THE INFLUENCE OF SULFUR ON THE CREEP-RUPTURE PROPERTIES AND HOT WORKING CHARACTERISTICS OF SEVERAL EXPERIMENTAL NICKEL-BASE ALLOYS

by

Jay Ward Schultz

A dissertation submitted in partial fulfillment
of the requirements for the degree of
Doctor of Philosophy in the
University of Michigan
1965

Doctoral Committee:

Professor James W. Freeman
Professor Richard A. Flinn
Professor Lars Thomassen
Professor Lawrence H. Van Vlack
Professor Gabriel Weinrich

To

L. R. S.

for patience, understanding, and encouragement

PREFACE

TABLE OF CONTENTS

LIST OF TABLES

LIST OF FIGURES

x

INTRODUCTION

The elevated temperature properties of nickel-base heat-resistant alloys can be highly sensitive to trace elements introduced from melting stock or by contamination during melting. Sulfur is one of the more notorious trace elements and, under present technology, is always present in commercially made nickel-base alloys. Producers have long considered it harmful to hot working characteristics. Sulfur is also thought to have an effect on creep-rupture properties. In fact, there has been speculation that the complete removal of sulfur from current nickel-base superalloys would result in a marked improvement of both hot working characteristics and creep-rupture properties.

Although it is widely accepted that sulfur can have harmful effects on the elevated temperature properties of nickel-base alloys [1, 2, 3, 4, 5, 6, 7 *], the validity of this concept has not been documented. Sulfur's reputation apparently stems from a combination of its ability to severely embrittle unalloyed nickel when present even in minute amounts [8, 9, 10, 11, 12] and mill experience with nickel alloys of various sulfur contents. Thus, this investigation was undertaken to establish the role of sulfur in nickel-chromium-titanium-aluminum alloys.

Boron and zirconium can be highly beneficial to the creep-rupture properties of nickel-base superalloys [13, 14] and are commonly added to them during manufacture. For these reasons it was deemed necessary to investigate the effects of sulfur without and with the presence of boron and zirconium. One main objective was to determine if these two elements produced marked property improvements by counteracting detrimental effects of sulfur.

The creep-rupture properties and hot rolling characteristics of high

---

* The superscripts refer to literature listed under REFERENCES.

1

purity experimental alloys of various chromium, aluminum and titanium contents were evaluated at sulfur levels fully encompassing those encountered in commercial practice. A major objective was to evaluate properties at an extraordinarily low level of sulfur as well as over a systematically varied range of sulfur contents and thus find out how beneficial the complete elimination of sulfur might be. Composition control was maintained by using the best raw materials available in the quantities required and vacuum-induction melting in high purity crucibles.

Boron and zirconium effects were separated from other compositional effects by splitting every heat and adding boron and zirconium to only the second ingot. This allowed the direct comparison of materials without and with boron and zirconium, but otherwise identical.

Initially one alloy was studied. It had a nominal composition of 20 percent chromium, 3.8 percent titanium, 1.2 percent aluminum and the balance nickel. The composition and strength of this alloy made it representative of several of the most successful commercial alloys. Sulfur levels were varied from 0.0020 to 0.0700 percent. Sufficient creep-rupture tests were run at 1200° and 1500°F to establish stress-rupture time curves between 10 and 1000 hours. 100-hour rupture strength and reduction of area were used to compare heats. Visual observation of the degree of corner cracking resulting from the direct rolling of ingots to barstock at 2150°F was used to evaluate hot working characteristics.

Because of an apparent titanium-sulfur interaction preventing sulfur damage in the initial alloy and the desire to more fully evaluate the role of sulfur the following materials were investigated:

Cr (%)	Ti (%)	Al (%)	Ni (%)
20	1.2	3.8	balance
20	0.1	3.8	balance
20	0	3.8	balance
20	0	0	80
0	0	0	100

The four alloys were studied at two levels of sulfur, nominally 0.0070 and 0.0350 percent. Nickel was investigated at three levels of sulfur, nominally 0.0005, 0.0030, and 0.0070 percent. All materials were again studied without and with boron and zirconium additions. Stress-rupture time curves and reduction of area were used to compare creep-rupture properties and the same method of evaluating hot rolling characteristics was employed. The nickel heats were rolled at 2000°F and creep-rupture tested only at 1200°F. Tensile properties were evaluated for nickel at 1200°F to provide a basis for selecting stresses for creep-rupture tests and also to compare with the effects of sulfur found by Kraai and Floreen[12].

Extensive structural studies were made throughout all phases of the investigation. Metallographic, X-ray diffraction and electron microprobe techniques were used to relate properties and composition to microstructure.

Several experimental heats were made when results indicated the likelihood of a "critical experiment" concerning the role of sulfur. These are fully described within the body of this dissertation.

REVIEW OF THE LITERATURE

The Influence of Sulfur on Nickel-Base Alloys

Those discussing the general topics of the melting [1, 2, 15], physical metallurgy [3, 4, 7], properties [5], and applications [6, 16, 17] of nickel-base alloys classify sulfur and the metallic elements of low melting point and limited solubility as deleterious trace elements which may adversely affect elevated temperature properties. Although several of the low melting point metals have been shown to be harmful to the creep-rupture properties and hot working characteristics of nickel-base alloys [18, 19, 20, 21] no documented evidence was found in the case of sulfur. Apparently sulfur's reputation was a result of its known effects on unalloyed nickel.

Sulfur Embrittlement of Nickel

The sulfur embrittlement of nickel was first suggested by Flietman in 1870, but it was not until 1925, when Merica and Waltenberg [10] published their classic paper on "The Malleability of Nickel", that the effects of sulfur as a trace element in nickel were fully recognized. From their work, Merica and Waltenburg concluded that sulfur in excess of 0.005 percent was harmful to the malleability of nickel during forging at 2000°F. The loss of malleability was attributed to liquid formation at the grain boundaries as a result of the 1190°F eutectic in the nickel-sulfur system. Moreover, they found that the addition of magnesium to high sulfur nickel would fully restore malleability by the formation of MgS. The MgS was formed in the melt and entrapped during solidification as innocuous inclusions. Manganese was also found to improve the malleability of high sulfur nickel, but not to the extent of magnesium. A manganese-nickel-sulfur eutectic was reported at 2425°F and MnS globules were distributed along the grain boundaries after solidification. Magnesium was thought

to form a sulfide preferentially to manganese. From the results of their work Merica and Waltenburg stated that "embrittlement of sulfur was suspected to be characteristic of nickel alloys".

More recently others [4, 10, 11, 12] have demonstrated the sulfur embrittlement of nickel. Kraai and Floreen [12] performed a definitive study involving high temperature tensile properties. They investigated the effects of from 0.0001 to 0.0050 percent sulfur on the tensile properties of nickel between 800° and 1400°F. A loss of strength and ductility was found on increasing sulfur for the entire range of temperatures studied. There was a maximum effect at about 1200°F, very close to the 1190°F eutectic in the nickel-sulfur system, and there appeared to be a measurable effect of as little as 0.0010 percent sulfur. From the fact that embrittlement occurred below the eutectic temperature, it was concluded that embrittlement could not be due only to a liquid phase. Magnesium additions completely eliminated sulfur embrittlement. Also, it was noted that up to 0.0050 percent sulfur did not affect malleability at 2100°F, which suggested a ductility increase above 1400°F.

Although a number of articles were found pertaining to various aspects of the creep of nickel, none dealt with or even considered the influence of sulfur on creep-rupture properties.

Sulfur in Other Metals and Alloys

To obtain a broader insight into what might be expected in the way of sulfur effects on the mechanical properties of nickel-base alloys, other metal-sulfur systems were reviewed.

Martin [22] investigated the effects of trace amounts of sulfur on the high temperature tensile properties and forgeability of cobalt. He claimed that his results indicated embrittlement by the same mechanism as in nickel. A eutectic reaction occurs in the cobalt-sulfur system at about 880°C (1615°F) and there is also limited sulfur solid solubility. Both

phenomena were said to lead to embrittling grain boundary films. Tensile tests at 800° and 900°C (1472° and 1652°F), above and below the eutectic temperature, revealed severe embrittlement at greater than 0.0050 percent sulfur. Cobalt containing more than 0.0150 percent sulfur could not be forged at 1000°C (1832°F). Also, magnesium and manganese were found to be effective sulfur neutralizers in cobalt, just as they were in nickel.

Ogawa et al [23] investigated the effects of up to 0.1 percent sulfur on the ductility of unalloyed iron from 1600° to 2400°F. High strain-rate tensile tests were used to evaluate cast material. Similar to the nickel-sulfur and cobalt-sulfur systems, a eutectic reaction occurs in the iron-sulfur system at 1810°F. This was said to result in sulfide precipitation or liquid formation at the grain boundaries. Sulfur, in sufficient quantities to produce sulfide or liquid films, was harmful throughout the entire temperature range of 1600° to 2400°F. Also, the authors demonstrated the effectiveness of manganese in neutralizing sulfur by the formation of stable MnS. Josefsson et al [24] investigated the influence of sulfur on the red-shortness in steel using high temperature impact tests. Their results were in agreement with Ogawa et al [23].

Others [25, 26] have found that the forgeability of manganese-free steels is very sensitive to sulfur. Good forging characteristics are apparently not obtained above 0.0020 percent sulfur [25]. Urban and Chipman [27], while studying the effects of various alloying additions on the nonmetallic inclusions formed in high sulfur iron, found that iron containing 0.158 percent sulfur was hot short. But similar materials having additions of 0.26 percent titanium, 0.3 percent zirconium or 0.43 percent manganese were readily forgeable, thus demonstrating a sulfur neutralizing ability for these elements.

Sulfur is not only harmful to high temperature properties; excessive numbers of preferentially orientated sulfides can severely affect room

temperature impact properties, as shown for plain carbon steels by Wright and Quarrell[28], Franklin and Tegart[29], and Vogels and Bruning[30]. Novak and Diran[31] found similar effects in the case of maraging steel plate.

The Titanium-Sulfur Interaction in Nickel and Iron-Base Alloys

Early in this investigation, phase identification work indicated that a stable titanium sulfide phase formed in all alloys containing titanium. This sulfide was identified as the tau-Ti_2S reported in the "X-Ray Powder Data File" published by the ASTM. The literature was then reviewed to find out what was known about the formation and effects of tau-titanium sulfide.

A diffraction pattern for tau-Ti_2S was obtained by Brown et al[32] during an investigation of 18Cr-8Ni-Ti and 18Cr-8Ni-Ti-Mo stainless steels. The phase was extracted and analyzed chemically as containing 69 percent titanium, 9.7 percent nitrogen, 5.7 percent carbon and 4.4 percent sulfur. The authors assumed that all the carbon and nitrogen were tied up as Ti (C, N) and arrived at Ti_2S for the formula of the phase. They apparently named the phase tau. Knop[23] suggested from comparison of X-ray diffraction data that a Y-phase reported by Gemmill et al[34] in a Cr-Mo-Ti steel was identical to tau-Ti_2S.

More recently, several investigators[35, 36, 37] have attributed extra lines in the X-ray diffraction patterns of extracts obtained from Udimet 500, a 55Ni-20Cr-15Co-4Mo-3Ti-3Al commercial heat-resistant alloy, to Y-phase or tau-Ti_2S. Amy[37] was able to obtain X-ray diffraction patterns for tau-Ti_2S in Udimet 500 only when the alloy contained boron. On the basis of limited data, he postulated a boron-sulfur interaction and suggested that this introduced uncertainties into previous work on the effects of boron.

Novak and Diran[31] reported the existence of tau-phase in maraging

steels having high sulfur contents and low impact strength. Electron microprobe studies of tau in situ indicated a composition of 34 percent titanium, 21 percent iron, 2 percent cobalt, 3 percent nickel, and 25 percent sulfur. The iron, cobalt, and nickel were attributed to matrix interference.

Frick and Rohde [38] investigated odd shaped inclusions formed in very slowly cooled 4.0C-3.6Si-0.3Mn-0.7P-0.05S-0.4Ti pig-iron melts. Metallographic observations indicated anisotropic rosette crystals with hexagonal symmetry. Microanalysis of extracted crystals indicated their composition to be 10.3 percent carbon, 23.3 percent sulfur, 5.3 percent iron and 61.9 percent titanium. The authors suggested the possibility of a $Ti_xS_xC_x$ compound. Kudielka and Rhode [39] employed a 4.3C-0.25S-1.0Ti pig-iron to grow similar large crystals. They gave the same chemical analysis for the phase as reported by Frick and Rhode [38]. Kudielka and Rhode made a detailed investigation of the crystal structure of this compound using precise single crystal X-ray diffraction techniques. They found it to have a hexagonal unit cell with lattice parameters c = 11.18kx and a = 3.20kx. Calculated "d" values and intensities were noted to be in excellent agreement with those obtained by others for tau-Ti_2S. A formula of $Ti_4C_2S_2$ was suggested on the basis of composition and crystal structure analysis. The authors further stated that the compound was similar to Ti_3S_4, but with carbon stabilizing the lattice. They also suggested that there was some solubility for iron.

After finding that tau-phase formed in iron as well as nickel-base alloys, the literature pertaining to the interaction of titanium and sulfur in iron-base materials was reviewed.

It was immediately apparent that many had observed titanium sulfides during metallographic examinations [27, 40, 41, 42, 43, 44, 45, 46, 47, 48, 49, 50]. All of the morphological descriptions of the titanium sulfides suggested that they were the tau-$Ti_4C_2S_2$ compound. Although

many of the investigators called the phase TiS, they did not supply proof
of this identification. In no case were these sulfides found to affect pro-
perties.

The literature seems to strongly indicate that titanium reacts with
sulfur and carbon in either iron or nickel alloys to form tau-$Ti_4C_2S_2$.
Tau usually has a lamellar-eutectic appearance in the cast structure
and appears blue-red to grey to tan, depending on the preparation of the
sample and the light-transmitting media.

EXPERIMENTAL PROCEDURE

The general procedure was to make, process, and evaluate small laboratory heats of experimental nickel-base alloys having both very low and systematically varied sulfur levels. Melting and casting was performed exclusively in a vacuum-induction furnace using carbon de-oxidation. Cast ingots were hot rolled directly to barstock. The bar-stock was then heat treated and machined into test specimens. The specimens were subjected to creep-rupture and short-time tensile tests. Structural studies were performed on various material conditions using metallographic, X-ray diffraction, and electron microprobe techniques.

Experimental Alloys

The alloy initially studied had the following aim composition in weight percent:

C	Cr	Al	Ti	Ni
0.06	20.0	1.2	3.8	balance

The hardener content (aluminum plus titanium) was selected to provide a level of the γ'-Ni_3 (Al, Ti) strengthening precipitate representative of successful wrought superalloys and also to give an atomic ratio of titanium to aluminum of 1.8 to 1. This particular ratio was suggested by Decker[51] as the one providing the greatest difference between the lattice parameters of the γ matrix and the γ'-Ni_3 (Al, Ti) precipitate, and the greatest strengthening for a given total hardener content.

All heats were made with and without boron and zirconium additions by splitting each heat, no boron and zirconium being added to the first ingot and 0.0035 percent boron and 0.045 percent zirconium being added

to the second. Boron and zirconium are frequently added to nickel-base alloys because they can have marked beneficial effects on creep-rupture properties. One objective of this investigation was to determine if their effects were due to an interaction with sulfur. Also it was evident that the role of sulfur could not be successfully clarified unless the alloy was made with and without boron and zirconium. The split heat technique was employed to reduce the possibility of misleading results from the comparison of separate heats. The amounts of boron and zirconium added represent common practice.

As will be shown by the data, remarkably little variation in properties was noted in the 20Cr-1.2Al-3.8Ti alloy for a wide range of sulfur contents. Preliminary structural studies indicated that this was due to the formation of an innocuous titanium sulfide phase. At that time it was decided to determine the role of titanium in preventing sulfur from adversely affecting creep-rupture properties. Thus, alloys were investigated having the following air compositions in weight percent:

C	Cr	Al	Ti	Ni
0.06	20.0	3.8	1.2	balance
0.06	20.0	3.8	0.3	balance
0.06	20.0	3.8	0	balance
0.06	20.0	0	0	balance
0.04	0	0	0	balance

Again the split heat technique was employed in making these alloys to provide the comparisons with and without the addition of boron and zirconium.

In the alloys containing aluminum and titanium, the aluminum was maintained at 3.8 percent while the titanium was varied to evaluate its influence. A high aluminum content was used to maintain the amount of the γ'-Ni$_3$ (Al, Ti) precipitate at a level that would provide reasonably good creep-rupture properties.

The 80Ni-20Cr alloy and unalloyed nickel were included to obtain data which would further clarify the role of sulfur in materials based on nickel. Factual creep-rupture data defining the effects of sulfur were unavailable for even these materials.

The sulfur content of the 20Cr-1.2Al-3.8Ti alloy was varied from about 0.0020 to 0.0700 percent. The other alloys were made at two levels of sulfur, about 0.0070 and 0.0350 percent. Three levels of sulfur were studied in nickel, about 0.0005, 0.0030, and 0.0070 percent.

Melting Stock and Crucibles

Generally, the purest materials available in the quantities needed for the investigation were utilized.

Nickel

Mond carbonyl nickel pellets were used for all but one heat. These were furnished in 200-pound lots by The International Nickel Company, Inc. Their chemical analysis of several pellets from one lot gave the following results:

%C	%S	%Pb	%B	%Si	%Mn	%Fe
0.013	0.0030	<0.001	<0.001	<0.005	<0.005	0.011

%Co	%Cu	%P	%Mg	%Al	%Ti	%Zr
<0.01	<0.005	0.002	<0.005	<0.01	<0.01	<0.01

From analyses of vacuum melted heats using this type of nickel, it appeared that the sulfur content varied from approximately 0.002 to 0.003 percent between the different lots of nickel shot.

UHP nickel was used for one heat of very low sulfur nickel. This material was made by melting Mond Type A carbonyl nickel powder under argon and remelting under hydrogen, a method similar to that described by Olsen[52]. It had the following chemical composition:

%C	%S	%B	%Si	%Mn	%O	%N
0.004	0.0003	<0.001	0.006	0.005	0.0070	nil

%Cu	%Fe	%Co	%Al	%Ti	%Mg
0.0046	0.094	<0.005	<0.005	<0.005	<0.002

Chromium

Except for the lowest sulfur heats, Shieldalloy aluminum-reduced "VMG" chromium was used. Elchrome chromium was used for the lowest sulfur heats. The analyses furnished for the various lots of Shieldalloy chromium were nearly identical. Typical reported compositions of the two types of chromium were:

	%C	%S	%Si	%Fe	%Al	%Cr	O(ppm)	H(ppm)	N(ppm)
Shieldalloy	0.01	0.012	0.12	0.21	0.06	99.43	-	-	-
Elchrome	0.007	0.0060	-	0.004	-	99.94	8.9	0.3	8

Sulfur

Sulfur was added as chemically pure nickel monosulfide.

Titanium

Dupont sponge titanium metal was used for all heats. The only impurity reported for the lot used was 0.06 percent iron. A sulfur analysis performed by The International Nickel Company, Inc. indicated 0.0020 percent of that element.

Aluminum

The aluminum was supplied gratis by the Aluminum Company of America as 99.99 percent Aluminum Ingot (1-pound notch bars) with the following composition:

%Cu	%Fe	%Si	%Mg
0.001	0.001	0.003	0.002

Boron

Boron was added as a nickel-boron alloy purchased from the Electromet Division of Union Carbide. The chemical composition furnished for

the alloy was:

%Ni	%B	%Al	%Fe	%C	%Si
77.25	16.38	0.11	2.98	0.44	0.01

Zirconium

Reactor Grade chunk zirconium was purchased from the Malloy Sharon Metals Company. They reported the following impurity content:

%C	%Si	%Mn	%Fe	%Pb
0.025	0.006	0.002	0.0309	0.002

Carbon

Spectrographically pure graphite rods were turned on a lathe to produce coarse powder which was used for all carbon additions.

Crucibles

All melting was carried out in Norton Alundum 99-percent fused alumina crucibles. The crucibles had an inside diameter of 3.5 inches and were 7.0 inches high. The following typical chemical composition was reported for the refractory:

$\%Al_2O_3$	$\%SiO_2$	$\%Fe_2O_3$	$\%Na_2O_3$	other
99.01	0.58	0.11	0.17	balance

A personal communication from the Norton Company stated that this grade of crucible material is spectrographically free from boron or boron compounds.

Melting Procedure

All melting was done in a vacuum-induction melting furnace designed and built at the University of Michigan. The furnace had a 30-cubic foot cylindrical tank and a 6-inch booster-diffusion pump and mechanical fore pump combination capable of maintaining pressures of less than 10 microns of Hg during the melting of the usual 5500-gram (12 pound) charges.

The melting procedure established to provide reproducible results was as follows:

1. All heats were the same size, 5500 grams.

2. All the Cr and C and as much Ni as possible were charged into the crucible. When S was to be added, the nickel-sulfide was also charged into the crucible. The remaining necessary additions were placed in charging buckets in the vacuum tank. The B and Zr were wrapped in aluminum foil to prevent losses during addition.

3. The tank was evacuated to a maximum pressure of 2 microns with a maximum apparent leak-up rate of 4 microns per minute.

4. The power was then turned on and the melting of the initial charge and the remainder of the Ni completed in about 45 minutes. Shorter melting times were not possible due to the power limitations of the furnace. In most cases no carbon boil was observed when the melt surface was finally visible, indicating that deoxidation occurred mainly during melt-down. If a boil was observed, the melt was held until the boil subsided before proceeding with further additions or pouring.

5. The Al and Ti were added (when required) and the melt superheated 200°F.

6. One half of the heat was poured.

7. B and Zr additions were made, superheat re-established, and the second half of the heat was poured. The total elapsed time from the start of melting was about one hour.

The molds used were 4-inch sections of 2-inch I. D. steel pipe. A 2-inch high hot-top, made from insulating brick, was mounted on each mold.

Hot Rolling Procedure

All ingots were hot rolled directly to barstock on a 2-Hi Reversing Bar Mill. The procedure normally used was to soak the ingots for two hours at the rolling temperature, 2150°F, and then roll them to ½-inch square barstock. The rolling schedule included 21 passes with a 10-minute reheat between each pass to maintain the temperature at 2150°F. The reduction of area per pass, as calculated from roll geometry, was as follows:

Pass Number:	1 through 4	5 through 10	11 through 21
Reduction of Area:	13% total	10% each	12 to 16% each

Initial square-up of an ingot took place in passes 1 through 4, resulting in a low true reduction of area per pass. Total contact of the material with the rolls occurred during passes 4 or 5. Passes 16 and 17 were diamond-shaped as opposed to square and, although the reduction per pass was not varied at this point, the overall shape of a bar was severely changed on going through these passes. The last pass was followed by air cooling.

Several deviations from the above procedure were introduced. The ingots from several heats of the 20Cr-1.2Al-3.8Ti alloy (Heats 1379, 1380, 1383, and 1384) had an "accelerated" rolling schedule in that they were reheated only after every three passes. This allowed the material to cool substantially and increased the severity of the working conditions.

The two ingots from Heat 1319 of the 20Cr-1.2Al-3.8Ti alloy were rolled to 1.5-inch wide by 0.4-inch thick strips using flats on the rolls. The normal heating and rolling schedule, as outlined above, was used.

Finally, all the ingots from nickel heats were held two hours at 2000°F and rolled from this same temperature to ½-inch square barstock using the "accelerated" rolling schedule outlined above.

The evaluation of hot working characteristics was based solely on the severity of corner cracking observed. This was recognized as qualitative, but corner cracks were the only significant defects expected with the conservative reduction schedules that were considered necessary for the assurance of obtaining some usable material.

Chemical Analyses

All chemical analyses were performed by the Research Laboratory of The International Nickel Company, Inc.

The sampling procedure consisted of taking a 1.5-inch section from the center of each piece of barstock and machining chips from this section. This provided a 1.5-inch by 0.5-inch by 0.25-inch sample for spectrographic analysis and sufficient chips for other methods. Small slices were also cut from several bars and ground to 0.25-inch cubes to provide samples for gas analysis by vacuum fusion.

Heat Treatments

The following heat treatments were used on the hot rolled material before creep-rupture and tensile testing:

1. Al and Ti-bearing alloys: 8 hours at 1975°F, air cooled, plus 16 hours at 1300°F, air cooled.

2. 80Ni-20Cr alloy: 1 hour at 1975°F, air cooled.

3. Nickel: 1 hour at 1600°F, air cooled.

Specimens were machined from barstock after heat treatment.

Mechanical Testing

Specimens

Coarse (1/2-13) and standard*(3/8-16) thread specimens were used for creep-rupture and tensile tests. Both had 0.250-inch diameter

---

* - Standard for the University of Michigan creep testing apparatus

by 1.00-inch long gage sections. The coarse-thread specimen resulted from previous refinements of the standard-thread specimen necessary to overcome the following technical difficulties:

1. Fracture in the threads.

2. Sticking of fractured specimens in specimen holders.

3. Destroying of reference threads used for gage marks.

The gage marks of the coarse-thread specimens were machined on the fillets. Thus accurate elongation measurements were possible around the entire circumference of the specimens. Not one specimen fractured at these gage marks.

Standard-thread specimens were used only where necessitated by lack of material.

Creep-Rupture Tests

Creep-rupture properties were evaluated at 1200° and 1500°F to determine if effects were the same at temperatures near the upper and lower limits of the useful range for wrought nickel-base heat-resistant alloys.

Creep-rupture properties were established at each temperature by conducting tests over a range of stresses so as to define stress-rupture time curves from about 10 to 1000 hours. The deviations of the test points from smooth curves on a log stress versus log rupture time plot gave an indication of the reproducibility of test results. More important, the slope variations within and between curves enabled the determination of effects produced by stress variations. This insured that erroneous conclusions from comparative tests at a single stress, a widely used procedure for studies of this nature, would be avoided if compositional effects should prove to be dependent on stress.

Elongation and reduction of area were measured for the fractured specimens. Ductility comparisons were made using reduction of area,

as the values were more consistent and more accurately measurable
than elongation values.

All of the creep-rupture tests were conducted in conventional beam
loaded creep-rupture units in accordance with ASTM recommended
procedure. The specimens were placed in the furnaces which were
at temperature, and allowed a maximum of four hours to attain proper
test temperature and temperature distribution prior to application of the
load. Temperature variation along the gage length was limited to $\pm3°F$.
Rupture times were recorded by automatic timers. Creep (time-
elongation) measurements were made during the tests with modified
Martens-type extensometers having sensitivities of 10^{-5} inches. These
measurements are available as a matter of record.

Tensile Tests

Tensile tests were conducted on unalloyed nickel materials at 1200°F
to guide in the selection of stresses for creep-rupture tests and to fur-
ther evaluate the possible effects of sulfur.

Specimens and procedure for obtaining test temperature were the
same as used for creep-rupture tests. Stress-strain data were obtained
with the same type of optical extensometer system used for creep-rupture
tests. The head speed used for all tests was 0.05-inches per minute.

Structural Studies

Metallography

Optical techniques were used for the metallographic investigation
of microstructures in this study. The as-cast, as-heat treated, and
tested samples were surveyed as to general structure and the relation-
ships between type, size, and distribution of sulfide phases and the nor-
mal microconstituents.

Metallographic samples were mechanically polished on wet silicon

carbide papers through 600 grit; then on cloths impregnated with 6 and 1 micron diamond paste; the final polish was obtained on either a Syntron vibratory polishing unit or cloth wheel using a mixture of Linde B aluminum powder and distilled water.

Specimens were examined before etching and after to ascertain the effect of the etch on sulfide phases. All etching was done electrolytically. A 2 percent aqueous solution of sulfuric acid at a current density of about 0.5 amps per square inch was found to be satisfactory for the 80Ni-20Cr alloy and nickel. The procedure developed by Bigelow and Amy[53] employing an etchant composed of 12 parts phosphoric acid (85 percent), 47 parts sulfuric acid (96 percent), and 41 parts nitric acid (70 percent) at current densities of 0.1 to 0.3 amps per square inch was used for all the aluminum and titanium-bearing alloys. By the selection of proper etching time, which varied with the alloy, a satisfactory delineation of the microstructure could be obtained without over-attacking the different sulfide phases.

X-Ray Diffraction Techniques

X-ray diffraction patterns were obtained from powder residues extracted from solid samples or turnings. Sulfide extracts were a problem. No successful method was found for extracting sulfides from titanium-free alloys. The sulfides in the titanium-bearing alloys were readily extracted with hot concentrated hydrochloric acid. All residues were thoroughly washed in alcohol and dried.

Powder samples were prepared with glass capillary tubes or Duco cement, the former giving the most uniform results.

Patterns were obtained using 114.6-mm. Debye-Sherrer cameras with the film loaded unsymmetrically (Straumanis method). Filtered copper radiation was used with the filter (nickel) placed over the film instead of between the source and sample. This eliminated most of the fluorescent radiation due to poor matching of the K absorption

edge of the specimen and the characteristic wavelength of the radiation, especially a problem with titanium-rich compounds. The positions of the diffracted lines were measured on an X-ray film comparator equipped with a Vernier scale. Shrinkage corrections were made in all cases. Intensities were estimated visually.

Electron Probe Microanalysis

Selected samples and residues were examined on electron probe microanalyzers at the Research Laboratory of The International Nickel Company, Inc. and the Babcock and Wilcox Company's research laboratory. One microprobe unit was equipped with a scanning device that could be connected to either a strip-chart and recorder or oscilloscopes. These arrangements made it possible to obtain linear concentration profiles and two-dimensional concentration images over the surface of a specimen.

The solid specimens investigated were prepared using the metallographic procedure outlined above. Polishing was stopped after the 1-micron diamond finish because the final step using alumina abrasive tends to leave a surface residue which can emit characteristic aluminum radiation. The powder samples were those left over from X-ray diffraction studies.

CHEMICAL COMPOSITION OF EXPERIMENTAL ALLOYS

In an investigation of this type, the importance of accurate chemical analyses cannot be over-emphasized. Reliable knowledge of composition is essential for the sound evaluation of minor element effects. This is true not only for the element under consideration, but for all other elements in an alloy. Thus, this section is devoted to the description of the results of chemical analyses.

The compositions of the experimental materials made for this investigation are presented in Table 1.

The sulfur content of the 20Cr-1.2Al-3.8Ti alloy was controlled by the grade of chromium used and sulfur (NiS) additions. Sulfur varied from 0.0017 to 0.1510 percent. Heats 1389 and 1313, lowest in sulfur, were made with Elchrome chromium. All other heats were made with Shieldalloy chromium. Sulfur (NiS) was added to produce levels above approximately 0.0090 percent.

Two levels of sulfur were used in the 20Cr-3.8Al-1.2Ti, 20Cr-3.8Al-0.1Ti, 20Cr-3.8Al, and 80Ni-20Cr alloys. The lower level of about 0.0070 percent resulted from melting with Shieldalloy chromium and Mond nickel shot, while the higher level of about 0.0350 percent required a sulfur (NiS) addition.

The various levels of sulfur in nickel were obtained by using two different grades of nickel and by adding sulfur (NiS). Heat 1346, lowest in sulfur, was made with UHP nickel; all other heats were made with Mond nickel shot. Sulfur (NiS) was added to obtain the higher levels in Heats 1348, 1376Zr-S, and 1377B-S.

The observations made during the investigation (mainly consistency of recovery during melting and microstructures) indicated that analyzed sulfur contents were accurate. The results of the chemical analyses for carbon, titanium, aluminum, boron and zirconium indi-

cated more variations from aim compositions than were desirable.
Only for carbon, however, could the test results be correlated with
the range in analyzed values.

Boron and zirconium analyses of the materials not having these
elements added, consistently indicated less than 0.0010 percent boron
and less than 0.01 percent zirconium. On the other hand, analyses
of the materials to which 0.0035 percent boron and 0.045 percent zir-
conium were added were quite erratic, frequently indicating well
over 100-percent recovery of either or both of the elements. Nothing
was found in the investigation to suggest that recovery variations were
due to segregation. On the contrary, the results seemed to agree with
the aim composition.

The analyzed titanium contents of Heats 1328 and 1334, both having
aim values of 0.3 percent, were less than 0.10 percent. It seemed
unlikely that the titanium recovery should be so poor. Moreover, the
creep-rupture tests indicated a slight improvement in strength, as
would be expected from a small amount of titanium. Consequently,
this alloy was considered to have about 0.1 percent titanium in order
to distinguish it from the 20Cr-3.8Al alloy.

Manganese was less than 0.01 percent in all heats. Silicon contents
ran close to 0.01 percent in heats made with Shieldalloy chromium.

Oxygen, hydrogen and nitrogen analyses were made on many of the
heats as a quality control check. Results indicated the levels of these
elements to be as expected from the type of vacuum melting procedure
used.

The levels of other elements were very low and consistent from
heat to heat. Thus, they were considered uninfluential for the pur-
poses of this investigation.

CREEP-RUPTURE PROPERTIES

A 20Cr-1.2Al-3.8Ti alloy was investigated initially because it closely resembled engineering alloys in composition and properties. The 1200° and 1500°F creep-rupture properties of this alloy were unaffected by varying sulfur from approximately 0.0020 to 0.0700 percent. Structural studies revealed that this was a result of the formation of a stable sulfide phase, tau-$Ti_4C_2S_2$, which in effect removed the sulfur from the alloy. Moreover, the distribution of the sulfide was such that it did not interfere with creep and fracture mechanisms.

The 20Cr-1.2Al-3.8Ti alloy was studied without and with combined additions of 0.0035 percent boron and 0.045 percent zirconium. These elements invariably improved creep-rupture properties, but with no apparent relation to sulfur content.

Other alloys were then investigated to determine how much titanium, if any, was required to eliminate sulfur effects. Accordingly, it was found that sulfur in the range of approximately 0.0070 to 0.0350 percent had no influence on the 1200° and 1500°F creep-rupture properties of a 20Cr-3.8Al-1.2Ti alloy, a 20Cr-3.8Al-0.1Ti alloy, a 20Cr-3.8Al alloy, and an 80Ni-20Cr alloy. Again structural studies revealed that stable sulfides formed, effectively tying up the sulfur. Furthermore, they were distributed so as not to interfere with creep and fracture mechanisms. Tau-$Ti_4 C_2S_2$ was the sulfide in the alloy containing 1.2 percent titanium and a chromium sulfide formed in the other three having little or no titanium. Thus, chromium was also found to interact with sulfur to prevent embrittlement.

Adding 0.0035 percent boron and 0.045 percent zirconium to these alloys again markedly improved creep-rupture properties; but, as before, the effect was not related to sulfur content.

Finally, the 1200°F creep-rupture and tensile properties of nickel

were evaluated to demonstrate conditions where sulfur was deleterious. Sulfur embrittlement was found as expected, but only when boron and zirconium had not been added. Both creep-rupture and tensile strength decreased linearly on increasing sulfur from 0.0004 to 0.0067 percent. Severe embrittlement was indicated by an almost total loss of ductility at the highest level of sulfur.

For nickel, the combined addition of 0.0035 percent boron and 0.045 percent zirconium eliminated embrittlement at 0.0071 percent sulfur. Investigating heats with separate additions of each element revealed that zirconium counteracted sulfur while both further improved proper- ties by a mechanism not related to sulfur embrittlement.

Other elements also had significant effects. An extensive investiga- tion of the 20Cr-1.2Al-3.8Ti alloy revealed that variations in carbon content caused heat-to-heat variations in properties. At least 0.05 percent carbon was necessary to obtain optimum properties. The dif- ferent aluminum and titanium contents used in the alloys demonstrated that the high titanium alloy had creep-rupture properties far superior to those of the high aluminum alloys.

The creep-rupture test data for all the materials investigated are presented in Tables II, III, and IV. The tensile test data for nickel are presented in Table V.

<u>Influence of Sulfur</u>

20Cr-1.2Al-3.8Ti Alloy

There were no significant effects of sulfur on the 1200° and 1500°F creep-rupture properties, summarized as 100 hour rupture strength and average reduction of area (ductility)* in Figure 1 and Table VI. Boron and zirconium additions substantially increased strength and duc-

---

* The terms reduction of area and ductility are used interchangeably.

tility at both temperatures, but with no relation to sulfur content (Fig. 1). Certainly boron and zirconium did not improve properties by nullifying detrimental effects of sulfur.

The summary data were derived from test data in Table II and the stress-rupture time curves in Figures 2, 3, 4, and 5. Since the wide variation in sulfur contents did not produce any consistent change in the slopes of the stress-rupture time curves, the 100-hour rupture strengths in Figure 1 are not subject to qualification on a time basis for a period of about 10 to 1000 hours. Thus, raising the sulfur content of the 20Cr-1.2Al-3.8Ti alloy to approximately 0.0700 percent did not reduce strength or ductility at 1200° and 1500°F; nor were these properties measurably improved by reducing sulfur to as low as approximately 0.0020 percent.

The 100-hour rupture strength data at 1200°F and the average reduction of area data at 1500°F exhibited considerable scatter (Fig. 1). Most of this, as will be shown later, resulted from heat-to-heat variations of carbon content. The scatter bore no apparent relationship to the heat-to-heat variations of titanium, aluminum, boron or zirconium.

Microstructural studies were undertaken as part of an investigation to reveal the reasons for the lack of sulfur effects. Examination of the as-heat treated materials disclosed sulfur was present as small rod-like rose-grey sulfides orientated parallel to the direction of rolling (compare Figs. 6 and 7). The sulfides were distributed as stringers and their location was random, i. e., they were not preferentially associated with other microstructural features. Chromium carbides were precipitated during heat treatment and are seen as the white intra and intergranular particles in Figures 6 and 7. The γ'-Ni$_3$ (Al, Ti)* matrix strengthening precipitate also formed during heat treatment, but it is not resolved in the photomicrographs.

---

* This phase will henceforth be referred to as γ'.

Employing X-ray diffraction and electron microprobe techniques, it was found that the sulfide phase present in this alloy was the titanium carbosulfide compound tau-Ti_4 C_2S_2. This sulfide was found at all sulfur levels, even in Heat 1313A with only 0.0017 percent sulfur. The specific results of the phase identification work will be presented in a subsequent section.

No evidence was found during examination of the fractured creep-rupture specimens (Figs. 8 and 9) to indicate that the sulfides, even in the numbers present in the high sulfur heats, influenced creep-rupture properties. The sulfides did not participate in the structural changes that resulted from testing (compare Figs. 8 and 9 to Figs. 6 and 7). The structural changes observed are characteristic of this type of alloy and were as follows:

a. The γ' intragranular precipitate grew in size and tended to become preferentially orientated along the direction of greatest grain deformation. This is well illustrated in Figure 8a.

b. The areas adjacent to the grain boundaries were denuded of γ'. This denudation was most extensive along the boundaries transverse to the direction of testing.

c. Carbide precipitation and agglomeration took place (compare Figs. 8 and 9 with Figs. 6 and 7). Moreover, although not evident from the photomicrographs, a carbide transformation occurred. This transformation is reported to be instrumental in causing the γ' denudation along the grain boundaries.

d. Microcracks formed along the grain boundaries, especially those transverse to the direction of testing (Figs. 8c and 9a).

These structural changes were generally greater as the exposure time was increased, and occurred sooner and were more extensive at 1500°F than at 1200°F.

Not only were the sulfide particles innocuous with respect to structural

changes, they were unaffected by long time exposure at 1500°F (compare Figs. 8 and 9 to Figs. 6 and 7). They maintained both their shape and relative positions, although sometimes their orientation was changed by matrix deformation and carbides tended to precipitate on them.

Thus, the presence of the seemingly stable titanium carbosulfide at even the lowest levels of sulfur and the non-participation of the phase in creep and fracture mechanisms accounts for the lack of effects from a wide range of sulfur contents. This apparently strong titanium-sulfur interaction then led to the investigation of other alloys, the original intent being to define how much titanium was necessary to eliminate sulfur effects.

20Cr-3.8Al-varied Ti Alloys

Increasing sulfur from about 0.0070 to 0.0350 percent had no significant effect on the creep-rupture strength of the 20Cr-3.8Al-1.2Ti alloy, the 20Cr-3.8Al-0.1Ti alloy, or the 20Cr-3.8Al alloy at 1200° and 1500°F (compare the stress-rupture time curves in Figs. 10, 11, and 12). Such differences as were found were too small to be meaningful, even if other composition effects were not likely. The addition of 0.0035 percent boron and 0.0045 percent zirconium substantially increased the strength of each alloy at both 1200° and 1500°F without relation to sulfur content (Figs. 10, 11, and 12).

Sulfur had no influence on the 1200°F ductility of the alloys without or with boron and zirconium; but at 1500°F there appeared to be an effect of sulfur on all three since the low sulfur heats had substantially higher ductility (Table III and Figs. 10, 11, and 12). However, as will be described below, microstructural examination indicated that these ductility differences at 1500°F were due to extensive carbide reactions and not sulfur.

Microstructural examination of as-heat treated specimens (Figs. 13 and 14) suggested that two different sulfides were present. Phase iden-

tification work, to be described later, verified this; the 20Cr-3.8Al-1.2Ti alloy contained tau-Ti_4 C_2S_2 and the 20Cr-3.8Al-0.1Ti and 20Cr-3.8Al alloys contained a chromium sulfide. Note that tau-$Ti_4C_2S_2$ was also found in the 20Cr-1.2Al-3.8Ti alloy discussed previously. The tau-Ti_4 C_2S_2 in the 20Cr-3.8Al-1.2Ti alloy was present as small grey particles associated with massive white carbides, both being distributed in stringers orientated parallel to the rolling direction (Figs. 13c and 13d). The chromium sulfide in the 20Cr-3.8Al-0.1Ti and 20Cr-3.8Al alloys was seen as large grey elongated particles, also associated with massive carbides and distributed as stringers (Figs. 14c and 14d).

With the exception of the difference in sulfides present, these three high aluminum alloys, without or with boron and zirconium, had essentially identical microstructures in the as-heat treated condition (compare Figs. 13 and 14). The most striking feature was the presence of the large white carbide particles. Their stringer-like distribution strongly suggested that they resulted from breaking down the cast structure, i.e., they went undissolved through the 2150°F rolling treatment. Moreover, there was little precipitation of carbides on the grain boundaries during heat treatment. This was in marked contrast to the 20Cr-1.2Al-3.8Ti alloy where the carbides were in solution after hot rolling and precipitated mostly on the grain boundaries during heat treatment (Figs. 6 and 7).

Metallographic examination of creep-rupture specimens (Figs. 15 and 16) indicated that extensive structural changes had occurred during testing, but these had no relation to the sulfides. Both the tau-$Ti_4C_2S_2$ in the 20Cr-3.8Al-1.2Ti alloy (Figs. 15c and 15d) and the chromium sulfide in the 20Cr-3.8Al alloy (Figs. 16c and 16d) appeared unaffected by long time exposure to stress at 1500°F. The sulfides did not change in appearance regardless of the boron and zirconium contents; nor were

they associated with structural changes that might affect creep-rupture properties. This, of course, does not explain the above-mentioned ductility effect; but it does indicate that one should look elsewhere for the reasons.

The changes in the microstructure were the same as those noted for the 20Cr-1.2Al-3.8Ti alloy. However, the degree was much greater for a given test condition, especially with respect to grain boundary reactions such as carbide precipitation and γ' denudation. These will be taken up in detail when the question of the ductility effect in these alloys is re-examined.

80Ni-20Cr Alloy

The 1200° and 1500°F creep-rupture properties of the 80Ni-20Cr alloy were unaffected by increasing sulfur from about 0.0075 to 0.0350 percent (compare the stress-rupture time curves in Fig. 17). Again boron and zirconium additions improved properties without relation to sulfur content. Other than this, there was remarkably little variation in the properties between heats.

Because of the lack of sulfur effects, structural investigations were limited to those required for identification of the sulfide present. Optically, the sulfide appeared identical to the chromium sulfides found in the 20Cr-3.8Al and 20Cr-3.8Al-0.1Ti alloys (Figs. 14c and 14d). The large grey particles were elongated and distributed as stringers parallel to the rolling direction with no relationship to grain boundaries. Phase identification by electron microprobe analysis, to be described later, verified that this alloy contained a chromium sulfide.

Unalloyed Nickel

Small amounts of sulfur were highly deleterious to the 1200°F creep-rupture and tensile properties of nickel when boron and zirconium were not added. The 100-hour rupture strength and tensile strength both

decreased linearly on increasing sulfur from 0.004 to 0.0067 percent
(Figs. 18 and 19). Furthermore, severe embrittlement was clearly
shown by the almost total loss of creep-rupture and tensile test ductil-
ity at 0.0067 percent sulfur (Figs. 18 and 19). The 100-hour rupture
strength data were obtained from the stress-rupture time curves pre-
sented in Figure 20. These curves dramatically show the effects of
sulfur over a wide range of rupture time, from less than 1 to more
than 1000 hours. The effects of sulfur on the tensile properties of
nickel agree with the findings of Kraai and Floreen [12].

As with previous materials, split heats were made and 0.0035 per-
cent boron and 0.045 percent zirconium were added to the second ingot.
Nickel containing boron and zirconium exhibited no sensitivity to sul-
fur in the range of 0.0007 to 0.0071 percent. Moreover, the addition
of these elements further improved creep-rupture and tensile proper-
ties over those of the lowest sulfur nickel with no addition of boron and
zirconium (Figs. 18, 19, and 20).

To establish the individual effectiveness of boron and zirconium in
counteracting sulfur, heats were made with separate additions of each.
Again the heats were split, but this time with sulfur added to the second
ingot. This provided material with 0.0035 percent boron at two levels
of sulfur and material with 0.045 percent zirconium at two levels of
sulfur. Creep-rupture and tensile test results revealed that zirconium
counteracted sulfur embrittlement while boron did not (Figs. 18, 19,
and 21). Adding only boron resulted in a substantial loss of strength
and ductility on increasing sulfur from 0.0044 to 0.0079 percent, but
properties were still superior to those of the boron and zirconium-free
nickel at similar sulfur levels. This suggests either a slight interaction
of boron with sulfur off-setting some sulfur damage or property improve-
ment by some other mechanism. Although the results show that boron
and zirconium both improve properties over and above what can be

accounted for by a sulfur interaction, the more important effects with regard to this investigation are the elimination of sulfur embrittlement by zirconium and the slight reduction of damage by boron.

Microstructural investigations of nickel did not directly reveal the whereabouts of sulfur. In the as-heat treated condition (Fig. 22) the only indication of the presence of a sulfide was the tendency of some of the grain boundaries in the high sulfur boron and zirconium-free nickel to become deeply etched, suggesting the prior presence of sulfide films (Fig. 22c). The nickel with boron and zirconium added had no suggestion of sulfide films in the high sulfur heat (Fig. 22d), but exhibited fine matrix and grain boundary precipitates at all sulfur levels (Figs. 22b and 22d). These precipitates were not evident in the nickel without boron and zirconium added (Figs. 22a and 22c).

Efforts to extract sulfides for phase identification were unsuccessful.

To obtain further insight into the embrittling mechanism, creep-rupture specimens from the high sulfur material without boron and zirconium added, Heat 1348A, were examined microstructurally. The evidence showed conclusively that the grain boundaries were extraordinarily weak. The specimen that ruptured after 0.067 hours under a load of 3000 psi had a completely intergranular fracture and little or no grain deformation (Fig. 23a). In fact numerous grains had fallen out, apparently during examination or etching. Figure 23a illustrated this lack of grain cohesion rather strikingly with a grain pulled out and lying upside down beside the cavity. The sulfur content, however, was apparently not high enough to produce a continuous film around all boundaries, as illustrated in Figure 23b by the partially ductile partially brittle fracture noted in the test lasting 31.9 hours at 2250 psi.

Grain boundary embrittlement was also obvious in the test specimen shut off after 4700 hours at 1500 psi (Fig. 23c). Although this specimen (not fractured during the test) had over 20 percent measured elong-

ation, most of the deformation was attributed to void formation rather than creep strain. It was riddled with oxide-filled voids where boundaries had parted and the grains showed little evidence of having been deformed.

The effectiveness of the boron and zirconium addition in eliminating sulfur embrittlement at the grain boundaries was evident in the micro-structures of the creep-rupture specimens of the high sulfur material, Heat 1348B (Fig. 24). The grain boundaries were fully capable of with-standing severe deformation and the fractures were ductile (transgran-ular).

Although the evidence available is limited to the visual observation of severely weakened grain boundaries, the data are all consistent with embrittlement by grain boundary films. Moreover, the Ni-S phase dia-gram exhibits a 1190°F eutectic and very limited sulfur solubility in nickel. Thus, sulfur embrittlement at 1200°F certainly seems due to the formation of liquid films at the grain boundaries and zirconium some-how prevents these films from forming by preferentially reacting with sulfur.

Influence of Boron and Zirconium

The addition of 0.0035 percent boron and 0.045 percent zirconium invariably produced material with superior creep-rupture properties at 1200° and 1500°F. This was true for all the materials investigated. Conclusive evidence is readily apparent when the following figures are reviewed:

Alloy	Figures
20Cr-1.2Al-3.8Ti-balance Ni	1, 2, 3, 4, and 5
20Cr-3.8Al-1.2Ti-balance Ni	10
20Cr-3.8Al-0.1Ti-balance Ni	11
20Cr-3.8Al-balance Ni	12
20Cr-balance Ni	17
Nickel	18 and 20

With the exception of nickel, the effects of boron and zirconium were not found to be related to sulfur content. Moreover, there was an improvement in the properties of nickel over and above the elimination of sulfur embrittlement.

Again with the exception of nickel, the addition of boron and zirconium did not affect microstructures of the as-heat treated alloys. Reviewing the following figures will verify this:

Alloy	Figures
20Cr-1.2Al-3.8Ti	6 and 7
20Cr-3.8Al-1.2Ti	13
20Cr-3.8Al-balance Ni	14
Nickel	22

Boron and zirconium obviously produced a general precipitate in nickel (Fig. 22) which could readily increase the strength of such a simple material; but the elimination of sulfur embrittlement by the addition of these elements was the greater effect and apparently not related to the precipitate.

The creep-rupture properties of the γ'-strengthened alloys with boron and zirconium added were substantially better than those of the same alloys without the addition. Microstructural evidence of the mechanisms causing these differences was limited to the observations that the structural changes were about the same without or with boron and zirconium for equivalent rupture times. Compare the following figures:

Alloy	Figures
20Cr-1.2Al-3.8Ti	8 and 9
20Cr-3.8Al-1.2Ti	15a and 15c with 15c and 15d
20Cr-3.8Al	16a and 16c with 16b and 16d

Of course stresses for a given rupture time were much higher for the alloys containing boron and zirconium. This situation confirms the observations of Decker et al[13] that boron and zirconium retard the structural changes that lead to failure and, in so doing, increase the creep strength together with the deformation possible before fracture.

Influence of Carbon on the 20Cr-1.2Al-3.8Ti Alloy

The heat-to-heat variations in creep-rupture properties of the 20Cr-1.2Al-3.8Ti alloy were for the most part, attributed to variations in carbon content (Tables I and VI). Moreover, when evaluating the effects of carbon it was necessary to take into account the wide variations in sulfur content, since appreciable carbon could be present in the stable sulfide tau-$Ti_4C_2S_2$. Thus, "effective" carbon content was defined as that carbon available to the alloy after all the sulfur had formed tau-$Ti_4C_2S_2$, i.e.:

effective carbon = total carbon - carbon in $Ti_4C_2S_2$

The amount of carbon in the sulfide is, from the formula $Ti_4C_2S_2$, equal to 0.376 times the total sulfur content. Thus:

effective carbon = total carbon - 0.376 total sulfur

Effective carbon contents were calculated for all the heats of the 20Cr-1.2Al-3.8Ti alloy and are included in a summary Table VI.

The 100-hour rupture strength and average reduction of area data (Table VI) are presented in Figure 25 as a function of effective carbon content. Also included are data from two heats with intentionally low carbon contents at two levels of sulfur, Heat 1383 (about 0.030 percent carbon and 0.0050 percent sulfur) and Heat 1380 (about 0.015 percent carbon and 0.0300 percent sulfur). These heats were made with the intent of defining the influence of very low effective carbon contents. It is quite evident from Figure 25 that most of the data scatter observed in Figure 1 (creep-rupture properties versus sulfur content) for 100-hour rupture strength at 1200°F and average reduction of area at 1500°F was due to heat-to-heat variations in carbon content. These properties were severely reduced by decreasing the effective carbon content, with or without boron and zirconium added (Fig. 25). There seemed to be a critical level of effective carbon at about 0.05 percent. Above this level a good combination of properties was obtained at both temperatures and below

it scatter increased and properties fell off.

Comparing the stress-rupture time curves for the two low carbon heats (Fig. 26) with those of the more normal carbon materials (Figs. 2, 3, 4 and 5) revealed that low effective carbon contents not only changed the stress levels of the curves at both 1200° and 1500°F, but also decreased the slopes at 1500°F. In effect this meant that short time properties were more severely affected by low carbon than the long time properties and was likely a result of the greater influence of limited ductility at high stresses.

Others [54, 55, 56, 57, 58] have observed similar effects of carbon in Ni-Cr-Al-Ti alloys. It is generally agreed that good creep strength and ductility rely on both a sufficient number and favorable distribution of carbides in grain boundaries as obtained by proper heat treatment and carbon content. The mechanism for the beneficial effects of these carbides is highly complex and still under investigation. However, there has been enough experimental evidence accumulated to suggest that in these alloys, at least in part, the carbides are nothing but a means to an end. The creep-rupture properties, especially ductility, are directly reliant on grain boundary denudation of γ' and this in turn depends on carbide precipitation and transformation.

The sequence of events that leads to grain boundary denudation of γ' involves the reaction $Cr_7 C_3 \rightarrow Cr_{23} C_6$, which occurs below and about 1920°F. $Cr_7 C_3$ is precipitated, mostly on grain boundaries during heat treatment above 1920°F (1975°F in this investigation) and transforms to $Cr_{23} C_6$ during exposure to lower temperatures. Some transformation takes place during aging (1300°F in this investigation), but most occurs during creep exposure (1200° and 1500°F in this investigation). The reaction requires more chromium than is available in $Cr_7 C_3$ and it is obtained by diffusion along the grain boundaries, leaving the areas adjacent to the boundaries depleted of chromium. The chromium-depleted areas have a high solubility for titanium and aluminum than the matrix and

the γ'-Ni$_3$ (Al, Ti) precipitate is thus dissolved. This results in grain boundary zones of reduced creep strength and increased ductility which can absorb more deformation before the onset of intergranular fracture, thus lengthening life and increasing ductility.

At low carbon contents (less than about 0.04 percent) the reduced carbide precipitation and transformation results in less γ' depletion along grain boundaries. At very low carbon contents (less than about 0.02 percent) $Cr_{23}C_6$ precipitates in a cellular manner along the grain boundaries and the cellular type of precipitation is known to be very harmful to ductility.

The effect of carbon content on the microstructural changes that resulted from creep-rupture testing were in agreement with the above mechanism. Comparing the higher carbon materials (Figs. 8 and 9) with the lower (Fig. 27) showed that high carbon content resulted in extensive carbide precipitation and agglomeration at the grain boundaries with wide zones along the boundaries denuded of γ'. Low carbon contents resulted in greatly reduced carbide precipitation and decreased γ' solution at the boundaries. Moreover, in the very low carbon Heat 1380 (Figs. 27c and 27d) carbide precipitation occurred in a cellular manner.

The Ductility Difference at 1500°F in the 20Cr-3.8Al-Varied Ti Alloys

The ductility difference found at 1500°F in the 20Cr-3.8Al-1.2Ti, 20Cr-3.8Al-0.1Ti, and 20Cr-3.8Al alloys with boron and zirconium added could easily be attributed to sulfur; but closer examination revealed that the explanation was more logically related to extensive carbide reactions which took place in all three alloys during creep exposure.

When the reduction of area values were plotted as a function of rupture time (Fig. 28), it was obvious that the high sulfur heats had

significantly lower ductility and that the differences in ductility increased substantially with rupture time. Microstructural examination of creep-rupture specimens of the three alloys disclosed, however, that the sulfides did not interfere with creep and fracture mechanisms. Furthermore, the carbide precipitation and transformation reactions in these high aluminum alloys were quite extensive and unusual when compared to those observed in the high titanium alloy (compare Figs. 15 and 16 with Figs. 8 and 9). Also, comparing the specimens with the greatest differences in ductility (Fig. 32a with Fig. 32b) revealed that the grain boundary carbide precipitation and γ' denudation were substantially greater in the high ductility specimens and cracking far more prevalent in the low ductility specimens. These microstructural differences account for the variations in ductility quite well, since the observed grain boundary reactions are said to control ductility in Ni-Cr-Al-Ti alloys, as discussed in the preceding section.

An explanation of what ultimately caused the differences in structure that led to the ductility effect is not clear; but it certainly appears related to the great number of large intragranular carbide particles in the as-heat treated material (Figs. 13 and 14) and the rate of the $Cr_7C_3 \rightarrow Cr_{23}C_6$ reaction during creep. The large intragranular carbides, assumed to be Cr_7C_3, dissolved during creep exposure, leaving white areas in the grains devoid of γ' (this is best seen in Figs. 15a, 15b, and 15c and by close examination of Fig. 29). The solution of these carbides presumably supplied the carbon for the precipitation of the carbides, assumed to be $Cr_{23}C_6$, in the grain boundaries.

For some reason the carbide solution and reprecipitation was more extensive in certain heats, which led to higher ductility. There was a consistent difference in composition that may hold the key; the high ductility heats had slightly lower aluminum contents and higher carbon contents than the low ductility heats. Compare the following:

Alloy	Heat	C (%)	Al (%)	Ductility
20Cr-3.8Al	1327B	0.07	3.87	high
	1333B	0.06	4.43	low
20Cr-3.8Al-0.1Ti	1328B	0.08	4.02	high
	1334B	0.07	4.27	low
20Cr-3.8Al-1.2Ti	1329B	0.10	4.00	high
	1335B	0.09	4.35	low

There is no conclusive evidence in the literature to suggest that these composition differences should affect carbide reactions, but the limited results here suggest that they do.

The Effect of the Ratio of Titanium to Aluminum

One the basis of Decker's research [51], the 20Cr-1.2Al-3.8Ti alloy was designed specifically to have an atomic ratio of titanium to aluminum of 1.8 to 1 to provide the greatest difference between matrix γ and the strengthening precipitate γ'. This was supposed to result in maximum strength for a given amount of titanium plus aluminum. Comparing the results obtained at 1500°F for Heat 1314 of the 20Cr-1.2Al-3.8Ti alloy and Heat 1329 of the 20Cr-3.8Al-1.2Ti alloy suggests this prediction was correct:

Heat	Atomic Ratio Ti:Al	Lattice Parameters [59] γ (A)	γ' (A)	100-Hr. Rupture Strength (psi)
1314A	1.8	3.57	3.60	25,300
1329A	0.18	3.57	3.58	17,000
1314B	1.8	3.57	3.59	34,500
1329B	0.18	3.57	3.56	26,000

The degree of misfit between γ and γ' appears to be the controlling factor for what should be about equal amounts of γ'. Nordheim and Grant [60] found a like difference in strength at 1500°F between a 20Cr-1.0Al-3.3Ti alloy and a 20Cr-3.8Al alloy, which they attributed to a similar lattice parameter misfit.

HOT WORKING CHARACTERISTICS

Observation of cracking characteristics during almost isothermal hot rolling indicated a general lack of sulfur effects except in the 80Ni-20Cr alloy, where high sulfur clearly caused cracking. Increasing the severity of rolling for the 20Cr-1.2Al-3.8Ti alloy resulted in cracking due to high sulfur only in an abnormally low carbon material.

Other effects were noted that were not related to sulfur content. High aluminum alloys cracked severely while the high titanium alloy did not, and adding titanium to the high aluminum alloys decreased cracking. Boron and zirconium had no beneficial effects and, furthermore, were observed to induce slight cracking in the low sulfur heat of the 80Ni-20Cr alloy.

When cracking occurred, it did so during breakdown of the cast structure. The tendency to crack was directly related to the condition of the grain boundaries just prior to rolling; the greater the amount of a second phase in the boundaries the greater the cracking tendency. Furthermore, the properties of the second phase were thought to have an influence in that cracking was more severe when the second phase was more resistant to deformation.

Before describing the results in detail, the rolling procedure will be reviewed to emphasize the limitations involved. Small, relatively homogeneous ingots were direct hot rolled to barstock using light reductions and reheats between each rolling pass. This process cannot then be directly compared to the working of large ingots having significant segregation; nor to forging or rolling operations where large variations in temperature and deformation rates are experienced.

The evaluation of hot rolling characteristics was limited solely to the visual observation of the number and severity of corner cracks formed in the barstock.

Cracking During Breakdown of the Cast Structure

The results of visual observations made during rolling are sum-
marized graphically in Figure 30, wherein an important general result
is apparent. When cracking occurred, it was always observed to start
during the initial square-up of the ingot and to stop before the final
rolling passes. This is taken to mean that the tendency to crack depen-
ded mainly on the alloy structure just prior to rolling, i.e., a cast struc-
ture partially homogenized by the pre-rolling soak; and that after this
structure was broken down during rolling, cracking stopped. This con-
cept was used in explaining the effects observed.

Influence of Sulfur

20Cr-1.2Al-3.8Ti Alloy

Varying the sulfur content of the 20Cr-1.2Al-3.8Ti alloy from 0.0017
to 0.0550 percent did not cause any significant corner cracking during
normal rolling at 2150°F (Figs. 30, 31, and 32). The finished barstock
of several high sulfur heats tended to have more very slight defects
(Fig. 32), but the trend was not consistent enough to attribute to sulfur.
Plate made from Heat 1319 having about 0.07 percent sulfur was success-
fully rolled using the normal schedule of reductions (Fig. 32).

Heat 1349B purposely had excessively high sulfur 0.1510 percent,
with the intention of inducing a sulfur effect. Excess titanium was added
to made up for that lost during sulfide formation. This material was
successfully rolled to sound barstock with the normal procedure (Fig. 32e).
There was some minor cracking, but this and other surface defects were
mostly attributed to the poor initial surface condition of the ingot. Need-
less to say, this material dramatically demonstrated the lack of influence
that sulfur had on the hot working characteristics of this alloy under the
restricted working conditions used.

Several heats were rolled using triple the normal severity, i.e., three

passes between each reheat. With this rolling procedure the 20Cr-1.2Al-3.8Ti alloy showed a tendency to crack which sulfur intensified at low carbon levels. Normal carbon Heats 1384B (0.09C and 0.0055S) and 1379B (0.06C and 0.0400S) had about equal numbers of slight corner cracks (Fig. 33). However, for the low carbon heats (0.03C and 0.0045S) and 1380 (0.015C and 0.03S) increased sulfur caused rather heavy corner cracking (Fig. 33). Thus, sulfur had an effect under these more severe rolling conditions.

Gibson's [61] experience with low (0.007 percent) and high (0.07 percent) sulfur heats of a 20Cr-0.8Al-2.5Ti-0.05C nickel-base alloy containing boron and zirconium bears this out. Attempting to hammer forge 2-inch square ingots at 2150°F, he found that the low sulfur material was readily reduced to 3/4-inch diameter barstock with no reheats; but the high sulfur material broke up during this operation. However, using light reductions at 2050°F, the high sulfur material could be successfully reduced. It was concluded that cracking depended somehow on deformation rate and temperature.

Throughout the processing of all the heats of the 20Cr-1.2Al-3.8Ti alloy there were no differences noted due to boron and zirconium (compare the A and B parts of each heat in Figs. 31, 32, and 33).

Microstructural investigations were performed to explain the role of sulfur. To compare materials that did and did not show sulfur effects for the same working conditions, Heat 1380A (0.017C and 0.0370S) and Heat 1379B (0.06C and 0.0400S) were examined in the as-cast, as-cast plus two hours at 2150°F, W.Q., and as-rolled and heat treated conditions. The treatment of two hours at 2150°F, W.Q., was employed to simulate the structure just prior to rolling.

Figure 34 illustrates the microstructures found. In the as-cast condition the tau-titanium sulfide in Heat 1379B occurred in a lamellar-eutectic pattern. It was generally interdendritic and intergranular, but

did not lie particularly in the grain boundaries - tending to fan out into the grains. In Heat 1380A the tau-sulfide had the same lamellar-eutectic appearance, but more closely associated with the grain boundaries. The differences in carbon content may account for the slight variation in microstructures. After exposing the materials to a temperature of 2150 °F for two hours, the difference in sulfide distribution was more obvious. The sulfides in the high sulfur-high carbon material, Heat 1379B, seemed unaffected, while the sulfides in the high sulfur-low carbon material, Heat 1380A, agglomerated and were distributed as globules in the grain boundaries. Note that the 2150°F treatment also dissolved the chromium carbides and γ'.

The reason for the increased cracking in the high sulfur-low carbon material then appeared to be the sulfide distribution; globules in the grain boundaries were more harmful than lamellae fanning out from them. Also, the unyielding nature of the sulfide itself may have been a factor. The agglomerated sulfide in the low carbon material did not change shape or size much on rolling (compare Fig. 34d with Fig. 34f), while the lamellar sulfide in the high carbon material was readily broken up into very small particles (compare Fig. 34c and Fig. 34e). Apparently the long thin lamellae were much easier to break up and tended to act less like crack initiators than the globules. A friable nature for tau-$Ti_4C_2S_2$ is certainly likely from the anisotropy and layer-like structure of its hexagonal lattice. Kudielka and Rohde [39] suggested separate layers of sulfur and carbon atoms in the tau-$Ti_4C_2S_2$ structure, and the Ti-S bonds may be fairly weak.

The microstructure of Heat 1349B (0.1510 percent sulfur) was examined for further information on the nature of the tau-titanium sulfide and how it reacted to rolling. The as-cast structure in Figure 35 shows the interdendritic precipitation of the lamellar sulfide phase (the white acicular phase is eta-Ni_3 Ti resulting from high titanium due to unexpectedly low sulfur recovery). Exposure at 2150°F for two hours did not affect

the sulfide, but tended to dissolve the other phases (Fig. 35c). Finally, rolling broke up the sulfide particles and re-distributed them rather uniformly in the wrought product (Fig. 35d). The rounded shapes of the sulfides in the as-rolled condition indicated that some spheroidization took place during rolling. It seems clear that the lack of influence that the large tau-$Ti_4 C_2 S_2$ lamellae had on hot working characteristics was due in part to their fragile nature.

20Cr-3.8Al-varied Ti Alloys

The 20Cr-3.8Al-1.2Ti, 20Cr-3.8Al-0.1Ti, and 20Cr- 3.8Al alloys all underwent corner cracking during the normal rolling operation at 2150°F, as shown in Figure 36. No differences were noted between heats of high and low sulfur contents; thus, there were no observable effects of sulfur. Sulfur effects might have been hidden, however, by the cracking tendencies of these alloys.

Evidently high aluminum was very detrimental to hot working properties, as these three alloys were more susceptible to cracking than the 20Cr-1.2Al-3.8Ti alloy discussed previously. Furthermore, titanium somehow improved the hot working properties of these high aluminum alloys. This is evident from comparing the as-rolled barstock of the three alloys in Figure 36. The 20Cr-3.8Al-1.2Ti alloy was less prone to cracking than two essentially titanium-free alloys. The reasons for the effects of titanium and aluminum will be considered in a subsequent section.

Boron and zirconium had no observable influence on the rolling characteristics of these alloys, as they cracked without or with these elements added (compare the A and B parts of each heat in Fig. 36).

Microstructural investigations were performed in search of an explanation for the severe cracking experienced by these alloys and what role sulfur might play. Again, a 2 hour exposure at 2150°F was used to simulate the structure present just before rolling. The sulfide in the

20Cr-3.8Al and 20Cr-3.8Al-0.1Ti alloys was identified as chromium sulfide and tau-$Ti_4C_2S_2$ was present in the 20Cr-3.8Al-1.2Ti alloy. Photomicrographs of the as-cast structures revealed the different solidification patterns of the two sulfides (Figs. 37b and 38b). The tau-$Ti_4C_2S_2$ had the characteristic lamellar appearance and was distributed along the grain boundaries (Fig. 37b). The chromium sulfide was globular and located in the grain boundaries within carbide films (Fig. 38b). After two hours at 2150°F, both sulfides tended to be associated with undissolved carbide particles, forming globules of the two phases.

The possible effects of the sulfides on cracking is not clear; but the presence of the undissolved carbides after the 2150°F treatment is in marked contrast to the easy solution of carbides in the high titanium alloy (Fig. 34c). As will be discussed in a subsequent section, the cracking tendencies of the high aluminum alloys seemed directly related to the undissolved carbides.

80Ni-20Cr Alloy

The effects of compositional variations on the rolling characteristics of the 80Ni-20Cr alloy are illustrated by the as-rolled barstock in Figure 39. Comparing the low and high sulfur heats without boron and zirconium added (Heats 1331A and 1332A), it is clear that high sulfur caused cracking. Moreover, comparing the two halves of the low sulfur heat, 1331A and 1331B, it is apparent that boron and zirconium induced cracking.

Microstructures of the as-cast and as-cast plus two hours at 2150°F, W.Q. conditions were studied to find the reasons for cracking (Fig. 40). Increased sulfur caused numerous large grain boundary sulfides to form on solidification (compare Figs. 40a with 40c). These sulfides were not affected much by the 2150°F exposure, only tending to assume a somewhat spherical shape. The increasing number of these large grain boun-

dary sulfides with increasing sulfur contents accounts for greater crack-
ing tendencies of the high sulfur material.

The reason for boron and zirconium inducing cracking was also
attributed to secondary grain boundary phases. More grain boundary pre-
cipitation was evident in the as-cast structure with these two elements
added (compare Figs. 40a and 40b). Furthermore, after the 2150°F ex-
posure simulating pre-rolling homogenization, a yellowish grain boun-
dary precipitate was seen in the boron and zirconium-containing material
and not in the other (compare Figs. 40d and 40e).

Unalloyed Nickel

No cracking was noted during or after rolling the nickel materials at
2000°F (Fig. 41). Thus, increasing sulfur from 0.0007 to 0.0067 per-
cent did not cause ceacking, nor did boron and zirconium have any ef-
fects. It is interesting to note that the severe sulfur embrittlement
found in rensile and creep-rupture properties at 1200°F was not evident
during hot rolling at 2000°F. This agrees with Kraai and Floreen's [12]
experiences with nickel at about the same sulfur levels. They suggested
that the lack of embrittlement was due to either the greatly increased
malleability or an increased sulfur solubility at the hot working tem-
peratures.

The Effect of Aluminum and Titanium Contents

Variations of the aluminum and titanium contents had the greatest
single effect on hot rolling characteristics noted during this investigation.
The alloys containing 3.8 percent aluminum and negligible titanium under-

went almost catastrophic cracking during rolling, while the 20Cr-1.2Al-3.8Ti alloy showed no tendency to crack under the same restricted rolling conditions. Moreover, adding 1.2 percent titanium to the 20Cr-3.8Al alloy greatly decreased the severity of cracking. The effect of increasing the titanium was then to improve the hot workability. This seems to be one explanation of the reasons why successful wrought alloys generally contain considerable amounts of titanium, while high aluminum alloys have been mainly limited to castings because of their limited hot workability.

Microstructural investigation immediately revealed that the lack of carbide solutioning before rolling was the most likely cause of the increased cracking in the high aluminum alloys. The as-cast structures (Figs. 37 and 38) had continuous grain boundary films of a chromium carbide. That this was chromium carbide was evident from an electron microprobe analysis of Heat 1327A showing that the grain boundary film, as pictured in Figure 38a, contained over 80 percent chromium and no other detectable element (the electron microprobe could not analyze for carbon). After two hours at 2150°F, which simulated the pre-rolling soak, the carbide films agglomerated into large blocky particles along the grain boundaries (Figs. 37c, 37d, 38c, and 38d). This was in marked contrast to the 20Cr-1.2Al-3.8Ti alloy, where the carbides went into solution after two hours at 2150°F (Fig. 34c). The fact that the carbides in the 20Cr-3.8Al-varied Ti alloys were never in solution during the entire rolling operation is shown by the structures after rolling where the large white carbide particles are distributed as stringers preferentially orientated parallel to the rolling direction (Figs. 37e, 37f, 38e, and 38f).

The heavy grain boundary carbide concentration in the high aluminum alloys during rolling then seems to account for the increased cracking, but it does not explain why the 20Cr-3.8Al-1.2Ti alloy was better than the 20Cr-3.8Al alloy. Quite obviously the titanium changes the solution

temperature of chromium carbide, but microstructural investigation did not indicate a difference between 20Cr-3.8Al and 20Cr-3.8Al-1.2Ti alloys in this respect (compare Figs. 37 and 38).

The Effects of Secondary Grain Boundary Phases
on Cracking Characteristics

If the results of the hot rolling study are evaluated in terms of a general tendency towards increased cracking, the presence of undissolved phases in grain boundaries of a solution treated cast ingot seems to be the major factor. This was arrived at because during breakdown of the cast structure a particular distribution of sulfides in the 20Cr-1.2Al-3.8Ti alloy caused cracking, undissolved carbides in the 20Cr-3.8Al-varied Ti alloys caused cracking, and sulfides and an unidentified precipitate associated with boron and zirconium in the 80Ni-20Cr alloy caused cracking. Combining the following set of conditions then generally accounts for the effects observed:

1. The highly alloyed face centered cubic structure of the alloys in question is inherently difficult to deform at high temperatures.

2. The columnar grain structure noted in all the ingots produces a condition of non-uniform deformation during hot rolling.

3. Combining conditions 1 and 2 results in severe grain boundary strains and a susceptibility to cracking along these boundaries during hot rolling.

4. Introducing a secon d phase into the grain boundaries increases their cracking tendencies by weakening them.

5. Increasing the amount or deformation resistance of the second phase further weakens the grain boundaries and cracking is commensurately easier to introduce.

6. Increasing the severity of the rolling operation by raising the deformation rate or decreasing the temperature for a given cast structure increases the tendency for the grain boundaries to crack.

One can then say that, under appropriate conditions, sulfides will induce cracking. Moreover, any other undissolved phase should do the same.

IDENTIFICATION OF SULFIDES

A summary of the results of sulfide identification is presented in Table VII according to alloy and method used. Where positive identifications were not accomplished, a prediction was made of the sulfide most likely to form. Tau-$Ti_4C_2S_2$ was the only sulfide found in the 20Cr-1.2Al-3.8Ti and 20Cr-3.8Al-1.2Ti alloys. A chromium sulfide formed in the 20Cr-3.8Al-0.1Ti, 20Cr-3.8Al, and 80Ni-20Cr alloys. A nickel sulfide was predicted in pure nickel on the basis of existing phase diagrams. However, for nickel with 0.045 percent zirconium added, a zirconium sulfide was predicted on the bases that zirconium lies among strong sulfide formers in the periodic table of elements, exhibits the ability to form a carbosulfide like titanium[39], and prevented sulfur embrittlement of nickel.

Of the methods available for minor phase identification, X-ray diffraction analysis of the extracted phase is one of the most positive. Only tau-$Ti_4C_2S_2$ could be identified in this manner; in all other cases no successful methods were found which would yield enough unreacted residue for proper analysis.

The tau-$Ti_4C_2S_2$ phase was readily extracted from all conditions of the 20Cr-1.2Al-3.8Ti and 20Cr-3.8Al-1.2Ti alloys, and in every case the X-ray diffraction patterns for tau exhibited more of the possible reflections than the patterns previously reported[32, 34, 39]. The pattern with the best line and intensity definition is presented in Table VIII along with Kudielka and Rohde's calculation[39] of possible reflections for tau-$Ti_4C_2S_2$. There were a number of weak reflections due to other phases in the experimental pattern that were deleted for the sake of clarity. There was excellent agreement between the experimental and calculated patterns for tau-$Ti_4C_2S_2$. The slight consistent deviation in "d" values was attributed to the small difference in lattice

50

parameters (see bottom of Table VIII).

The complete pattern obtained from a residue from Heat 1313A (0.0017S), the lowest sulfur heat of the 20Cr-1.2Al-3.8Ti alloy, is presented in Table IX. This pattern shows "extra" lines than can occur from second phases. Not only did the residue contain tau-phase, it also had a considerable amount of Ti(C, N) and some traces of Cr_7C_3, $Cr_{23}C_6$, and either γ or γ' in it. This particular pattern had the heaviest concentration of extra lines, most likely because the small amount of sulfide available in the alloy required that much material be dissolved to obtain sufficient residue for analysis. Nevertheless, the identification of the tau-phase was positive.

It was possible to distinguish between the visible sulfides using metallographic techniques. Tau-$Ti_4C_2S_2$ had a distinctive coloration of light rose-grey in unetched samples. However, the etches used for these types of alloys tend to stain and this can change the color of tau to reddish-grey, grey or even tan. Thus, color can be mis-leading. In cast material tau-$Ti_4C_2S_2$ was present as lamellar par-ticles (Figs. 34a, 34b, 35a, 35b, and 37b) and these lamellar particles were readily broken up on rolling (Figs. 34c and 35d). The most effec-tive method for recognizing tau-phase was through the use of polarized light. The phase is highly anisotropic and optically active (compare Figs. 42a and 42b). One again must be careful to avoid heavily stained samples as the stain can greatly change the sensitivity to polarized light. Also the orientation of particles is important because hexagonal crystals are isotropic when the "a" axis is parallel to the plane of polish. This isotropy was observed for some particles in every sample.

The chromium sulfide found in the 20Cr-3.8Al-0.1Ti, 20Cr-3.8Al and 80Ni-20Cr alloys was also distinctive and had decidedly different optical and morphological characteristics when compared to tau-$Ti_4C_2S_2$.

It was always a medium grey in color and sometime banded (Fig. 42c).
Examination under polarized light showed that it was not particularly
anisotropic, although some indication of optical activity was evident
(Fig. 42d). Moreover, the phase always tended to form as globules
in the grain boundaries during solidification (Figs. 38b and 40c), and
showed definite malleability by elongating during hot rolling (Fig. 38f
and 42c). Hall's description[7] of chromium sulfides in Inconel (14Cr-
7Fe-balance Ni) agrees very well with that presented here and the phases
sound identical.

In an effort to determine the composition of the sulfides encountered,
two electron microprobe studies were made; one with an instrument
capable only of stationary beam analyses and the other with an instru-
ment equipped with an electron beam scanning attachment capable of
producing concentration distribution images of an area of specimen sur-
face. The small size of the sulfide particles made the results from the
manual scanning semi-quantitative, since the beam overlapped and
possibly penetrated through the particles, hitting the matrix. Images
from the electron beam scan were only qualitative; but the results
were quite positive.

Figure 43 illustrates the results obtained on a large lamellar sul-
fide particle in a sample of as-cast Heat 1319A (0.0700S) of the 20Cr-
1.2Al-3.8Ti alloy. The back scattered electron image (Fig. 43a) gave
the distribution of elements according to atomic number, the higher the
atomic number the higher the intensity. Similar intensity images for
monochromatic sulfur K_α (Fig. 43b) and the titanium K_α (Fig. 43c)
radiation revealed the high concentration of titanium and sulfur in the
particle. The same thing was shown by four intensity profiles obtained
by a linear beam scan (Fig. 43d). The particle was obviously a titanium
sulfide.

Heat 1319A was also examined in the as-rolled condition. This time

the sulfide particles were small and in stringers as in Figure 7. The back scattered electron and characteristic X-ray images in Figure 44 again show the high titanium and sulfur concentrations in the particles. Semi-quantitative intensity profiles were obtained from a particle by moving the specimen at a set speed under the beam, and, as the particle was traversed, recording the characteristic X-ray intensities on a chart. These results (Fig. 45) clearly indicated the high titanium and sulfur concentrations as well as the decrease in chromium and nickel as the particle was traversed. Note that the particle was about one micron in width.

Results of a stationary analysis of sulfides in as-rolled Heat 1319A indicated the following:

Ti (%)		S (%)		Cr (%)	Ti (%)
28.2,	27.1	16.2,	18.5	7.5	50.2

The high concentrations of titanium and sulfur suggest a titanium sulfide while the high chromium and nickel contents show the matrix interference.

An electron microprobe study of the sulfide in Heat 1349B (0.1510 percent sulfur), both in situ and extracted, provided the following analyses:

Sample	Ti (%)	S (%)	Cr (%)	Ni (%)
sulfide in situ	30.1	22.4	7.3	30.4
sulfide extracted	51.2-57.8	22.0-38.2	3	3

The interference of the matrix is readily apparent from the high chromium and nickel contents indicated in the solid sample as compared with the low nickel and chromium levels in the extracted phase. The elimination of matrix interference by using the extracted phase certainly shows that the sulfide contained mainly titanium as a metallic element.

Figure 46 illustrates the results obtained from as-rolled samples of Heat 1333A of the 20Cr-3.8Al alloy (0.0320S) and Heat 1332A

of the 80 Ni - 20 Cr alloy (0. 0310S). The studies were made on large elongated sulfide particles similar to those in Figure 42c. The monochromatic X-ray intensity images (Figs. 46a and 46b) clearly revealed the high chromium and sulfur concentrations in these particles. The intensity profiles (Fig. 46c) showed the same and the lower nickel as well. The results for both alloys were identical and indicated the same phase in each. Results of stationary analyses indicated that the sulfides in these two alloys contained mostly chromium and sulfur; but accurate estimation of composition was not possible because of matrix interference:

Alloy	Heat	Cr (%)	S (%)	Ni (%)
20Cr-3.8Al	1333A	27.5	23.8	13.9
80Ni-20 Cr	1332A	40.3-44.8	21.2	17.9

The electron microprobe studies verify that tau-phase is a titanium sulfide and show that, in the absence of titanium, chromium sulfide forms. Unfortunately, the electron microprobes employed were not at the time capable of analyzing for carbon, so its presence in tau-phase was not verified.

THE STABILITY AND FORMATION OF TAU-$Ti_4C_2S_2$

Most wrought nickel-base superalloys contain at least one percent titanium[4] and the results of this investigation suggest that tau-$Ti_4C_2S_2$ would be likely to form in these materials. Thus, to enable a reasonable prediction of the role of sulfur in engineering alloys, the stability and effects of composition on the formation characteristics of tau-phase were evaluated.

After tau-phase once formed on solidification, it was remarkably stable. Prolonged exposures to high temperatures only caused the phase to agglomerate slightly; there was no observable tendency for it to dissolve. This held true up to the melting point, which was about 2400°F with boron and zirconium added and 2425°F without. Thus, it was concluded that no harmful solution and reprecipitation would occur at critical places, such as grain boundaries.

Alloy composition had a definite influence on the formation of tau-$Ti_4C_2S_2$. Experiments indirectly verified that the phase is a carbosulfide because it did not form at carbon levels estimated to be less than 0.01 percent. Moreover, experiments suggested that in nickel-base alloys chromium is necessary for tau-$Ti_4C_2S_2$ to form. The reasons for this were not clear, but the fact that nickel-base superalloys normally contain substantial amounts of chromium means that tau-phase would be one of the most likely sulfides to expect in these materials.

Stability of Tau-$Ti_4C_2S_2$

Normal processing procedures used in the investigation did little more than change the particle size and distribution of tau-phase. No tendency to dissolve was noted during the 2150°F pre-rolling homogenization, although tau did change shape in some cases (Figs. 34, 35, and 37). Rolling broke up the sulfide and redistributed it as stringers of

55

small particles (Figs. 34, 35, and 41). Subsequent heat treatments at 1975° and 1300°F had no observable effect on the phase. There were no significant differences in the X-ray diffraction patterns obtained on tau-phase extracted from as-cast and as-heat treated material (Table X).

Creep exposures of up to about 1000 hours at 1200° and 1500°F had no observable influence on tau-phase. It was not altered in appearance (Figs. 8, 9, and 15), nor structurally (Table X).

Attempts to dissolve tau-phase at high temperatures were unsuccessful, only some agglomeration was noted (Fig. 47). This was true right up to the melting point, which was about 2400°F with 0.0035 percent boron and 0.045 percent zirconium added and 2425°F without these elements added (Fig. 47). Sims[48] noted the same type of stability for MnS in steels. Moreover, he suggested that the titanium sulfide in steels is more stable than MnS.

Thus, at no time throughout this investigation was there any evidence that tau-phase could be dissolved and reprecipitated, and it required very high temperature exposures to even agglomerate slightly. One would not, then, expect any effects from this sulfide due to redistribution or massive particle growth during long-time high-temperature exposure.

Influence of Alloy Composition on the Formation of Tau-$Ti_4C_2S_2$

Four experimental heats were made to evaluate the influence of alloy composition on the formation of tau-$Ti_4C_2S_2$. Constant titanium and sulfur levels were used, while chromium and carbon were varied. The nominal compositions were as follows:

Heat	Cr (%)	Ti (%)	S (%)	C (%)	Ni
1393	20	1.0	0.10	0.06	balance
1394	20	1.0	0.10	<0.01	balance
1395	0	1.0	0.10	0.06	balance
1396	0	1.0	0.10	<0.01	balance

The as-cast structures of these heats (Fig. 48) suggested that tau-phase occurred only in the first alloy containing chromium, titanium, sulfur and carbon. The second alloy with nominally less than 0.01 percent carbon had a strikingly different sulfide eutectic. The last two alloys, without chromium, contained identical sulfides completely different in appearance from those in the first two. X-ray diffraction patterns of extracts from these alloys (Table XI) verified that Tau-$Ti_4C_2S_2$ was present in Heat 1393 and revealed than an unknown phase (or phases) was present in Heat 1394 and a second unknown phase (or phases) was present in both Heat 1395 and Heat 1396. The X-ray diffraction patterns for these two unknown phases have not previously been reported; but the ease with which they were extracted and the reactivity exhibited between titanium and sulfur seems to give good indication that they are titanium sulfides.

The results from this group of heats indirectly verified that carbon is essential to the formation of tau-$Ti_4C_2S_2$ and, furthermore, suggested that chromium is necessary in nickel-base alloys for tau to form. This requirement for chromium is puzzling because the phase has definitely been identified in chromium-free alloys by Kudielka and Rohde [39]. On the basis of finding a small amount of iron in extracted tau-phase, they suggested the formula $(Ti, Fe)_4C_2S_2$ might be more appropriate. However, the nickel-base alloys investigated here contained no iron and electron microprobe analyses indicated little, if any, chromium in tau-phase. Therefore it seems that there is insufficient evidence to explain just what the role of chromium is.

The possibility that the two unidentified sulfides found in this investigation might form in titanium-bearing nickel-base superalloys seems unlikely. Present alloys all contain sufficient chromium and carbon to force the formation of tau-$Ti_4C_2S_2$. The only other reason to suspect that tau might not form would be the possibility that other common alloy-

ing elements, such as manganese, molybdenum, tungsten, cobalt, columbium or vanadium might cause other sulfides to form. Amy[37] found tau-$Ti_4C_2S_2$ in Udimet 500, which nominally contains 0.08C-19Cr-19.5Co-4Mo-2.9Al-2.9Ti-4Fe-balance Ni. This would suggest that cobalt and molybdenum do not interfere with the formation of tau-phase. Of course manganese, the most notable sulfide former, might prevent the formation of tau by causing MnS to form. However, Koch and Artner[47] and Morrogh[42, 44] found that titanium sulfides formed in steels unless the manganese content exceeded the titanium. If the same held true in nickel-base alloys, tau would form since manganese contents are normally below titanium. If MnS did form, it would not be expected to introduce deleterious effects on creep-rupture properties because it is seemingly as stable as tau-phase[48]. But MnS could increase cracking tendencies during hot working if it were to exhibit the tendency to form as globules on grain boundaries during solidification, as it does sometimes in steel[48].

LIMITATIONS OF RESULTS

The lack of influence from sulfur was rather striking in view of its general reputation of being harmful to nickel-base alloys. This situation suggests that the limitations of the results be emphasized rather than their generality.

The creep-rupture test conditions were sufficiently critical so as not to limit the results. They could only have been made more critical by extending the testing to longer time periods or to higher temperatures; but nothing in the results suggested that either approach would be likely to turn up an effect of sulfur where none had been found. The procedures accurately delineated the embrittlement of nickel by sulfur in the range of 0.0004 to 0.0067 percent. Moreover, the same test procedures were used by the author in a previous investigation[21] and adequately defined the harmful effects of as little as 0.0010 percent lead in the 20Cr-1.2Al-3.8Ti alloy.

A major limitation of the investigation was the lack of sensitivity of the method used to evaluate hot working characteristics. Visual observation of cracking is by no means quantitative. Furthermore, the results obtained cannot be directly applied to actual practice because of the limited rolling conditions used and the small size of the ingots. Full scale mill operations would be expected to introduce greater variations in temperature and deformation rates than those experienced in this investigation. Larger ingots would certainly introduce the problem of macrosegregation, which could easily intensify the effects of sulfur on hot working characteristics. Nevertheless, the effects noted in the work may suggest some answers to problems encountered in engineering practice.

Due to sulfide stability, the heat treatments given the alloys limited the results only with respect to effects other than from sulfur. Thus, general improvement from boron and zirconium, the influence of carbon

59

on the 20Cr-1.2Al-3.8Ti alloy, the ductility effect in the high alum-
inum alloys, and the strength differences noted by changing the titan-
ium and aluminum contents are subject to some qualification. How-
ever, the heat treatment given the aluminum and titanium-bearing
alloys is one that is successfully used for many nickel-base alloys
strengthened by the precipitation of γ'.

The range of sulfur contents investigated does not seem to be a
limitation. The maximum allowable sulfur level in engineering alloys
is 0.03 percent and this was exceeded in every case where sulfur was
not found to be harmful. Sulfur in the alloys containing chromium could
have been carried to levels lower than those investigated, but the broad
range of sulfur contents studied together with the marked ability of
titanium and chromium to form stable sulfides gave no indication that
an improvement would result from even completely eliminating sulfur.

The possibility that alloying elements other than those considered
in this investigation might somehow change the influence of sulfur in
more complex alloys certainly exists. But if these elements were re-
active enough to prevent the formation of the titanium and chromium
sulfides noted in this study, it seems logical to think that the phases
formed would be stable and innocuous.

Finally, the properties measured in the investigation were a limit-
ation. This must be strongly emphasized to place them in their proper
perspective. Sulfide inclusions can certainly influence properties such
as fatigue and impact strength. Preferred orientation of tau-$Ti_4C_2S_2$
particles has been definitely established as a primary factor when low
short-transverse impact strength occurs in maraging steel plate[31].

CONCLUSIONS

Sulfur in the range of approximately 0.0020 to 0.0700 percent had no detectable influence on the creep-rupture properties of five Ni-Cr-Al-Ti, Ni-Cr-Al, and Ni-Cr alloys at 1200° and 1500°F. Boron and zirconium additions invariably improved the creep-rupture properties of these alloys without relation to sulfur content.

Increasing the sulfur from 0.0004 to 0.0067 percent severely reduced the creep-rupture and tensile properties of unalloyed nickel at 1200°F. Adding zirconium or boron and zirconium to nickel prevented sulfur embrittlement and further improved properties.

The lack of sulfur effects on the creep-rupture properties of the alloys was due to the formation of stable sulfide compounds that did not interfere with creep and fracture mechanisms. The formation of these compounds essentially removed sulfur from locations where it could have been damaging. Titanium and carbon reacted with sulfur to form $tau-Ti_4 C_2 S_2$. In the ansence of titanium, chromium reacted with sulfur to form a chromium sulfide. Zirconium in nickel apparently acted in a like manner by combining with sulfur to prevent the formation of embrittling grain boundary films.

In contrast to sulfur, carbon had a marked effect on the properties of a Ni-Cr-Al-Ti alloy. Low carbon led to decreased creep-rupture strength and ductility, while carbon contents of 0.05 percent or above provided good and reproducible properties. The effect of carbon was related to the influence of carbide distribution on the grain boundary reactions that occurred during creep.

A difference in rupture ductility at 1500°F was noted between heats of high aluminum alloys. This was apparently caused by unusually extensive carbide reactions which were an ultimate result of the effect of aluminum on carbide solution temperature.

A 20Cr-1.2Al-3.8Ti alloy had substantially better creep-rupture properites than a 20Cr-3.8Al-1.2Ti alloy. The superior strength of the high titanium alloy was related in part to a greater difference between the lattice parameters of the matrix and the strengthening precipitate γ'-Ni$_3$ (Al, Ti).

Aluminum and titanium contents had more influence than sulfur on cracking tendencies during hot rolling. Undissolved carbides associated with high aluminum contents induced severe cracking during breakdown of the cast structure. The carbides in a high titanium alloy were in solution with a resultant marked reduction in cracking. However, high sulfur did increase the susceptibility to cracking in the high titanium alloy, as became evident when the severity of rolling was increased. Sulfur was also detrimental to a Ni-Cr alloy. Boron and zirconium additions had no beneficial effects and even induced cracking in one alloy.

Cracking sensitivity was related to the number and nature of undissolved second phase particles remaining in the grain boundaries of cast ingots after the heating prior to rolling.

Sulfur does increase cracking during hot working. Therefore, even though sulfur does not affect creep-rupture properties, it is still essential to control sulfur in the production of nickel-base alloys. Under large-scale production conditions, the increased ingot size, segregation, and the more severe working procedures would intensify sulfur effects.

REFERENCES

1. Grubb, L. E.: "The Melting and Casting of Nickel and Nickel Alloys", Metals Handbook, 1948 Ed., Cleveland, ASM, 1948, p. 1027.

2. Bieber, C. G. and Decker, R. F.: "The Melting of Malleable Nickel and Nickel Alloys", Trans. AIME, Vol. 221, June 1961, pp. 629-636.

3. Bieber, C. G.: "Creative Metallurgy", Met. Eng. Quarterly, Vol. 1, Nov. 1961, pp. 92-108.

4. Lund, C. H.: "Physical Metallurgy of Nickel-Base Superalloys", DMIC Report 153, Battelle Memorial Institute, May 5, 1961.

5. Pridantsev, M. and Estalin, T. E.: "Influence of Impurities on the Properties of High Temperature Strength Nickel-Chromium Alloys", Henry Brutcher Translation No. 4088, 1958 (translated from Stahl', Vol. 17, 1957, pp. 636-64).

6. Khimushin, T. T.: "Heat Resistant Steels and Alloys for Gas Turbines", Chem. Abstracts, Vol. 54, 25 July, 1960, col. 11925c (abstracted from Sovremennye Spluvy i ikh Termichesk, Oct. 1958, p. 216).

7. Hall, A. M.: "Sulfides in Nickel and Nickel Alloys", Trans. AIME, Vol. 152, 1943, pp. 278-284.

8. Merica, P. D. and Waltenberg, R. T.: "The Malleability of Nickel", Trans. AIME, Vol. 71, 1925, pp. 709-719.

9. Rogelberg, I. L. and Shpichinettskie, E. S.: "Brittleness of Pure Nickel", Chem Abstracts, Vol. 54, 25 April, 1960, col. 7482g, (abstracted from Tsvetnye Metally, Vol. 28, 1955, pp. 63-66).

10. Rogelberg, I. L. and Shpichinettskie, E. S.: "Ductility of Nickel Containing Traces of Sulfur and Some Attempts to Desulfurize Nickel During Melting", Chem Abstracts, Vol. 52, 25 Nov., 1958, col. 19803d (abstracted from Tsvetnye Metally, Vol. 31, July 1958, pp. 61-65).

11. Olsen, K. M., Larkin, C. F. and Schmitt, P. N.: "Embrittlement of High Purity Nickel", Trans. ASM, Vol. 53, 1961, pp. 349-358.

12. Kraai, D. A. and Floreen, S.: "The Hot Ductility of Nickel", submitted for publication.

13. Decker, R. F., Rowe, J. P. and Freeman, J. W.: "Boron and Zirconium from Crucible Refractories in a Complex Heat-Resistant Alloy", NASA Report 1392, 1958.

14. Crawford, C. A.: Age-Hardenable Nickel-Chromium Alloys, New York, The International Nickel Company, Inc., 1959.

15. Bieber, C.: "The Melting and Hot Rolling of Nickel and Nickel Alloys", Metals Handbook, 1948 Ed., Cleveland, ASM, 1948, p. 1028.

16. Rhines, J. N.: "Nonferrous Metals", Effect of Residual Elements on the Properties of Metals, Cleveland, ASM, 1957, pp. 63-69.

17. Bradbury, E. J., Hancock, P. and Lewis, H.: "The Corrosion of Nickel-Base Material in Gas Turbine and Boiler Atmospheres", Metallurgia, Vol. 67, Jan. 1963, pp. 3-14.

18. Eash, J. I and Kihlgren, I. E.: "Effect of Composition on the Properties and Structure of Cast Metal", Trans. AFS, Vol. 57, 1949, pp. 535-544.

19. Peter, N. and Spitzer, H.: "Influence of Vacuum Melting and Some Trace Elements on the Behavior of a Heat Resisting Nickel-Base Alloy in Creep Testing", Archiv. F. d. Eisenhüttenwesen, Vol. 33, Nov. 1962, pp. 761-770 (German).

20. Wood, D. R. and Cook, R. M.: "Effects of Trace Contents of Impurity Elements on the Creep-Rupture Properties of Nickel-Base Alloys", Metallurgia, Vol. 67, Mar. 1963, pp. 109-117.

21. Schultz, J. W. and Freeman, J. W.: "The Effects of Lead on Two Ni-Cr-Ti-Al Alloys", unpublished report, University of Michigan, 1963.

22. Martin, D. L.: "Sulfur Embrittlement of Cobalt", Trans. AIME, Vol. 206, May 1956, pp. 578-579.

23. Ogawa, S. Y., King, T. B. and Grant, N. J.: "Deformation and Fracture Characteristics of Fe-S, Fe-S-O, and Fe-S-Mn Alloys At High Strain Rates and Temperatures", Trans. AIME, Vol. 224, Feb. 1962, pp. 12-18.

24. Josefsson, A., Koeneman, J. and Lagerberg, T.: "The Influence of Sulfur and Oxygen in Causing Red-Shortness in Steel", Journal of the Iron and Steel Institute, Vol. 191, Mar. 1959, pp. 240-249.

25. Anderson, S, Kimball, R. W. and Cuttoir, F. R.: "Effect of Various Elements on Hot-Working Characteristics and Physical Properties of Fe-C Alloys", Trans. AIME, Vol. 197, Apr. 1953, pp. 525-529.

26. Anderson, C. J. et al: "Forgeability of Steel with Varying Amounts of Manganese and Sulfur", Trans. AIME, Vol. 200, July 1954, pp. 835-837.

27. Urban, S. J. and Chipman, J.: "Nonmetallic Inclusions in Steels", "Part II Sulfides", Trans. ASM, Vol. 23, 1935, pp. 645-671.

28. Wright, J. A. and Quarrell, A. T.: "Effect of Chemical Composition on the Occurrence of Intergranular Fracture in Plain Carbon Steel Castings Containing Aluminum and Nitrogen", Journal of the Iron and Steel Institute, Vol. 200, Apr. 1962, pp. 299-307.

29. Franklin, A. T. and Tegart, W.: "Effect of Desulfurization on the Impact Properties of Some Low Alloy Steels", Journal of the Iron and Steel Institute, Vol. 202, July 1964, pp. 588-592.

30. Vogels, H. A. and Bruning, T.: "Influence of the Form of Non-Metallic Inclusions on the Mechanical Properties of Plates", Archiv. f. d. Eisenhüttenwesen, Vol. 35, No. 2, Feb. 1964, pp. 115-127, (German).

31. Novak, C. J. and Diran, L. M.: "What Are the Effects of Residual Elements in Maraging Steels", Journal of Metals, Mar. 1963, pp. 202-206.

32. Brown, J. T., Clark, W. D. and Parker, A.: "The Extraction of Minor Phases from Austenitic Steel", Metallurgia, Vol. 56, Nov. 1957, pp. 215-223.

33. Knop, O.: "The Identity of the Tau- and Y-Phases from Austenitic Steels", Metallurgia, Vol. 57, Mar. 1958, P. 137.

34. Gemmill, M. G., et al: "Study of 7% and 8% Chromium Creep-Resisting Steels", Journal of the Iron and Steel Institute, Vol. 184, Oct. 1956, p. 122.

35. Hagel, W. C. and Beattie, H. J., Jr.: "High Temperature Aging Structures in γ'-Hardened Austenitic Alloys", Trans. AIME, Vol. 215, Dec. 1959, pp. 967-975.

36. Kaufman, M. and Palty, A. E.: "Relationship of Structure to Mechanical Properties in Udimet 500", Trans. AIME, Vol. 218, Feb. 1960, pp. 107-116.

37. Amy, J.: "New Developments in the Electron Metallographic Study of Heat-Resistant Alloys", Ph. D. Thesis, University of Michigan, 1963.

38. Frick, C. and Rohde, H.: "Investigations of Odd Shaped Inclusions Containing Titanium and Sulfur in High Carbon Pig Iron Melts", Archiv. f. d. Eisenhüttenwesen, Vol. 31, July 1960, pp. 419-422 (German).

39. Kudielka, H. and Rohde, H.: "Structural Investigations of the Carbosulfides of Titanium and Zirconium", Z. Krist, Vol. 114, 1960, pp. 441-456, (German).

40. Blair, A. A. and Shimer, P. W.: "A Crystalline Sulfide in Pig Iron", Trans. AIME, Vol. 31, 1901, pp. 748-752.

41. Portevin, A. M. and Castro, R.: "Morphology of the Inclusions in Siderurgical Products, Parts IV and V", Journal of the Iron and Steel Institute, Vol. 135, 1937, pp. 223.

42. Morrogh, H.: "The Metallography of Inclusions in Cast Irons and Pig Irons", Journal of the Iron and Steel Institute, Vol. 143, 1941, pp. 207-253.

43. Roadley, J. A.: "Joint Correspondence", Journal of the Iron and Steel Institute, Vol. 143, 1941, pp. 264-268.

44. Morrogh, H.: "Author's Reply", Journal of the Iron and Steel Institute, Vol. 143, pp. 275-286.

45. Sims, C. E., Saller, H. A. and Boulger, F. W.: "Effects of Various Deoxidizers on the Structures of Sulfide Inclusions", Trans. AFS, Vol. 57, 1949, pp. 233-247.

46. Fishel, W. P., Roc, W. P. and Ellis, J. F.: "Desulfurizing Action of Titanium in Steels", Trans. AIME, Vol. 191, Aug. 1951, pp. 674-676.

47. Koch, W. and Artner, E.: "Contribution to the Isolation of Sulfides in Steels", Archiv. f.d. Eisenhüttenwesen, Vol. 29, Dec. 1958, pp. 737-744, (German).

48. Sims, C. E.: "The Nonmetallic Constituents of Steel", Trans. AIME, Vol. 215, June 1959, pp. 367-393.

49. Woodfine, B. C. and Quarrell, A. T.: "Effect of Al and N on the Occurrence of Intergranular Fracture in Steel Castings", Journal of the Iron and Steel Institute, Vol. 195, Aug. 1960, pp. 409-414.

50. Cochran, A. A. and Jensen, J. W.: "Autoradiography of Carbon and Sulfur in Titanium Steels", U. S. Bureau of Mines Reports of Investigations, No. 6122, 1962.

51. Decker, R. F.: "Phase Transformations in Nickel-Rich Nickel Titanium-Aluminum Alloys", Transcript of Presentations of a Research Seminar on High-Nickel Alloys for High Temperatures, New York, The International Nickel Company, Inc., 1960.

52. Olsen, K. M.: "Superpurity Nickel Melted Under Controlled Atmospheres", Metals Progress, Vol. 71, Sept. 1957, pp. 105-109.

53. Bigelow, W. C. and Amy, J. A.: "Electron Metallographic Studies of Nickel-Base Heat-Resistant Alloys", WADC TR No. 58-406, Aug. 1958.

54. Betteridge, W. and Franklin, A. N.: "The Effect of Heat Treatment and Structure on the Creep-Rupture Properties of Nimonic 80A", Journal of the Institute of Metals, Vol. 85, 1956-57, pp. 473-479.

55. Weaver, C. W.: "Influence of Heat Treatment and Composition on the Microstructure and Creep Behaviour of a Nimonic 80A-Type Alloy", Journal of the Institute of Metals, Vol. 88, 1959-60, pp. 462-467.

56. Heslop, J.: "Creep-Fracture in Nickel Chromium-Base Creep-Resistant Alloy", Journal of the Institute of Metals, Vol. 91, 1962-63, pp. 28-33.

57. Fleetwood, M. J.: "The Distribution of Chromium Around Grain Boundary Carbides in Nimonic 80A", Journal of the Institute of Metals, Vol. 90, July 1962, pp. 429-430.

58. Fell, E. A.: "The Effect of Thermal Treatment on the Constitution of 80-20 Nickel-Chromium Alloys Hardened With Titanium and Aluminum", Metallurgia, Vol. 63, April 1961, pp. 157-166.

59. Sundberg, D. V.: "Study of Gamma Prime in Experimental Nickel-Base Alloys", unpublished Master's Thesis, University of Michigan, 1964.

60. Nordheim, R. and Grant, N. J.: "Aging Characteristics of Nickel-Chromium Alloys Hardened with Titanium and Aluminum", Trans. AIME, Vol. 200, Feb. 1954, pp. 211-218.

61. Private Communication from R. C. Gibson, Paul D. Merica Research Laboratory, The International Nickel Company, Inc., Sterling Forest, Suffern, New York.

Table I

CHEMICAL COMPOSITION OF EXPERIMENTAL HEATS

(O, H and N reported in parts per million, others in weight percent)

20Cr-1.2Al-3.8Ti Alloy

Heat No.	Mode of Sulfur Addition	S	C	Cr	Al	Ti	B	Zr	Mg	Mn	Si	As	Sb	Pb	Bi	Cu	Fe	Sn	O	H	N
Aim Composition		(a)	0.06	20.0	1.2	3.8	(b)	(c)	LP	LP	LP	LP	LP	LP	LP	LP	LP	LP	LP	LP	LP
1289A	(d) and (g)	0.0024	0.05	20.18	1.28	4.07	<0.0010	<0.01	<0.01	<0.01	<0.01	ND	ND	T	ND	VW	W	ND	9.4	0.6	None
1289B		0.0022	0.04	20.36	1.31	4.03	0.0069	0.078	<0.01	<0.01	<0.01	ND	ND	T	ND	VW	W	ND	3.3	0.7	None
1313A	(d) and (g)	0.0017	0.10	20.17	1.01	3.67	<0.0016	<0.01	<0.01	<0.01	<0.01	ND	ND	T	ND	VW	W	ND			
1313B		0.0020	0.10	20.06	1.01	3.72	0.0020	0.03	<0.01	<0.01	<0.01	ND	ND	T	ND	VW	W	ND			
1247A	(e) and (g)	0.0035	0.024	20.94	1.12	3.42	0.0017	<0.01	VW			ND	T	ND	ND	VW		ND			
1247B		0.0028	0.024	20.94	1.12	3.41	0.0016	0.058	VW		0.033	ND	T	ND	ND	VW		VW			
1290A	(e) and (g)	0.0059	0.04	20.29	1.29	3.97	<0.0010	<0.01	<0.01	<0.01	0.013										
1290B		0.0043	0.04	20.29	1.30	4.03	0.0075	0.075	<0.01	<0.01	0.016										
1314A	(e) and (g)	0.0049	0.10	19.94	0.99	3.75	<0.0010	<0.01	<0.01	<0.01	0.014	ND	ND	T	ND	VW	W	ND	9.2	0.6	8.6
1314B		0.0089	0.10	19.85	1.01	3.70	0.0031	0.025	<0.01	<0.01	0.014	ND	ND	T	ND	VW	W	ND	8.2	0.7	6.1
1291A	(e), (g) and (h)	0.0145	0.04	20.41	1.27	4.05	0.0010	<0.01	<0.01	<0.01	0.013										
1291B		0.0162	0.04	20.35	1.26	3.85	0.0055	0.065	<0.01	<0.01	0.014										
1315A	(e), (g) and (h)	0.0092	0.10	20.00	0.92	3.70	<0.0010	<0.01	<0.01	<0.01	0.015	ND	ND	T	ND	VW	W	ND	7.7	0.6	6.8
1315B		0.0110	0.10	19.70	1.01	3.70	0.0048	0.031	<0.01	<0.01	0.012	ND	ND	T	ND	VW	W	ND	11.6	0.6	5.4
1316A	(e), (g) and (h)	0.0310	0.07	20.08	0.92	3.67	<0.0010	<0.01	<0.01	<0.01	0.012	ND	ND	T	ND	VW	W	ND	3.9	0.4	5.0
1316B		0.0300	0.08	19.90	0.96	3.63	0.0024	0.035	<0.01	<0.01	<0.01	ND	ND	T	ND	VW	W	ND	10.8	0.7	4.9
1317A	(e), (g) and (h)	0.0540	0.04	19.98	0.93	3.68	<0.0010	<0.01	<0.01	<0.01	0.015	ND	ND	T	ND	VW	W	ND	19.0	0.3	0.8
1317B		0.0550	0.04	19.92	0.92	3.68	0.0028	0.024	<0.01	<0.01	<0.01	ND	ND	T	ND	VW	W	ND	23.7	0.6	2.2
1319A	(e), (g) and (h)	0.0700	0.07	19.69	1.22	3.70	<0.0010	<0.01	<0.01	<0.01	0.021	ND	ND	T	ND	VW	W	ND	18.5	0.6	10.8
1319B		0.0640	0.06	19.69	1.13	3.62	0.0068	0.067	<0.01	<0.01	0.023	ND	ND	T	ND	VW	W	ND	20.5	0.6	11.2
1384B	(e) and (g)	0.0055	0.09	19.9	1.23	3.88	0.0075	0.057			0.051										
1379B	(e), (g) and (h)	0.0400	0.06	19.6	1.20	3.90	0.0072	0.057			0.043										
1383A	(e) and (g)	0.0043	0.037	20.0	1.31	3.72	ND	ND	<0.001		0.039										
1383B		0.0053	0.022	19.9	1.23	3.77	0.0060	0.049	<0.001		0.034										
1380A	(e), (g) and (h)	0.0310	0.017	19.9	1.20	3.80	ND	ND			0.037										
1380B		0.0293	0.014	19.9	1.18	3.69	0.0057	0.046			0.046										
1349B	(e), (g) and (h)	0.1510	0.06	19.3	1.00	5.5	0.0060	0.051	<0.001		0.020										

(a) Sulfur varied intentionally

(b) 0.0035% boron added to B ingot of each heat

(c) 0.045% zirconium added to B ingot of each heat

(d) Using Elchrome chromium

(e) Using Shieldalloy chromium

(f) Using UHP nickel

(g) Using Mond nickel shot

(h) Adding sulfur as NiS

LP - Low as possible

W - Weak - 0.01 to 0.1%

VW - Very weak - 0.001 to 0.01%

T - Trace - 0.0001 to 0.001%

ND - Element not detected

Table I (continued)

Heat No.	Mode of Sulfur Addition	S	C	Cr	Al	Ti	B	Zr	Mg	Mn	Si	As	Sb	Pb	Bi	Cu	Fe	Sn	O	H	N
20Cr-3.8Al-1.2Ti Alloy																					
Aim Composition	(a)		0.06	20.0	3.8	1.2	(b)	(c)	LP	LP	LP.	LP	LP	LP	LP	LP	LP	LP	LP	LP	LP
1329A	(e) and (g)	0.0066	0.11	19.15	3.60	1.21	<0.0010	<0.01	<0.01	<0.01	0.022	ND	ND	T	ND	VW	W	ND	136	0.6	60
1329B		0.0070	0.10	21.00	4.00	1.17	0.0036	0.030	<0.01	<0.01	0.022	ND	ND	T	ND	VW	W	ND			
1335A	(e), (g) and (h)	0.0330	0.09	21.03	4.35	1.20	0.0010	<0.01	<0.01	<0.01	0.021	ND	ND	T	ND	VW	W	ND	23.6	0.6	40
1335B		0.0320	0.09	20.95	4.35	1.18	0.0040	0.025	<0.01	<0.01	0.021	ND	ND	T	ND	VW	W	ND			
20Cr-3.8Al-0.1Ti Alloy																					
Aim Composition	(a)		0.06	20.0	3.8	0.1	(b)	(c)	LP	LP	LP	LP	LP	LP	LP	LP	LP	LP	LP	LP	LP
1328A	(e) and (g)	0.0070	0.10	21.53	3.95	0.10	0.0010	<0.01	<0.01	<0.01	0.016	ND	ND	T	ND	VW	W	ND			
1328B		0.0060	0.08	21.54	4.02	<0.10	0.0039	0.031	<0.01	<0.01	0.019	ND	ND	T	ND	VW	W	ND			
1334A	(e), (g) and (h)	0.0410	0.07	21.40	4.25	<0.10	0.0010	<0.01	<0.01	<0.01	0.018	ND	ND	T	ND	VW	W	ND			
1334B		0.0370	0.07	21.43	4.27	<0.10	0.0030	0.031	<0.01	<0.01	0.016	ND	ND	T	ND	VW	W	ND			
20Cr-3.8Al Alloy																					
Aim Composition	(a)		0.06	20.0	3.8	LP	(b)	(c)	LP	LP	LP	LP	LP	LP	LP	LP	LP	LP	LP	LP	LP
1327A	(e) and (g)	0.0080	0.09	19.15	3.60	<0.01	0.0010	<0.01	<0.01	<0.01	0.018	ND	ND	T	ND	W	W	ND			
1327B		0.0060	0.07	21.55	3.87	<0.10	0.0041	0.041	<0.01	<0.01	<0.01	ND	ND	T	ND	W	W	ND			
1333A	(e), (g) and (h)	0.0320	0.07	21.61	4.20	<0.10	0.0010	<0.01	<0.01	<0.01	0.018	ND	ND	T	ND	VW	W	ND			
1333B		0.0330	0.06	21.57	4.43	<0.10	0.0034	0.049	<0.01	<0.01	0.015	ND	ND	T	ND	VW	W	ND			
80Ni-20Cr Alloy																					
Aim Composition	(a)		0.06	20.0	LP	LP	(b)	(c)	LP	LP	LP	LP	LP	LP	LP	LP	LP	LP	LP	LP	LP
1331A	(e) and (g)	0.0080	0.06	21.64	<0.10	<0.10	0.0010	<0.01	<0.01	<0.01	0.010	ND	ND	T	ND	VW	W	ND	24.1	0.3	40
1331B		0.0070	0.05	19.31	0.042	<0.10	0.0034	0.032	<0.01	<0.01	0.011	ND	ND	T	ND	VW	W	ND			
1332A	(e), (g) and (h)	0.0310	0.09	21.97	<0.10	<0.10	0.0010	<0.01	<0.01	<0.01	<0.01	ND	ND	T	ND	VW	W	ND	71.5	0.5	20
1332B		0.0390	0.05	21.92	0.043	<0.10	0.0044	0.037	<0.01	<0.01	0.011	ND	ND	T	ND	VW	W	ND			
Nickel																					
Aim Composition		(a)	0.04	LP	LP	LP	(b)	(c)	LP	LP	LP	LP	LP	LP	LP	LP	LP	LP	LP	LP	LP
1346A	(f)	0.0004	0.036	0.004	0.023	<0.005	<0.0010	<0.005	<0.001	0.011	0.004	<0.005	<0.005	<0.005	<0.001	0.001	0.09	<0.001			
1346B		0.0007	0.033	0.005	0.028	<0.005	0.0034	0.034	<0.001	0.0085	0.006	<0.005	<0.005	<0.005	<0.001	0.003	0.10	<0.001			
1345A	(g)	0.0032	0.046	<0.001	0.020	<0.005	<0.0010	<0.005	<0.001	<0.001	0.002	<0.005	<0.005	<0.005	<0.001	0.003	0.014	<0.001			
1345B		0.0031	0.041	<0.001	0.027	<0.005	0.0029	0.040	<0.001	<0.001	0.002	<0.005	<0.005	<0.005	<0.001	0.003	0.014	<0.001			
1348A	(g) and (h)	0.0067	0.020	<0.001	0.021	<0.005	<0.0010	<0.005	<0.001	<0.001	0.002	<0.005	<0.005	<0.005	<0.001	0.008	0.016	<0.001			
1348B		0.0071	0.019	<0.001	0.025	<0.005	0.0023	0.020	<0.001	<0.001	0.003	<0.005	<0.005	<0.005	<0.001	0.004	0.018	<0.001			
1376 Zr	(g)	0.0022	0.04	0.0013	0.11	<0.005	<0.0010	0.016	<0.001	<0.001	0.0016	ND	<0.001	<0.001	<0.001	<0.001	0.015	<0.001			
1376 Zr+S	(g) and (h)	0.0067	0.05	0.0066	0.12	<0.005	<0.0010	0.012	<0.001	<0.001	0.0022	ND	<0.001	<0.001	<0.001	<0.001	0.032	<0.001			
1377B	(g)	0.0044	0.042	0.0062	0.13	<0.005	<0.0010	0.0066	<0.001	<0.001	0.022	ND	<0.001	<0.001	<0.001	<0.001	0.022	<0.001			
1377B+S	(g) and (h)	0.0079	0.04	0.0038	0.11	<0.005	<0.0010	0.0050	<0.001	<0.001	0.0042	ND	<0.001	<0.001	<0.001	<0.001	0.029	<0.001			

(a) Sulfur varied intentionally

(b) 0.0035% boron added to B ingot of each heat

(c) 0.045% zirconium added to B ingot of each heat

(d) Using Elchrome chromium

(e) Using Shieldalloy chromium

(f) Using UHP nickel

(g) Using Mond nickel shot

(h) Adding sulfur as NiS

LP - Low as possible

W - Weak - 0.01 to 0.1%

VW - Very weak - 0.001 to 0.01%

T - Trace - 0.0001 to 0.001%

ND - Element not detected

Table II

CREEP-RUPTURE TEST DATA FOR THE 20Cr-1.2Al-3.8Ti ALLOY

	No Boron or Zirconium Added								0.0035% Boron and 0.045% Zirconium Added						
Heat	Sulfur Content (%)	Effective Carbon Content (%)	Temp. (°F)	Stress (psi)	Rupture Time (hours)	Elong. (%)	R.A. (%)	Heat	Sulfur Content (%)	Effective Carbon Content (%)	Temp. (°F)	Stress (psi)	Rupture Time (hours)	Elong. (%)	R.A. (%)

Heats Made with Elchrome Chromium - No Sulfur Added

Heat	Sulfur (%)	Eff. Carbon (%)	Temp. (°F)	Stress (psi)	Rupture Time (hours)	Elong. (%)	R.A. (%)	Heat	Sulfur (%)	Eff. Carbon (%)	Temp. (°F)	Stress (psi)	Rupture Time (hours)	Elong. (%)	R.A. (%)
1289A	0.0024	0.049	1200	90,000	32.7	2	5	1289B	0.0022	0.039	1200	110,000	47.6	3	8
				80,000	64.7	2	4					105,000	66.2	3	7
				70,000	118.3	2	2					100,000	106.5	3	7
				65,000	207.3	2	2					90,000	740.7	3	4
				50,000	701.0	2	2								
			1500	30,000	25.1	3	4				1500	50,000	16.6	12	20
				25,000	50.6	2	2					40,000	54.3	14	18
				20,000	89.7	6	6					35,000	115.9	15	19
				20,000	146.3	3	6					30,000	195.1	12	17
				15,000	199.6	22	20					25,000	464.1	20	23
1313A	0.0017	0.099	1200	90,000	47.5	3	5	1313B	0.0020	0.099	1200	120,000	25.5	7	11
				70,000	145.1	2	3					100,000	145.7	6	8
				55,000	425.8	3	3								
			1500	35,000	16.0	5	5				1500	35,000	89.1	14	20
				25,000	103.0	7	6					25,000	430.8	19	24
				15,000	795.5	26	22								

Heats Made with Shieldalloy Chromium - No Sulfur Added

Heat	Sulfur (%)	Eff. Carbon (%)	Temp. (°F)	Stress (psi)	Rupture Time (hours)	Elong. (%)	R.A. (%)	Heat	Sulfur (%)	Eff. Carbon (%)	Temp. (°F)	Stress (psi)	Rupture Time (hours)	Elong. (%)	R.A. (%)
1247A	0.0035	0.023	1200	87,000	15.2	3	4	1247B	0.0028	0.023	1200	110,000	18.3	3	8
				87,000	19.2*	-	-					100,000	12.4	3	9
				87,000	12.8	4	7					90,000	374.5	2	5
				78,000	65.0	2	3					87,000	196.7	3	9
				70,000	62.4	3	7								
				60,000	328.0	<1	3								
				50,000	1790.9	1	2								
			1500	30,000	43.0	2	<1				1500	40,000	45.7	6	10
				26,000	110.8	2	3					34,000	112.7	9	12
				15,000	1924.3	5	3					26,000	407.4	10	12
1290A	0.0059	0.038	1200	90,000	9.7	2	6	1290B	0.0043	0.038	1200	110,000	40.3	2	8
				80,000	91.0	2	5					100,000	14.9	<1	6
				70,000	57.6	2	6					95,000	344.4	2	4
				70,000	177.1	1	4					90,000	412.7	3	5
				60,000	562.6	1	3								
			1500	30,000	35.2	<1	1				1500	50,000	17.6	6	11
				25,000	125.3	2	1					40,000.	65.4	7	6
				20,000	187.1	3	2					35,000	153.0	6	8
				20,000	180.5	5	4					30,000	316.0	8	9
				15,000	1348.3	-	4					25,000	797.4	11	12
1314A	0.0049	0.098	1200	90,000	59.1	3	3	1314B	0.0089	0.097	1200	120,000	18.4	10	13
				70,000	302.0	2	2					100,000	182.5	8	10
				60,000	364.2	2	4					90,000	644.3	5	7
			1500	40,000	9.6	3.	3				1500	50,000	12.2	15	20
				25,000	105.7	-	7					35,000	97.3	13	20
				15,000	758.9	21	21					25,000	487.5	19	26

Heats Made with Shieldalloy Chromium - Sulfur Added

Heat	Sulfur (%)	Eff. Carbon (%)	Temp. (°F)	Stress (psi)	Rupture Time (hours)	Elong. (%)	R.A. (%)	Heat	Sulfur (%)	Eff. Carbon (%)	Temp. (°F)	Stress (psi)	Rupture Time (hours)	Elong. (%)	R.A. (%)
1291A	0.0145	0.035	1200	100,000	15.0	2	8	1291B	0.0162	0.034	1200	110,0u0	24.7	3	8
				90,000	34.4	2	6					105,000	69.7	3	7
				80,000	46.6	<1	6					100,000	98.8	2	7
				70,000	244.8	2	6					90,000	310.7	2	6
			1500	30,000	30.2	2	2				1500	50,000	12.9	11	12
				25,000	69.2	<1	<1					40,000	59.0	9	12
				20,000	132.4	2	<1					35,000	108.5	9	12
				20,000	224.4	2	2					30,000	215.6	10	16
				15,000	836.4	9	7					25,000	648.0	17	17
1315A	0.0092	0.096	1200	90,000	61.7	3	5	1315B	0.0110	0.096	1200	120,000	15.8	7	11
				70,000	247.1	3	2					100,000	158.7	6	8
				60,000	537.1	2	2					90,000	444.9	5	9
			1500	40,000	7.5	6	6				1500	50,000	11.1	14	24
				25,000	106.8	7	8					35,000	89.4	15	21
				15,000	721.1	27	24					25,000	481.0	18	25
1316A	0.0310	0.058	1200	110,000	9.4	3	6	1316B	0.0300	0.068	1200	120,000	14.4	8	10
				100,000	43.9	3	5					110,000	70.2	5	9
				80,000	204.3	2	4					100,000	220.9	6	8
				60,000	707.6	1	4					90,000	545.0	7	9
			1500	35,000	23.8	7	8				1500	50,000	13.1	15	21
				25,000	147.7	14	18					35,000	130.6	16	23
				15,000	884.9		27					25,000	440.9	19	23
1317A	0.0540	0.019	1200	110,000	3.3	3	10	1317B	0.0550	0.019	1200	110,000	17.6	2	8
				90,000	55.6	2	3					100,000	76.2	4	7
				70,000	342.8	2.	4					90,000	196.8	2	8
				60,000	814.6	2	6					80,000	818.2	2	5
			1500	35,000	38.7	1	2				1500	50,000	13.2	7	10
				25,000	142.2	3	4					35,000	144.2	7	12
				15,000	1640.3	5	3					25,000	825.2	9	11
1319A	0.0700	0.043	1200	100,000	29.2	2	7	1319B	0.0640	0.035	1200	110,000	16.0	2	9
				80,000	288.5	2	4					100,000	46.1	2	8
				60,000	1045.0	2	3					90,000	588.4	3	7
			1500	40,000	11.7	4	5				1500	50,000	13.3	14	19
				25,000	118.2	5	6					35,000	92.4	13	21
				15,000	799.6	9	9					25,000	377.3	15	22

Heats Made with Intentionally Low Carbon - without and with Sulfur Added

Heat	Sulfur (%)	Eff. Carbon (%)	Temp. (°F)	Stress (psi)	Rupture Time (hours)	Elong. (%)	R.A. (%)	Heat	Sulfur (%)	Eff. Carbon (%)	Temp. (°F)	Stress (psi)	Rupture Time (hours)	Elong. (%)	R.A. (%)
1383A	0.0043	0.035	1200	80,000	16.2	2	6	1383B	0.0053	0.020	1200	100,000	21.0	2	8
				60,000	74.5	1	4					90,000	116.4	2	6
				45,000	1302.0	<1	2					80,000	40.0	2	8
			1500	25,000	9.5	2	2				1500	50,000	10.9	2	4
				20,000	136.8	<1	1					35,000	117.2	3	8
				15,000	1368.8	2	2					25,000	497.0	4	8
1380A	0.0310	0.005	1200	80,000	1.0	2	11	1380B	0.0293	0.003	1200	100,000	12.3	1	6
				60,000	16.0	<1	3					90,000	24.8	2	7
				45,000	60.1	1	2					75,000	85.0	1	5
			1500	25,000	0.8	1	<1				1500	50,000	0.6	<1	<1
				20,000	1.3	<1	1					35,000	33.7	2	2
				15,000	579.6	4	3					25,000	267.2	2	2

* - Fractured in Threads

Table III

CREEP-RUPTURE TEST DATA FOR THE 20Cr-3.8Al-VARIED Ti AND 80Ni-20Cr ALLOYS

	No Boron or Zirconium Added							0.0035% Boron and 0.045% Zirconium Added					
Heat	Sulfur Content (%)	Temp. (°F)	Stress (psi)	Rupture Time (hours)	Elong. (%)	R.A. (%)	Heat	Sulfur Content (%)	Temp. (°F)	Stress (psi)	Rupture Time (hours)	Elong. (%)	R.A. (%)
20Cr-3.8Al-1.2Ti Alloy													
1329A	0.0060	1200	70,000	7.9	<1	4	1329B	0.0070	1200	105,000	4.6	3	10
			50,000	82.3	<1	2				90,000	41.6	3	7
			40,000	281.1	2	2				80,000	121.4	3	5
										65,000	474.7	3	5
		1500	35,000	1.2	2	2			1500	35,000	17.6	10	11
			20,000	41.2	5	6				25,000	121.5	17	22
			15,000	168.9	15	13				18,000	546.5	37	43
			11,000	524.3	26	24				15,000	927.6	34	48
			9,000	748.0	33	28							
1335A	0.0330	1200	80,000	1.6	2	4	1335B	0.0320	1200	90,000	23.9	2	6
			50,000	83.3	2	3				80,000	84.9	2	6
			40,000	310.4	1	1				65,000	458.8	2	6
		1500	35,000	1.2	2	2			1500	45,000	2.5	5	5
			25,000	7.7	1	<1				35,000	10.9	6	6
			15,000	139.4	8	8				25,000	104.3	8	9
			11,000	437.4	17	15				18,000	331.4	21	15
			9,000	687.4	25	21				15,000	619.0	13	14
20Cr-3.8Al-0.1Ti Alloy													
1328A	0.0070	1200	80,000	3.0	.3	8	1328B	0.0060	1200	80,000	22.7	3	9
			60,000	18.4	<1	6				70,000	83.2	3	8
			50,000	117.7	2	4				60,000	363.2	4	4
			35,000	451.2	<1	2							
		1500	30,000	1.5	2	3			1500	30,000	15.1	16	17
			20,000	22.3	3	3				25,000	52.2	25	25
			15,000	127.0	9	9				20,000	110.7	35	47
			11,000	525.2	14	14				15,000	562.0	48	38
1334A	0.0410	1200	70,000	18.0	2	8	1334B	0.0370	1200	90,000	3.6	4	13
			60,000	24.2	<1	3				70,000	44.0	2	5
			50,000	61±9	<1	6				60,000	101.2	3	7
			40,000	171.5	<1	4				50,000	868.6	2	6
			30,000	937.9	1	2							
		1500	20,000	18.4	3	2			1500	30,000	10.4	7	7
			15,000	101.9	3	3				25,000	37.8	7	8
			11,000	440.8	7	7				20,000	151.0	5	6
										15,000	552.5	9	11
20Cr-3.8Al Alloy													
1327A	0.0080	1200	70,000	5.3	4	10	1327B	0.0060	1200	70,000	32.1	3	10
			50,000	71.8	2	8				60,000	151.5	3	6
			35,000	423.8	2	4				50,000	810.0	2	6
										50,000	237.4	2	8
										42,000	1780.9	2	4
		1500	30,000	2.7	2	4			1500	30,000	6.8	8	12
			20,000	21.5	2	4				25,000	32.8	14	18
			15,000	157.6	3	2				20,000	128.2	19	19
			11,000	793.7	6	5				15,000	548.4	23	34
1333A	0.0320	1200	70,000	8.4	2	9	1333B	0.0330	1200	80,000	5.4	5	9
			50,000	72.3	2	7				70,000	26.8	4	10
			35,000	904.1	1	4				60,000	69.4	2	8
										50,000	252.0	2	7
										42,000	1145.0	2	5
		1500	30,000	1.7	2	2			1500	35,000	2.7	6	7
			20,000	17.1	2	14				25,000	25.1	9	11
			15,000	123.2	3	3				20,000	99.0	9	9
			11,000	472±8	7	6				15,000	450.5	-	12
80Ni-20Cr Alloy													
1331A	0.0080	1200	40,000	7.0	16	20	1331B	0.0070	1200	40,000	8.8	·23	25
			25,000	70.9	11	12				25,000	194.4	45	46
			15,000	1526.9	14	18				19,000	1298.6	49	40
		1500	13,000	8.2	35	30			1500	10,000	50.0	70	69
			10,000	20.9	18	21				7,000	370.0	45	39
			7,000	76.8	18	15							
			4,000	1591.2	26	18							
1332A	0.0310	1200	40,000	5.9	16	18	1332B	0.0390	1200	40,000	12.2	42	38
			25,000	77.4	13	18				25,000	181.9	36	53
			15,000	1479.9	17	20				19,000	1129.5	50	47
		1500	13,000	5.5	26	25			1500	13,000	11.0	73	76
			10,000	33.0	34	26				10,000	46.3	65	64
			7,000	119.7	-	17				7,000	322.9	27	30
			4,000	1176.2	25	21							

Table IV

CREEP-RUPTURE TEST DATA FOR NICKEL AT 1200°F

	No Boron or Zirconium Added							0.0035% Boron and 0.045% Zirconium Added					
Heat	Sulfur Content (%)	Stress (psi)	Rupture Time (hours)	Min. Creep Rate (%/hour)	Elong. (%)	R.A. (%)	Heat	Sulfur Content (%)	Stress (psi)	Rupture Time (hours)	Min. Creep Rate (%/hour)	Elong. (%)	R.A. (%)
Heat Made with UHP Nickel - No Sulfur Added													
1346A	0.0004	16,000	0.6	48	52	81	1346B	0.0007	16,000	12.3	3.22	66	87
		12,000	16.7	<1.26	69	75			12,000	109‡8	0.225	75	90
		10,000	59‡8	-	54	87			9,000	731.9	0.038	83	81
		8,000	402.3	0.01	58	73							
		6,000	2480.0	0.0039	29	33							
Heat Made with Mond Nickel Shot - No Sulfur Added													
1345A	0.0032	12,000	0.3	>10	47	65	1345B	0.0031	18,000	3.0		66	92
		9,000	5.4	1.15	49	77			16,000	6.6	3.1	54	90
		7,000	54.6	0.11	36	80			12,000	94.2	0.24	66	94
		5,000	485.3	0.0143	28	59			9,000	799.1	0.03	71	72
Heat Made with Mond Nickel Shot - Sulfur Added													
1348A	0.0067	12,000	broke on loading		3	2	1348B	0.0071	16,000	8.5‡2	2.0	67	93
		3,000	0.07	>10	<1	<1			12,000	20.7	<0.7	27	42
		2,250	31.9	0.05	3	3			10,000	333.4	0.076	75	90
		1,500	>4708.6*		25*	10*			8,000	1766.1	0.0112	62	64

Heats Made with Mond Nickel Shot - Split with Sulfur

	0.045% Zirconium Added							0.0035% Boron Added					
1376ZR	0.0022	15,000	14‡7	1.5	79	95	1377B	0.0044	15,000	1.7		66	93
		12,000	76.0		58	94			12,000	15‡9		57	96
		9,000	595.0	0.031	52	73			9,000	245.1	0.055	53	94
1376ZR+S	0.0067	15,000	4.9	4.0	58	90	1377B+S	0.0079	9,000	1.6		14	20
		12,000	29.2		67	92			5,000	32.1	0.06	7	10
		9,000	289.3	0.059	63	92			3,000	248.3		12	13

* Test shut off, elongation and reduction of area measured on unbroken specimen

Table V

TENSILE TEST DATA FOR NICKEL AT 1200°F

Heat	Sulfur Content (%)	Tensile Strength (psi)	Elong (%)	R.A. (%)
Heat Made with UHP Nickel - No Sulfur Added				
1346A	0.0004	18,500	79	84
1346B	0.0007	24,600	56	92
Heat Made with Mond Nickel Shot - No Sulfur Added				
1345A	0.0032	14,600	67	92
1345B	0.0031	22,300	67	92
Heat Made with Mond Nickel Shot - Sulfur Added				
1348A	0.0067	9,100	4	5
1348B	0.0071	23,000	51	90
Heat Made with Mond Nickel Shot and 0.045% Zirconium - Split with Sulfur				
1376Zr	0.0022	22,300	62	93
1376Zr-S	0.0067	18,450	64	91
Heat Made with Mond Nickel Shot and 0.0035% Boron - Split with Sulfur				
1377B	0.0022	16,450	61	95
1377B-S	0.0067	13,780	31	42

TABLE VI

100-HOUR RUPTURE STRENGTH AND AVERAGE REDUCTION OF AREA
FOR THE 20Cr-1.2Al-3.8Ti ALLOY HEATS

Heat	Sulfur Content (%)	Carbon Content (%)	Effective Carbon Content (%)	1200°F 100-Hour Rupture Strength (psi)	1200°F Avg. Red. of Area (%)	1500°F 100-Hour Rupture Strength (psi)	1500°F Avg. Red. of Area (%)
1289A	0.0024	0.05	0.049	73,000	3	20,500	8
1289B	0.0022	0.04	0.039	102,000	7	36,000	19
1313A	0.0017	0.10	0.099	76,000	4	25,000	11
1313B	0.0020	0.10	0.099	104,000	10	34,000	22
1247A	0.0035	0.024	0.023	70,000	4	26,100	2
1247B	0.0028	0.024	0.023	96,000	8	34,500	11
1290A	0.0059	0.04	0.038	75,000	5	24,300	3
1290B	0.0043	0.04	0.038	101,000	6	37,500	9
1314A	0.0049	0.10	0.098	81,500	3	25,300	10
1314B	0.0089	0.10	0.097	106,000	10	34,500	22
1291A	0.0145	0.04	0.035	77,000	6	23,000	2
1291B	0.0162	0.04	0.034	99,500	7	35,500	14
1315A	0.0092	0.10	0.096	82,000	3	25,500	13
1315B	0.0110	0.10	0.096	104,000	9	34,000	23
1316A	0.0310	0.07	0.058	90,000	5	26,500	16
1316B	0.0300	0.08	0.068	107,000	9	36,500	23
1317A	0.0540	0.04	0.019	83,000	6	27,500	3
1317B	0.0550	0.04	0.019	96,000	7	37,000	11
1319A	0.0700	0.07	0.043	92,000	5	26,000	7
1319B	0.0640	0.06	0.035	99,000	8	34,500	21
Heats Made with Intentionally Low Carbon Contents							
1383A	0.0043	0.037	0.035	60,500	4	20,600	2
1383B	0.0053	0.022	0.020	82,000	7	36,000	7
1380A	0.0310	0.017	0.005	44,000	5	18,100	1
1380B	0.0293	0.014	0.003	73,000	6	30,000	1

75

TABLE VII

SUMMARY OF SULFIDE IDENTIFICATION

Results obtained by:

Alloy	X-ray Diffraction	Electron Microprobe	Metallography	Prediction
20Cr-1.2Al-3.8Ti	tau - $Ti_4C_2S_2$	titanium sulfide	tau - $Ti_4C_2S_2$	
20Cr-3.8Al-1.2Ti	tau - $Ti_4C_2S_2$	-	tau - $Ti_4C_2S_2$	
20Cr-3.8Al-0.1Ti	none	-	chromium sulfide	
20Cr-3.8Al	none	chromium sulfide	chromium sulfide	
80Ni-20Cr	none	chromium sulfide	chromium sulfide	
nickel (pure)	none	-	none	β-NiS at 1200°F
nickel + 0.045Zr	none	-	none	zirconium sulfide

TABLE VIII

COMPARISON OF CALCULATED AND EXPERIMENTAL X-RAY
DIFFRACTION DATA FOR TAU - $Ti_4C_2S_2$

Left panel:

hkl	Tau - $Ti_4C_2S_2$* d(A)	Io	Is	Tau-Phase Extracted from Heat 1335A d(A)	I
002	5.61	1.1	41.8	5.60	5
004	2.80	5.4	5.3		
100	2.78	62.7	23.9	2.77	60
101	2.70	6.6	23.7	2.69	20
102	2.492	7.5	15.4	2.463	50
103	2.232	262.4	211.0	2.224	100
104	1.974	11.9	33.4	1.968	15
006	1.867	20.8	11.8	1.864	20
105	1.745	7.1	2.6	1.741	10
110	1.607	64.7	64.7	1.601	70
106	1.550	13.2	30.9	1.548	30
112	1.544	0.2	5.3		
008	1.400	3.4	3.4	1.399	2
114	1.394	3.9	3.8		
200	1.391	6.3	2.7		
107	1.387	8.6	13.4	1.386	25
201	1.380	1.1	3.1		
202	1.350	0.5	1.3		
203	1.304	40.6	32.5	1.299	50
108	1.251	1.4	0		
204	1.246	2.4	7.34	1.242	7
116	1.219	32.5	17.9	1.214	50
205	1.182	2.4	0.8	1.177	1 diffuse
109	1.136	18.4	13.5	1.134	20
0010	1.120	1.9	3.9		
206	1.116	11.7	14.4	1.113	15
118	1.056	13.3	13.6		
210	1.052	8.8	3.5		
207	1.050	5.4	8.7	1.049	15
211	1.046	1.3	4.1		

a = 3.21A;   c = 11.20A

Right panel:

hkl	Tau - $Ti_4C_2S_2$ d(A)	Io	Is	Tau-Phase Extracted from Heats 1335A d(A)	I
1010	1.041	1.0	0.4	1.008	50
212	1.034	0.9	2.1	1.008	20
213	1.011	73.2	58.2		
208	0.986	1.60	0	0.981	1 diffuse
214	0.984	5.5	16.5	0.954	15
1011	0.956	22.3	15.9	0.949	10
215	0.951	7.3	2.5	0.933	1 diffuse
0012	0.932	4.4	5.6	0.924	20
209	0.927	38.4	28.4	0.924	7
300	0.927	56.2	56.7		
301	0.923	0	0		
1110	0.918	28.9	57.7	0.917	5
216	0.916	62.8	76.2	0.914	10
302	0.914	0.1	7.1	0.911	5
1012				0.884	1 diffuse
304, 2010				0.876	5
0013				0.876	2
306				0.867	1
2011				0.828	20
				0.828	10
1112				0.820	15
				0.820	7
0014				0.806	15
				0.806	7
				0.8005	30
				0.8005	10

a = 3.20A;   c = 11.19A

* - Derived by Kudielka and Rhode [39].

Table IX

X-RAY DIFFRACTION IDENTIFICATION OF TAU-$Ti_4C_2S_2$ IN LOW SULFUR HEAT OF THE 20CR-1.2Al-3.8Ti ALLOY

Residue from Heat 1313A (0.0017%S)		Reflections Assigned To:				
d (A)	I	tau-$Ti_4C_2S_2$	Ti(C, N)	Cr_7C_3	$Cr_{23}C_6$	γ or γ'
3.65	1					x
2.77	5	x				
2.69	2	x				
2.489	95		x			
2.399	1				x	
2.224	30	x				
2.156	100		x			
2.049	2					x
2.046	2			x	x	
1.977	1	x				
1.866	1	x				
1.818	1			x	x	
1.690	2				x	
1.602	10	x				
1.549	2	x				
1.526	60		x			
1.437	1			x		
1.386	1			x		
1.302	40	x	x			
1.246	30		x			
1.216	2	x				
1.136	1	x				
1.008	5	x				
1.008	2	x				
0.991	20		x			
0.991	10		x			
0.966	40		x			
0.966	30		x			
0.882	40		x			
0.882	30		x			
0.832	30		x			
0.832	20		x			

Table X

X-RAY DIFFRACTION DATA FOR TAU-$Ti_4C_2S_2$ EXTRACTED
FROM DIFFERENT CONDITIONS OF HEAT 1319A
OF THE 20Cr-1.2Al-3.8Ti ALLOY

hkl	I*	As-Cast d (A)	As-Heat Treated d (A)	After 800 hr. Creep Exposure at 1500° F d (A)
100	40	2.78	2.77	2.77
101	10	2.69	2.69	2.69
102	20	2.497	2.476	2.482
103	100	2.227	2.222	2.223
104	15	1.970	1.965	1.966
006	30	1.865	1.861	1.860
105	10	1.742	1.740	1.739
110	60	1.600	1.599	1.598
106	40	1.546	1.546	1.545
107	30	1.384	1.385	1.385
203	50	1.299	1.300	1.298
116	40	1.214	1.215	1.214
109	30	1.135	1.135	1.135
206	5	1.114	1.114	1.113
118	5	1.055	1.055	1.054
207	5	1.048	1.049	1.048
213	50	1.009	1.009	1.009

* - Line intensities were essentially the same for all three patterns

Table XI

X-RAY DIFFRACTION DATA FOR SULFIDES EXTRACTED FROM Ni-Cr-Ti-S-C ALLOYS

	Aim Heat Composition				
Heat	Cr	Ti	S	C	Ni
1393	20	1.0	0.1	0.06	balance
1394	20	1.0	0.1	<0.01	balance
1395	0	1.0	0.1	0.06	balance
1396	0	1.0	0.1	<0.01	balance

Tau-$Ti_4C_2S_2$ from Heat 1393		Unidentified Phase from Heat 1394		Unidentified Phase from Heats 1395 and 1396	
d (A)*	I*	d (A)	I	d (A)	I
2.76	60	2.94	50	5.69	60
2.68	20	2.64	80	5.23	1
2.463	50	2.445	15	4.68	1
2.217	100	2.084	100	2.96	40
1.962	20	1.699	60	2.62	100
1.857	30	1.640	20	2.064	50
1.738	15	1.498	20	2.046	95
1.600	70	1.478	15	1.900	1
1.544	40	1.430	15	1.714	40
1.384	30	1.320	40	1.705	70
1.297	60	1.278	5	1.611	2
1.211	50	1.224	5	1.593	40
1.131	20	1.183	5	1.439	20
1.113	10	1.119	30	1.423	30
1.052	20	1.096	15	1.322	5
1.045	20	1.044	30	1.309	40
1.008	60			1.164	5
		plus 11 lines to 0.789		1.098	5
plus 10 lines to 0.800				1.092	40
				1.062	5
				1.048	5
				1.038	20

plus 8 lines to 0.785

* - Compare with data in Table VIII
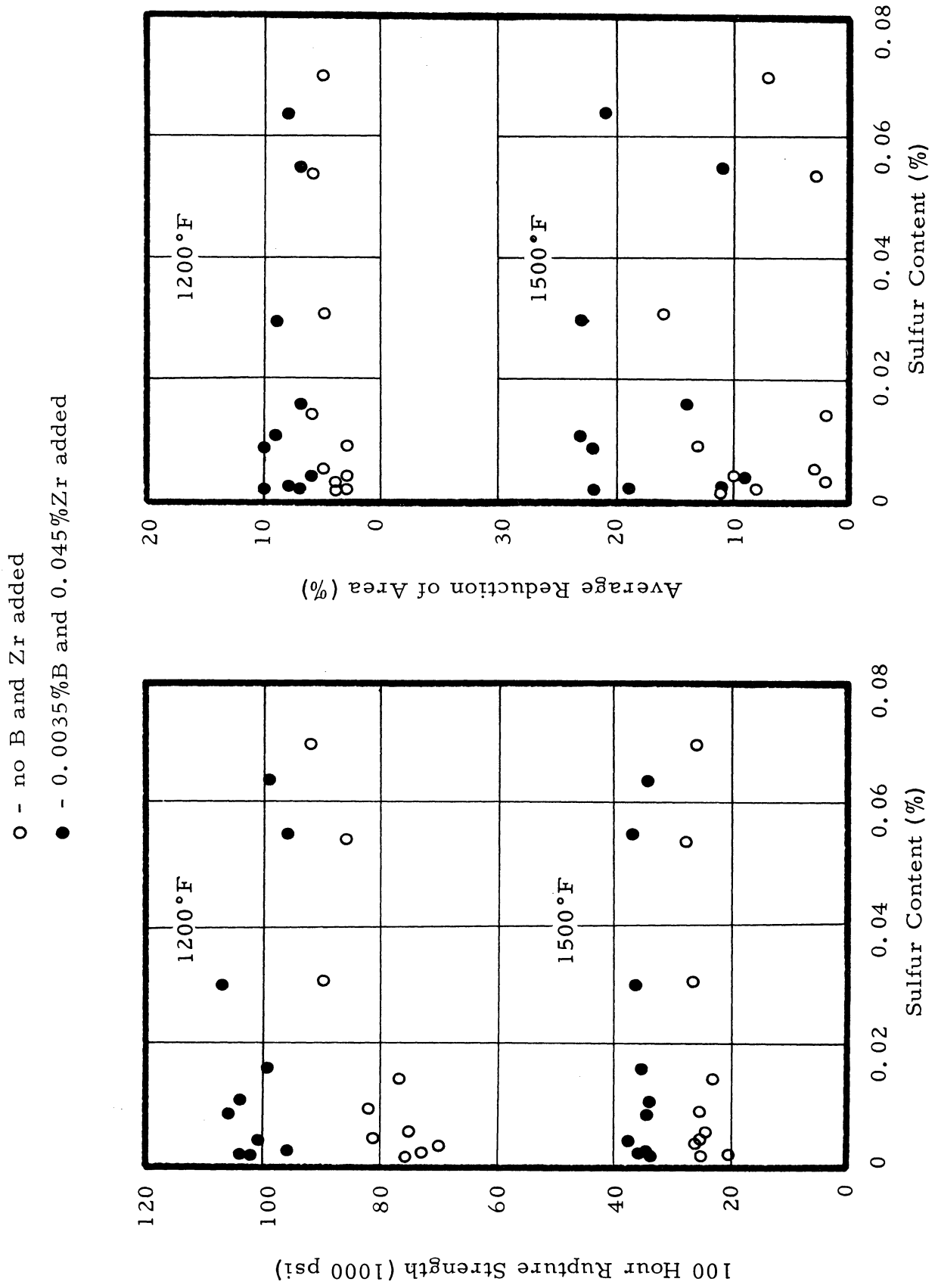
Figure 1. Relationships Between Creep-Rupture Properties and Sulfur Content for the 20Cr-1.2Al-3.8Ti Alloy at 1200° and 1500°F
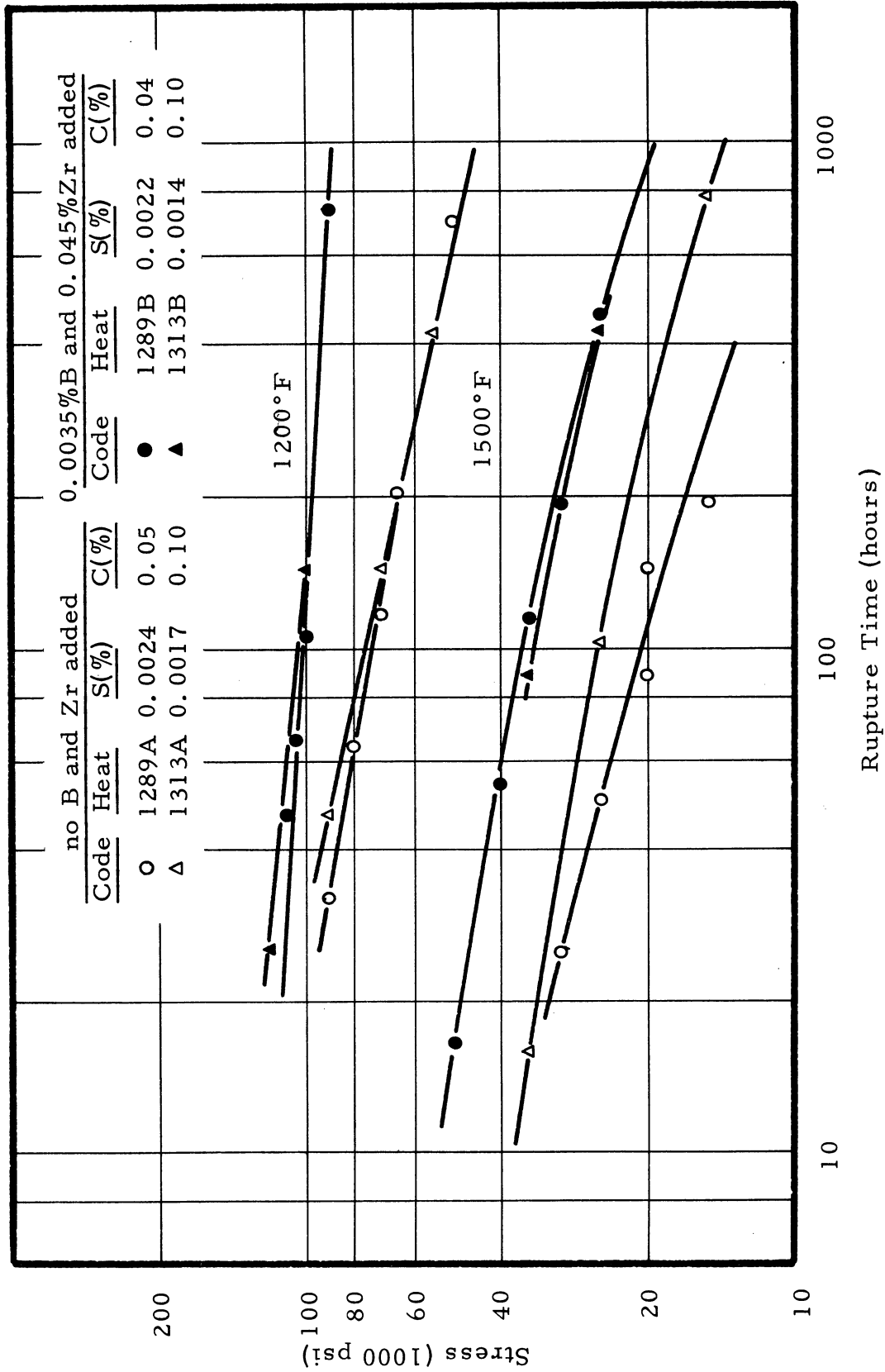
Figure 2. Stress-Rupture Time Curves for Very Low Sulfur Split Heats of the 20Cr-1.2Al-3.8Ti Alloy
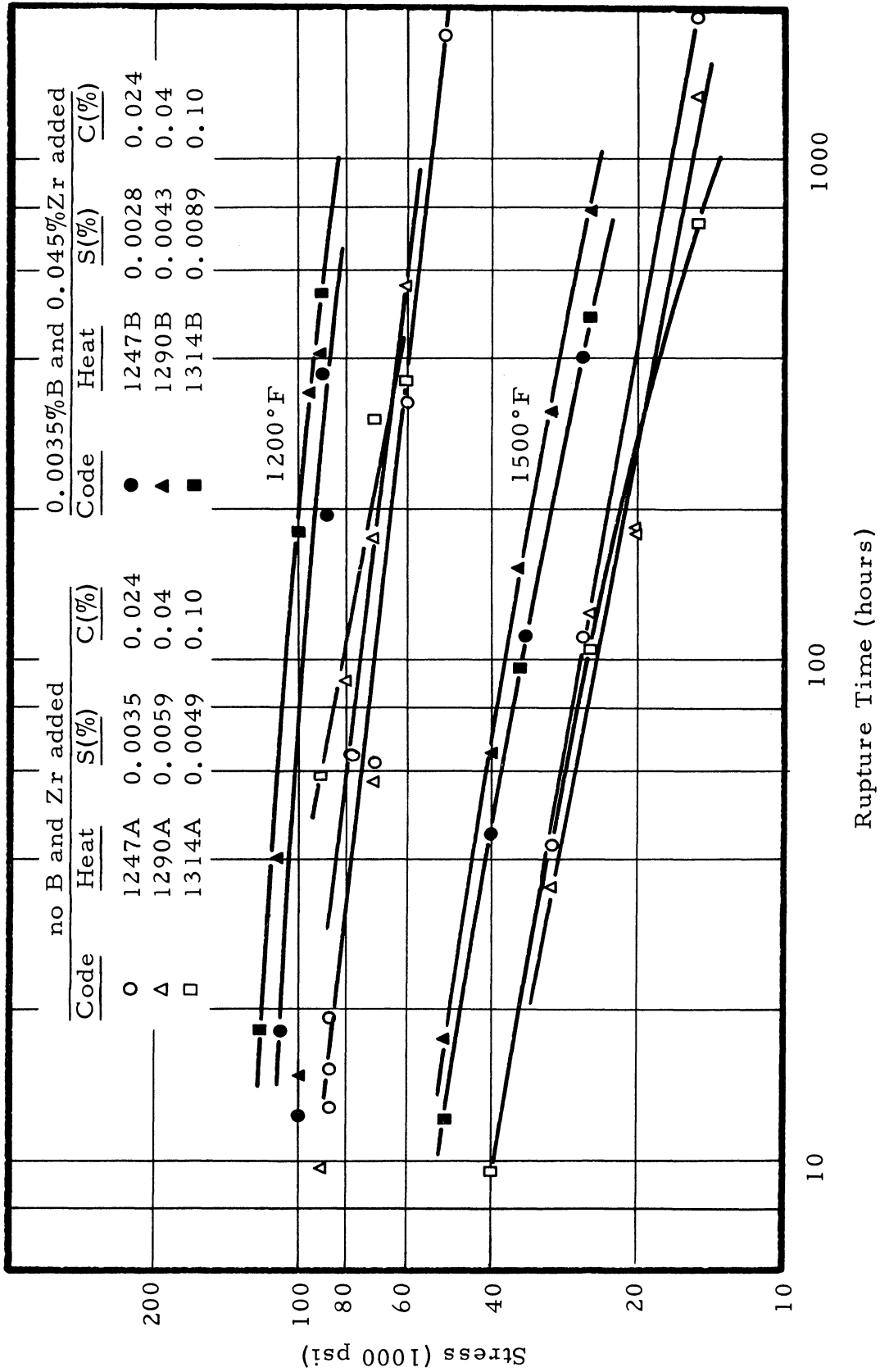
Figure 3. Stress-Rupture Time Curves for Low Sulfur Split Heats of the 20Cr-1.2Al-3.8Ti Alloy
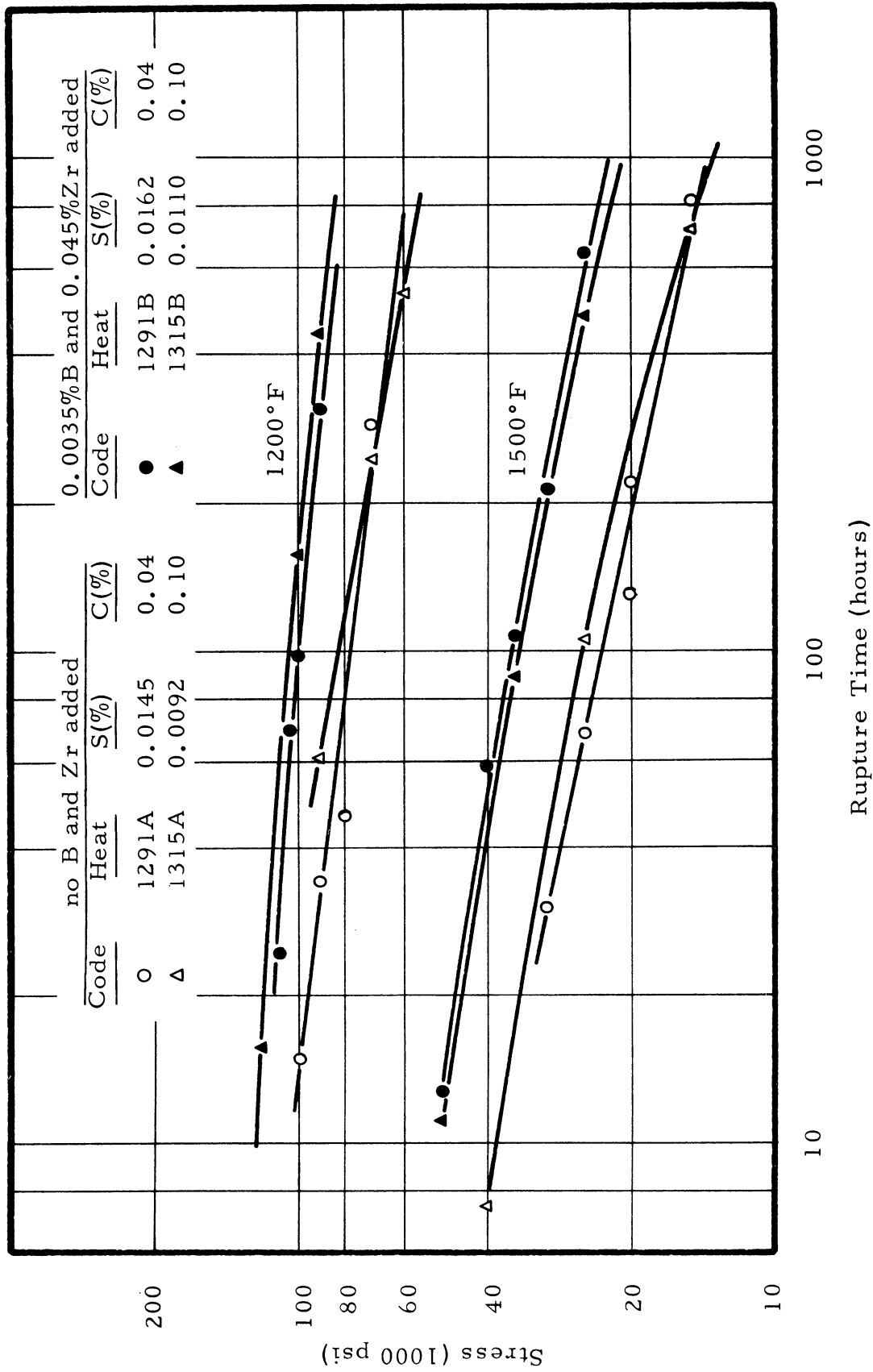
Figure 4. Stress-Rupture Time Curves for Moderate Sulfur Split Heats of the 20Cr-1.2Al-3.8Ti Alloy
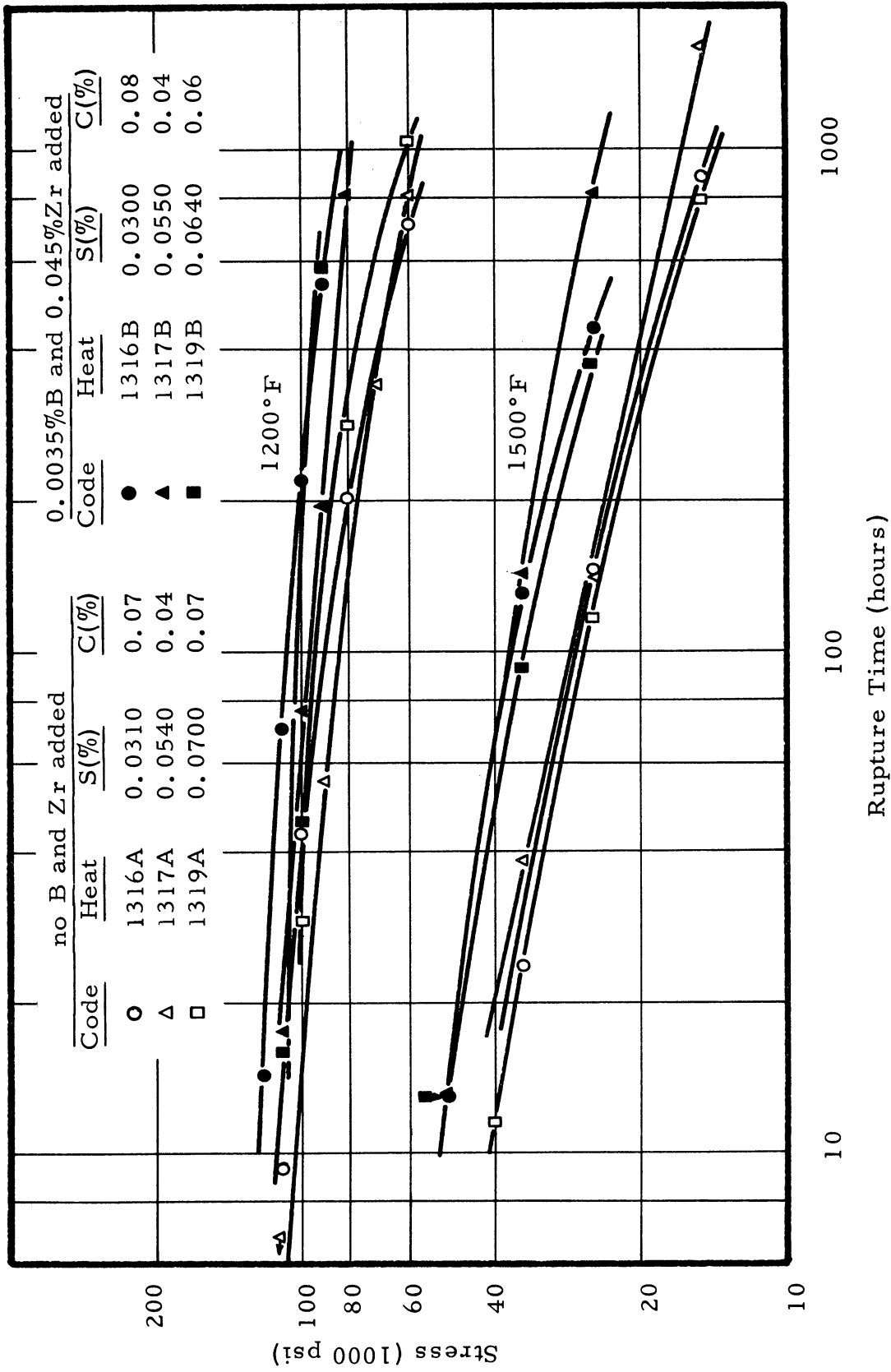
Figure 5. Stress-Rupture Time Curves for High Sulfur Split Heats of the 20Cr-1.2Al-3.8Ti Alloy

100X   1000X

(a) Heat 1314A - 0.0049%S, no B and Zr added
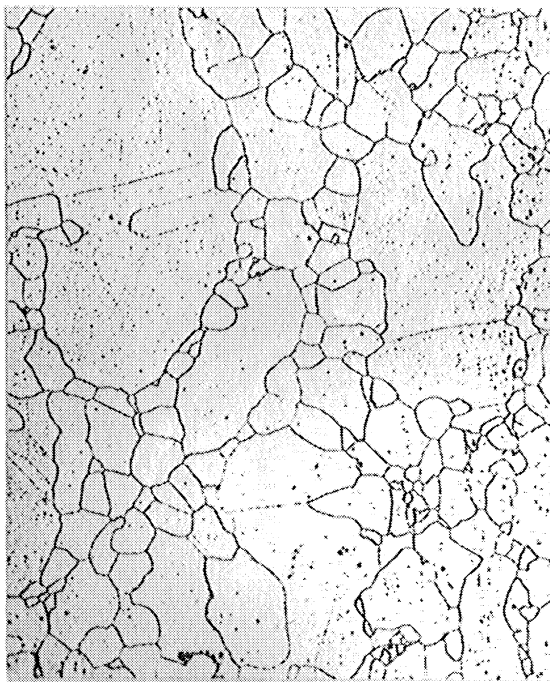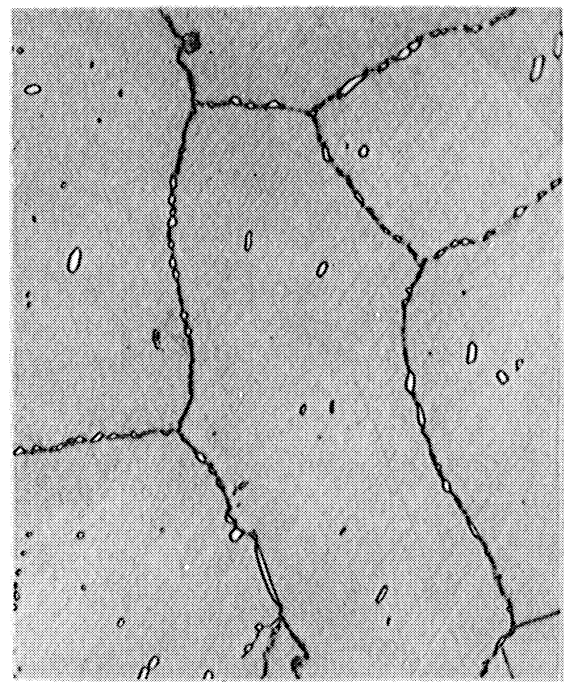
100X   1000X

(b) Heat 1314B - 0.0089%S, 0.0035%B and 0.045%Zr added

Figure 6.   Microstructure of a Low Sulfur Split Heat of the
20Cr-1.2Al-3.8Ti Alloy in the As-Heat Treated
Condition
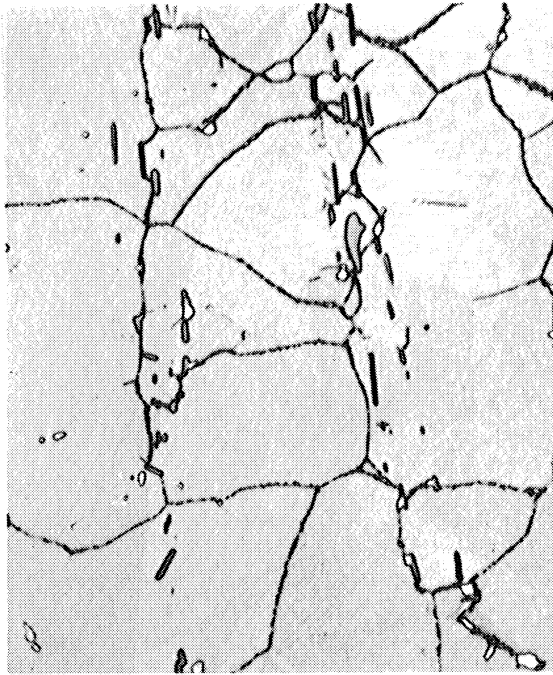
100X   1000X

(a) Heat 1319A - 0.0700%S, no B and Zr added
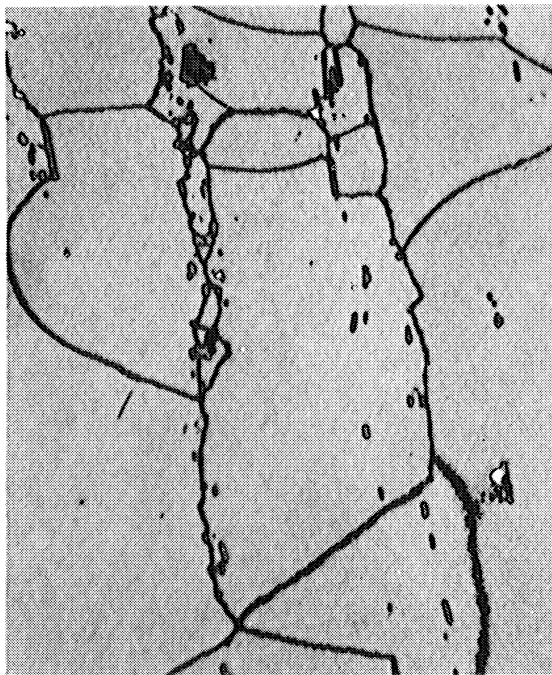
100X   1000X

(b) Heat 1319B - 0.0640%S, 0.0035%B and 0.045%Zr added

Figure 7. Microstructures of a High Sulfur Split Heat of the
20Cr-1.2Al-3.8Ti Alloy in the As-Heat Treated
Condition

(a) Heat 1314A - 0.0049%S
rupt. time - 758.9 hrs, RA - 21%
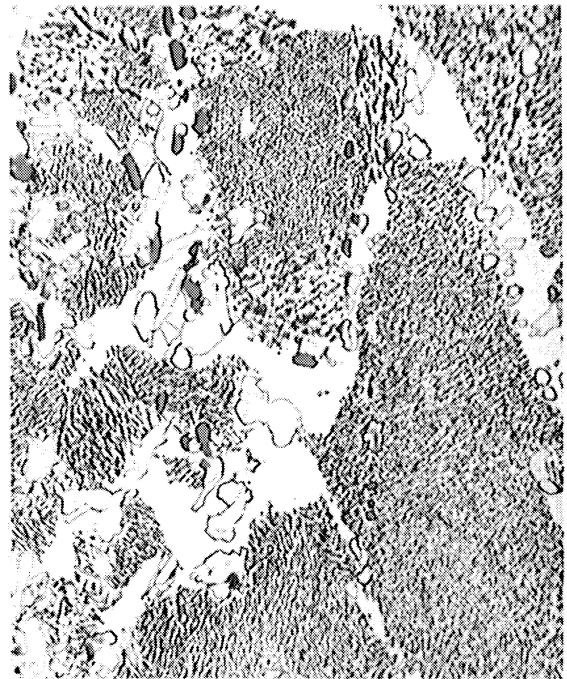
(b) Heat 1316A - 0.0310%S
rupt. time - 884.9 hrs, RA - 27%
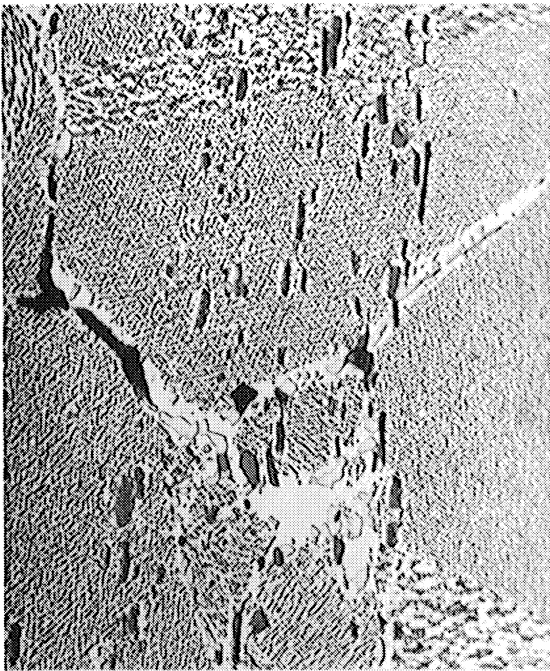
(c) Heat 1317A - 0.0540%S
rupt. time - 1640.3 hrs, RA - 3%
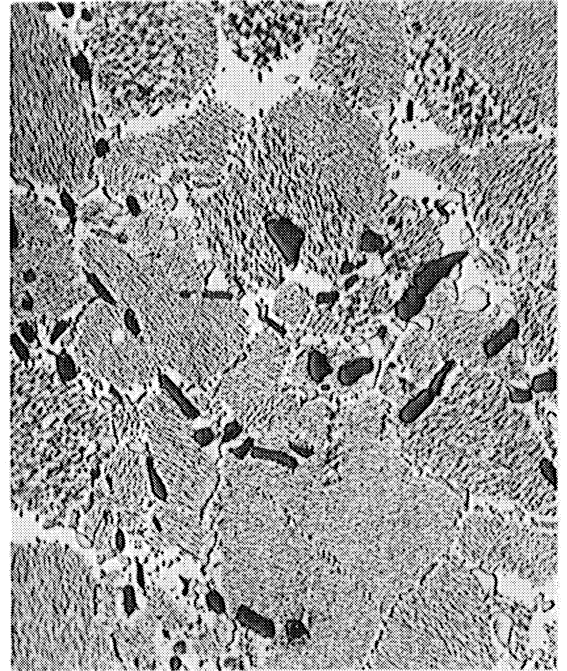
(d) Heat 1319A - 0.0700%S
rupt. time 799.6 hrs, RA - 9%

Figure 8. The 20Cr-1.2Al-3.8Ti Alloy with No Boron and
Zirconium Added. Microstructures After Creep-
Rupture Testing at 1500°F and 15,000 psi (1000X)
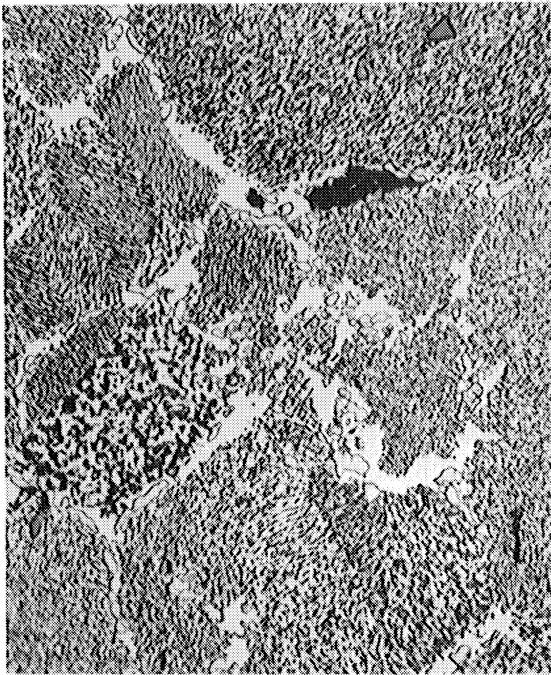
(a) Heat 1314B - 0.0089%S
rupt. time - 487.5 hrs, RA - 26%
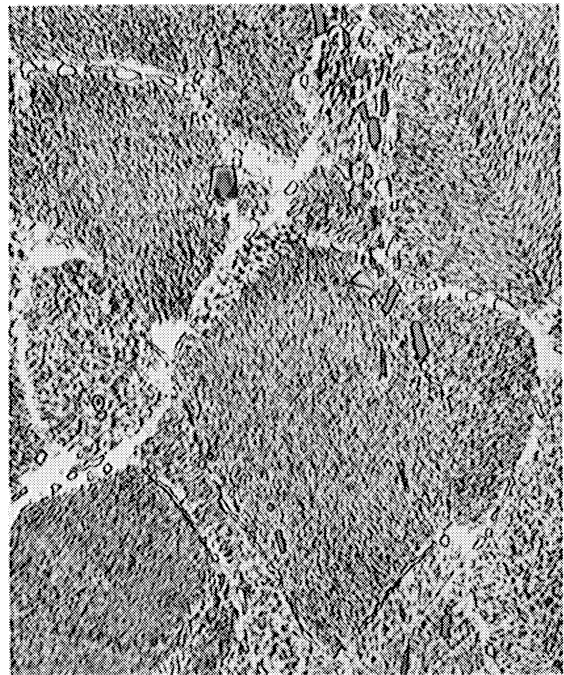
(b) Heat 1316B - 0.0300%S
rupt. time - 440.8 hrs, RA - 23%
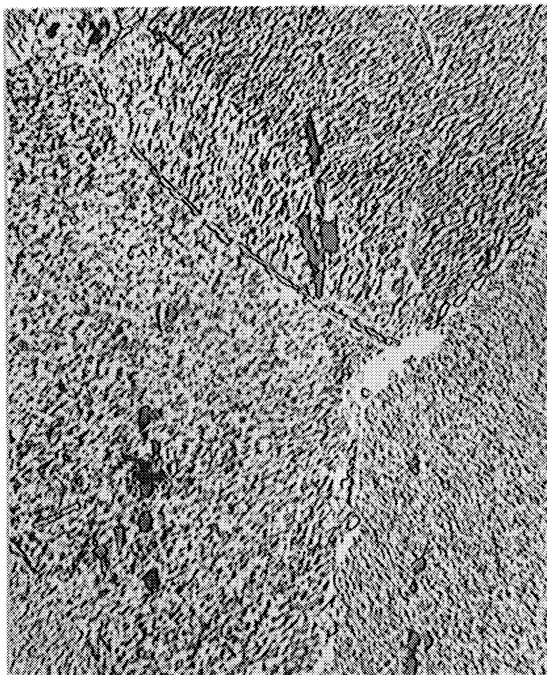
(c) Heat 1317B - 0.0550%S
rupt. time - 825.2 hrs, RA - 11%
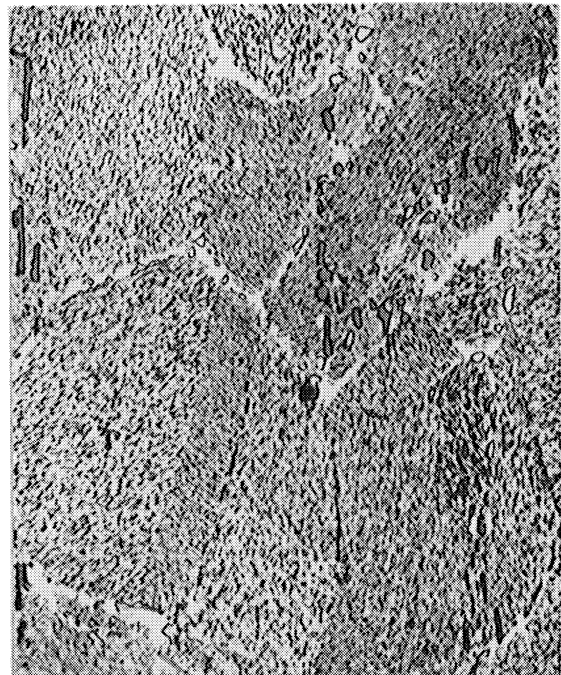
(d) Heat 1319B - 0.0640%S
rupt. time - 377.3 hrs, RA - 22%

Figure 9.   The 20Cr-1.2Al-3.8Ti Alloy with 0.0035 percent
Boron and 0.045 percent Zirconium Added. Micro-
structures After Creep-Rupture Testing at 1500°F
and 25,000 psi (1000X)
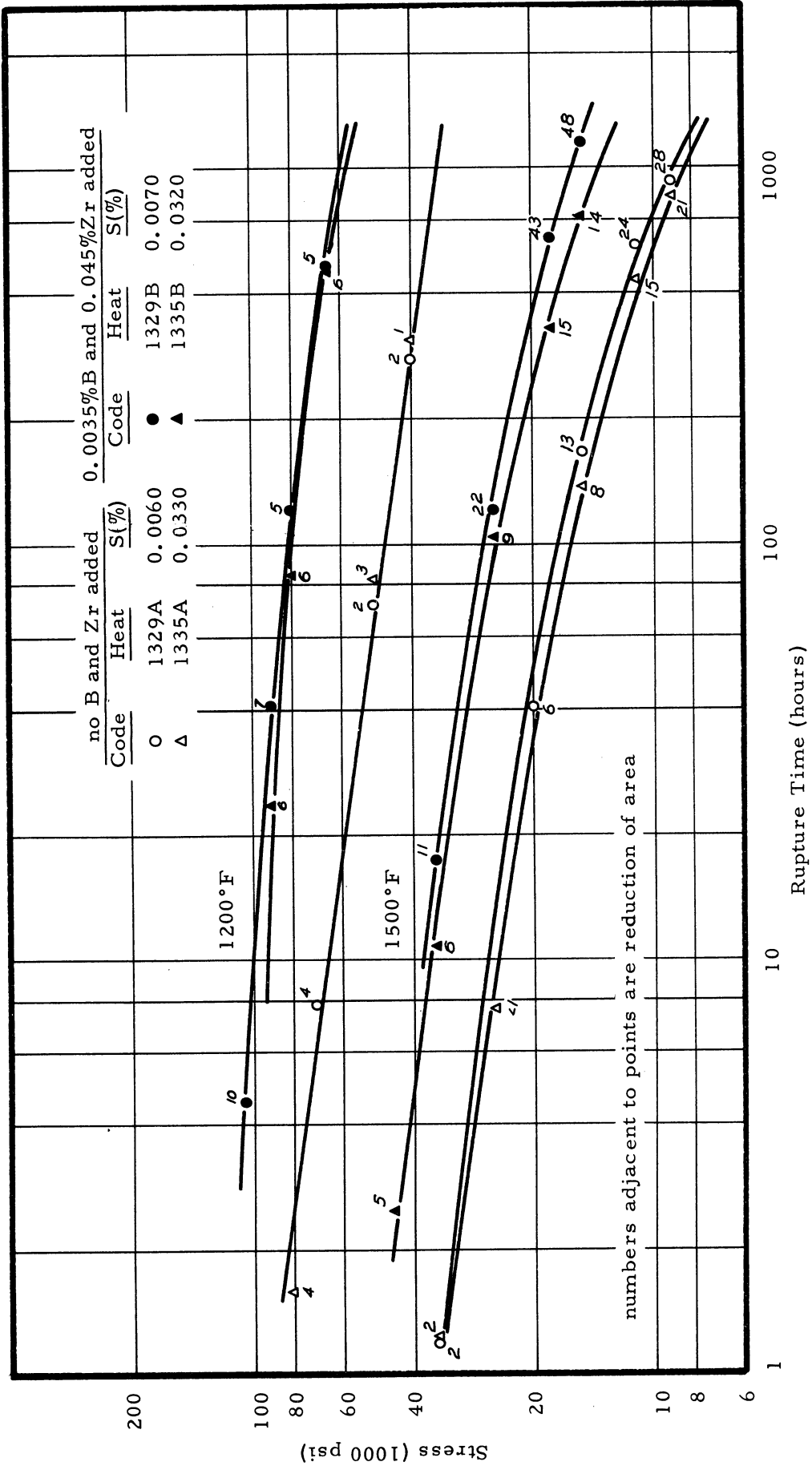
Figure 10. Comparative Stress-Rupture Time Curves for High and Low Sulfur Split Heats of the 20Cr-3.8Al-1.2Ti Alloy
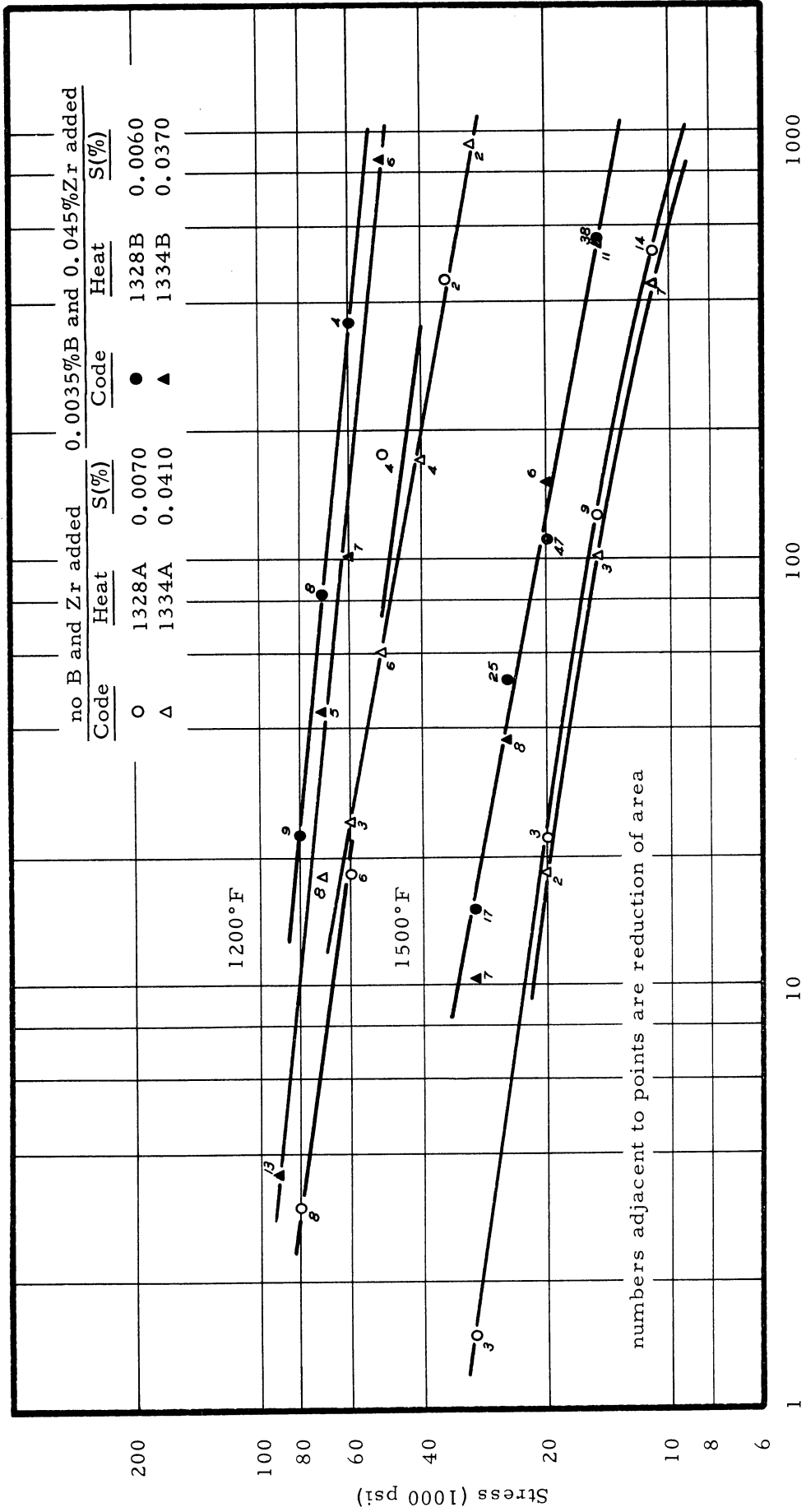
Figure 11. Comparative Stress-Rupture Time Curves for High and Low Sulfur Split Heats of the 20Cr-3.8Al-0.1Ti Alloy
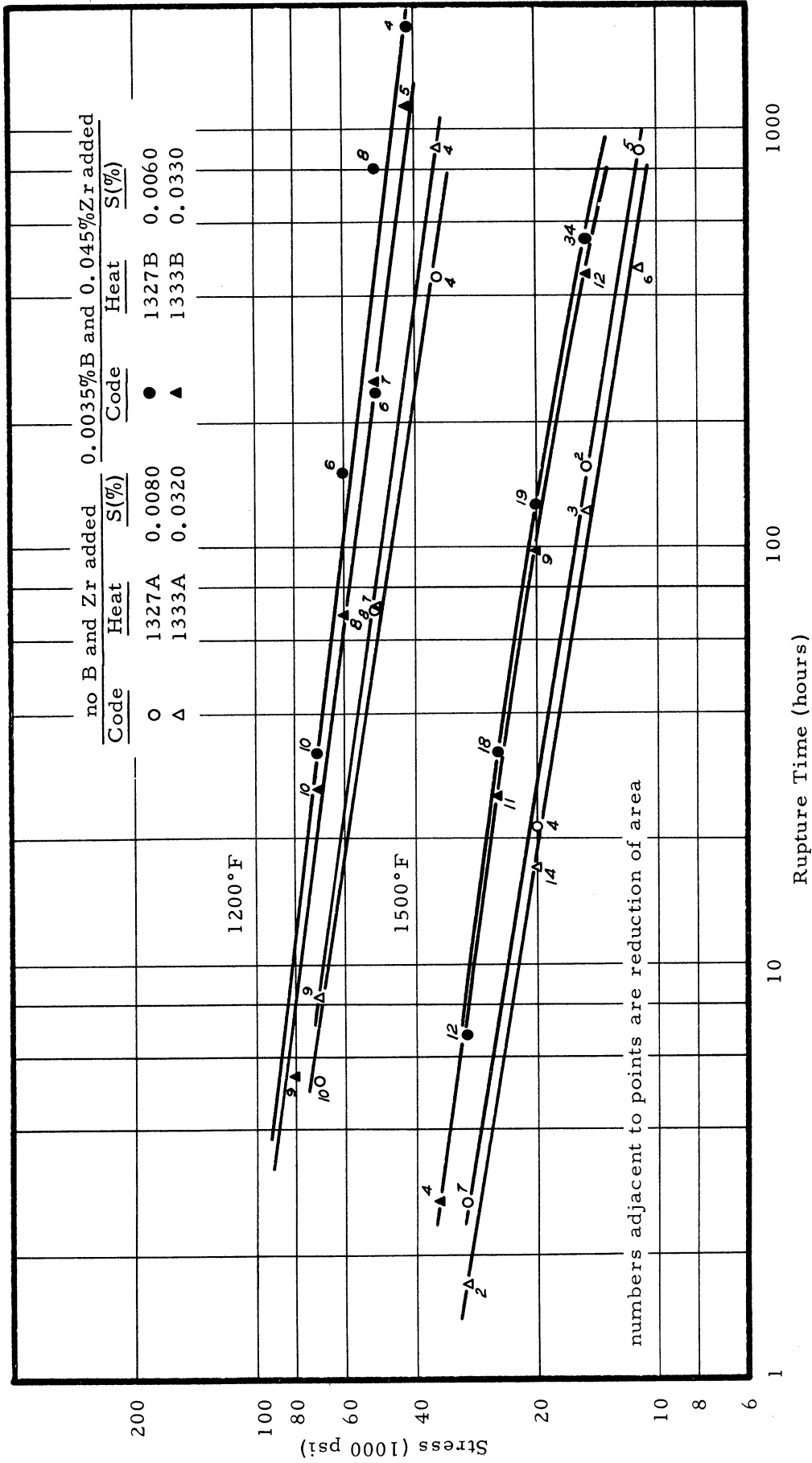
Figure 12. Comparative Stress-Rupture Time Curves for High and Low Sulfur Split Heat of the 20Cr-3.8Al Alloy

no B and Zr added   0.0035%B and 0.045%Zr added
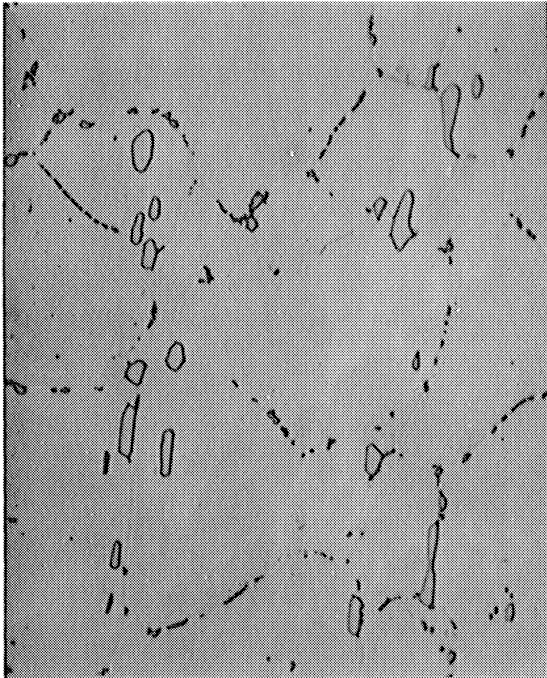
(a) Heat 1329A - 0.0060%S
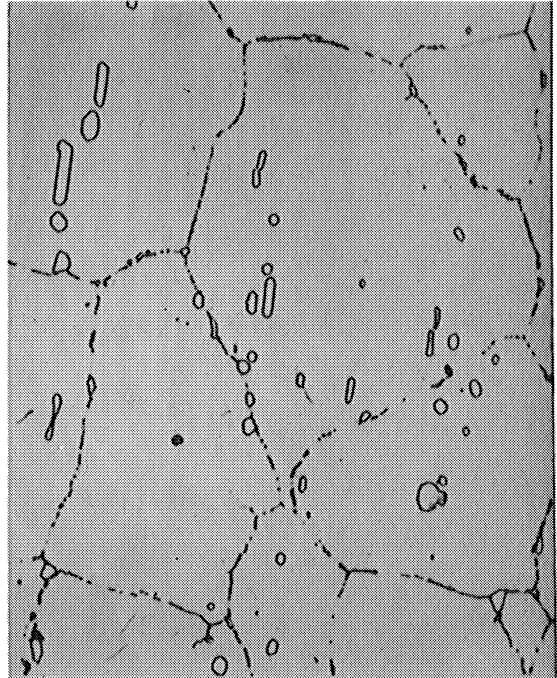
(b) Heat 1329B - 0.0070%S
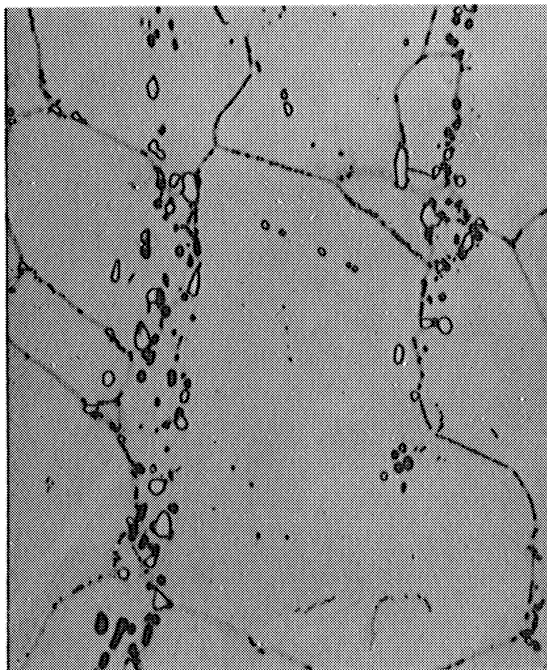
(c) Heat 1335A - 0.0330%S
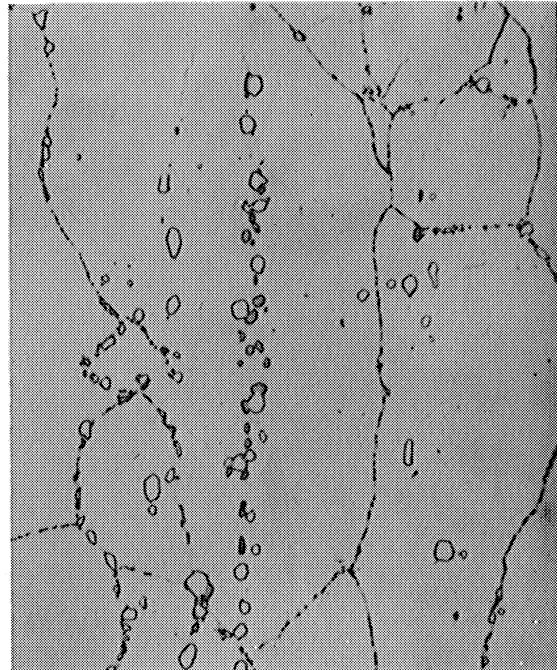
(d) Heat 1335B - 0.0320%S

Figure 13. Microstructures of Low and High Sulfur Split Heats
of the 20Cr-3.8Al-1.2Ti Alloy in the As-Heat
Treated Condition (1000X)
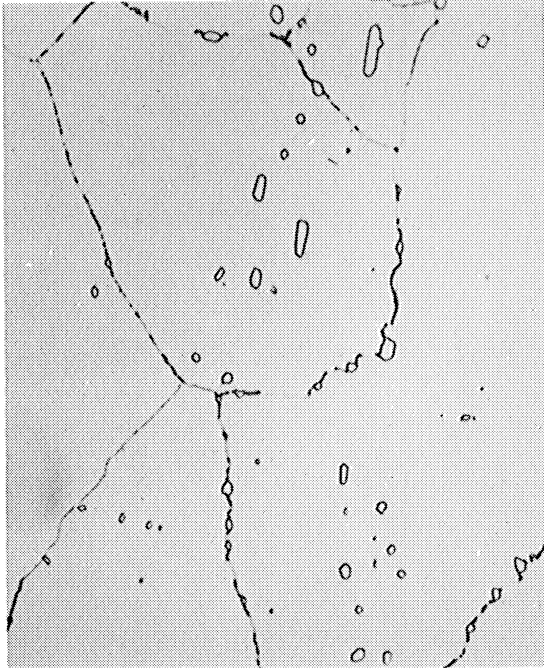
No B and Zr added   0.0035%B and 0.045%Zr added
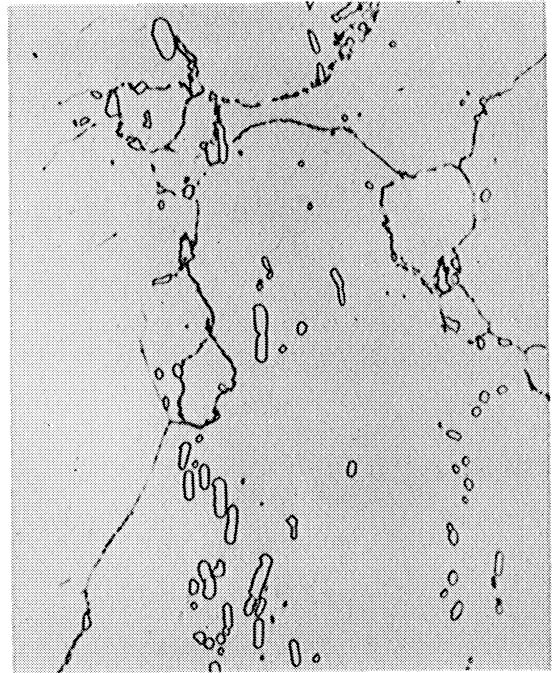
(a) Heat 1327A - 0.0080%S   (b) Heat 1327B - 0.0060%S
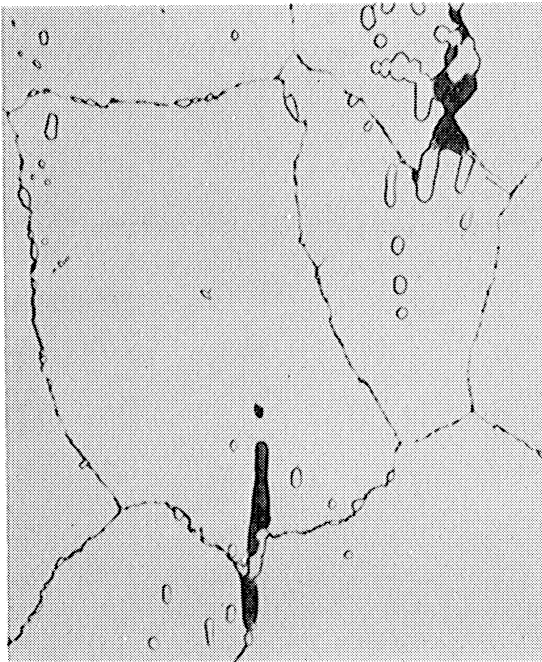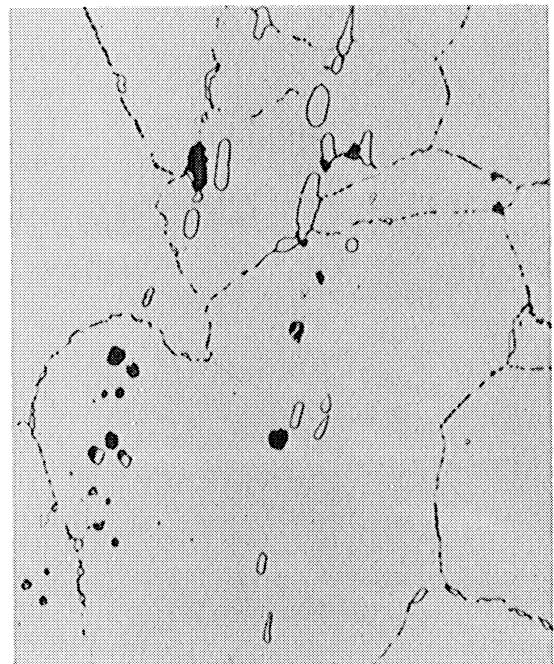
(c) Heat 1333A - 0.0410%S   (d) Heat 1333B - 0.0370%S

Figure 14. Microstructures of Low and High Sulfur Split Heats
of the 20Cr-3.8Al Alloy in the As-Heat Treated
Condition (1000X)

no B and Zr added   0.0035%B and 0.045%Zr added
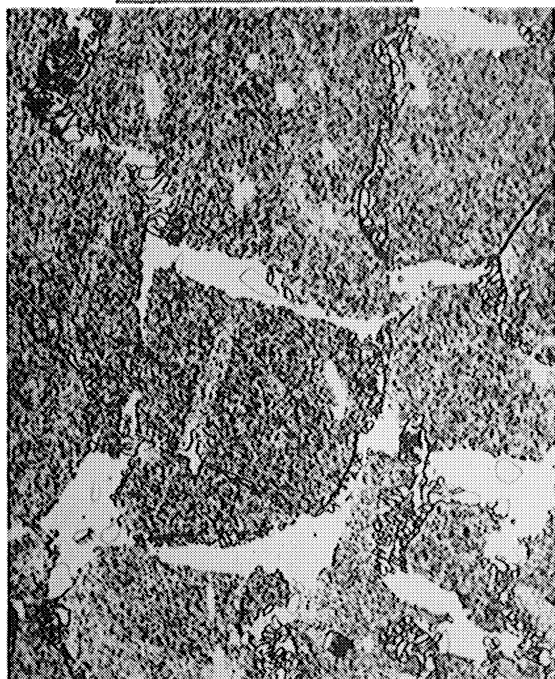
(a) Heat 1329A - 0.0060%S
    stress - 11,000 psi
rupt. time - 524.3 hrs, RA - 24%

(b) Heat 1329B - 0.0070%S
    stress - 15,000 psi
rupt. time - 927.6 hrs, RA - 48%
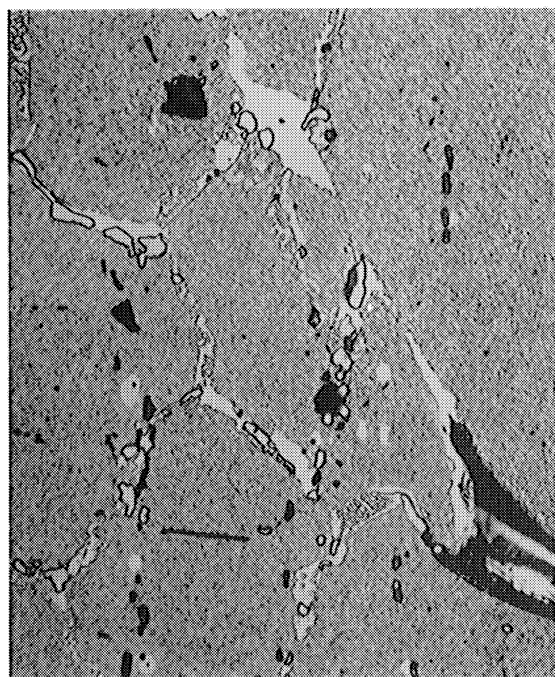
(c) Heat 1335A - 0.0330%S
    stress - 11,000 psi
rupt. time - 437.4 hrs, RA - 15%
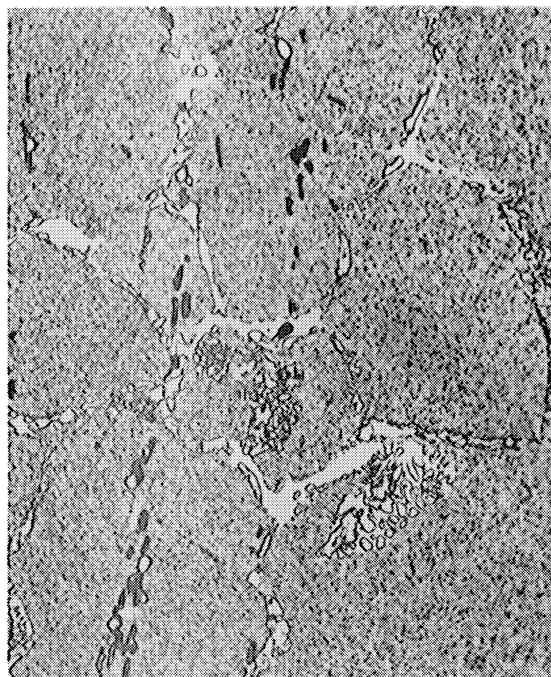
(d) Heat 1335B - 0.0320%S
    stress - 15,000 psi
rupt. time - 619.0 hrs, RA - 14%

Figure 15.   Microstructures of Low and High Sulfur Split Heats
             of the 20Cr-3.8Al-1.2Ti Alloy After Creep-Rupture
             Testing at 1500°F (1000X)

no B and Zr added   0.0035%B and 0.045%Zr added
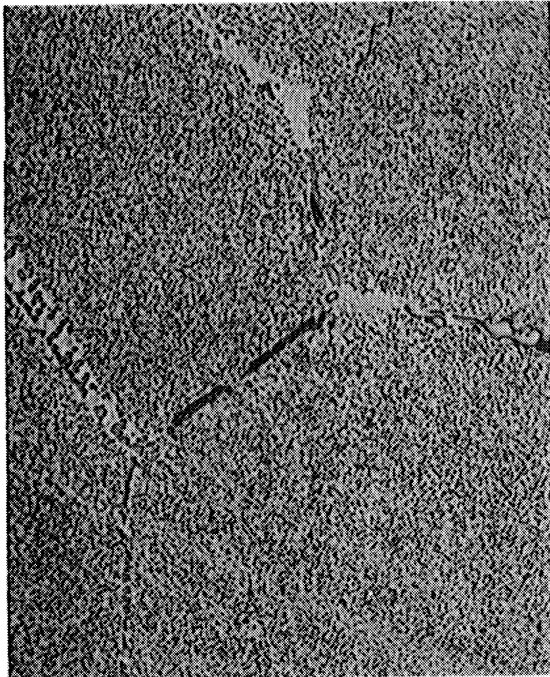
(a) Heat 1327A - 0.0080%S
stress - 11,000 psi
rupt. time - 793.7 hrs, RA - 5%
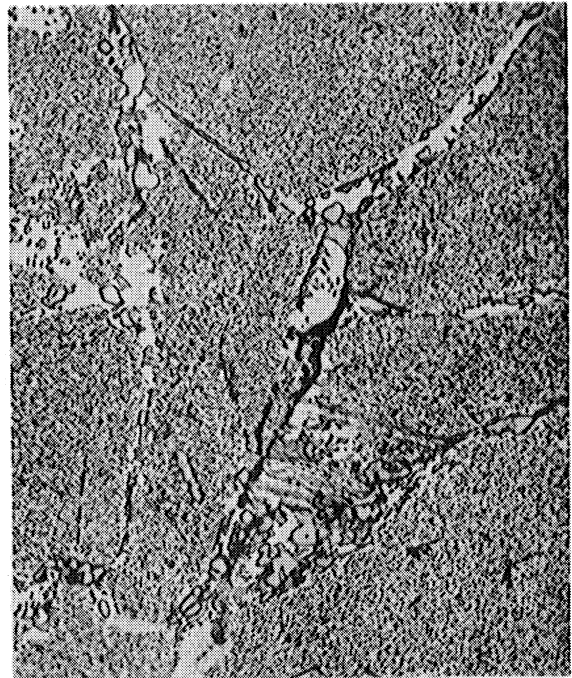
(b) Heat 1327B - 0.0060%S
stress - 15,000 psi
rupt. time - 548.4 hrs, RA - 34%
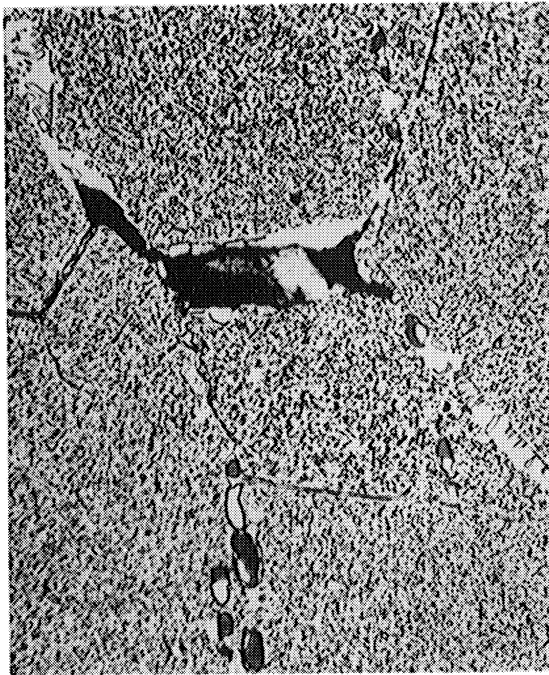
(c) Heat 1333A - 0.0320%S
stress - 11,000 psi
rupt. time - 472 hrs, RA - 6%

(d) Heat 1333B - 0.0330%S
stress - 15,000 psi
rupt. time - 450.5 hrs, RA - 12%

Figure 16. Microstructures of Low and High Sulfur Split Heats
of the 20Cr-3.8Al Alloy After Creep-Rupture Test-
ing at 1500°F (1000X)
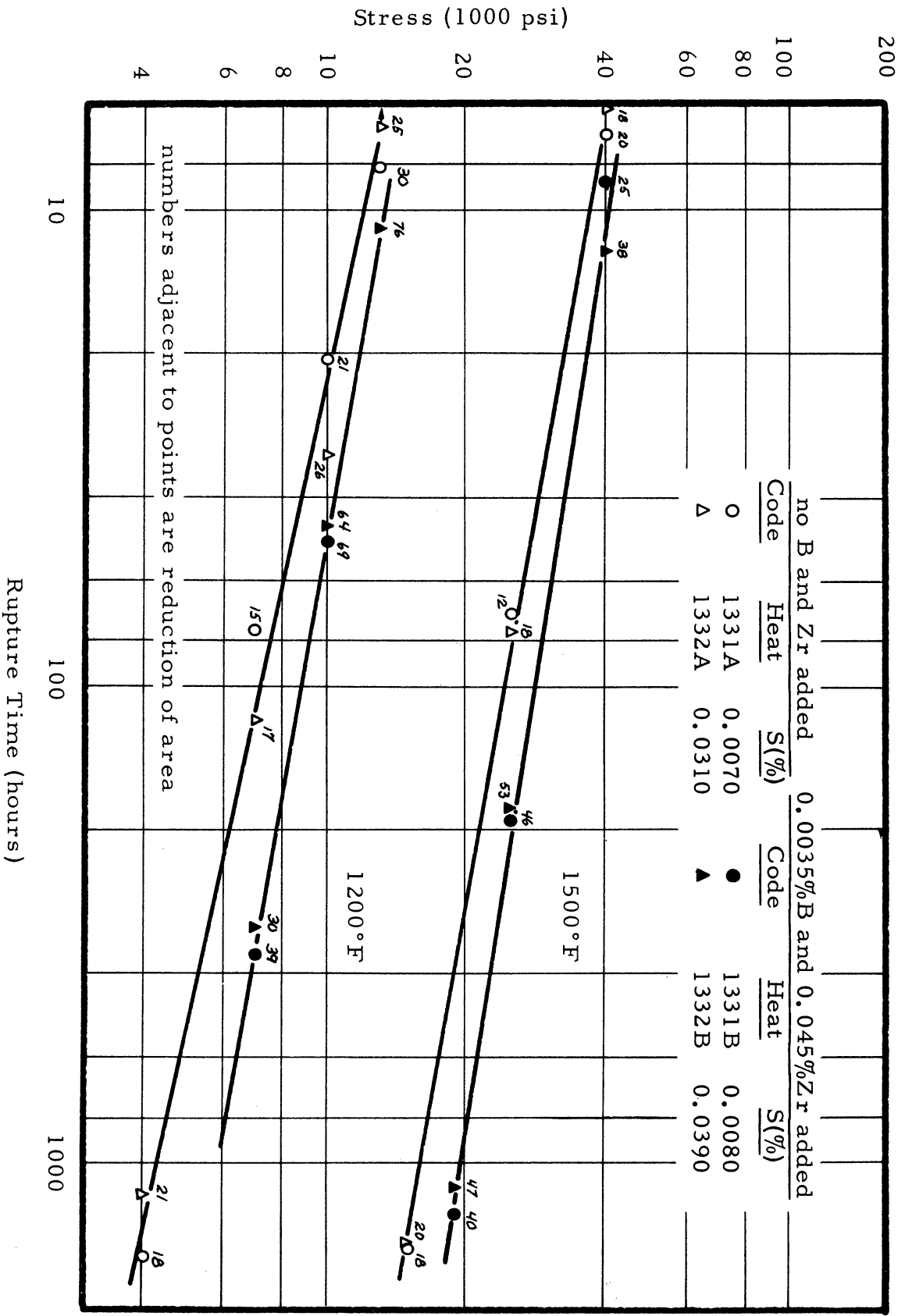
Figure 17. Comparative Stress-Rupture Time Curves for High and Low Sulfur Split Heats of the 80Ni-20Cr Alloy

96
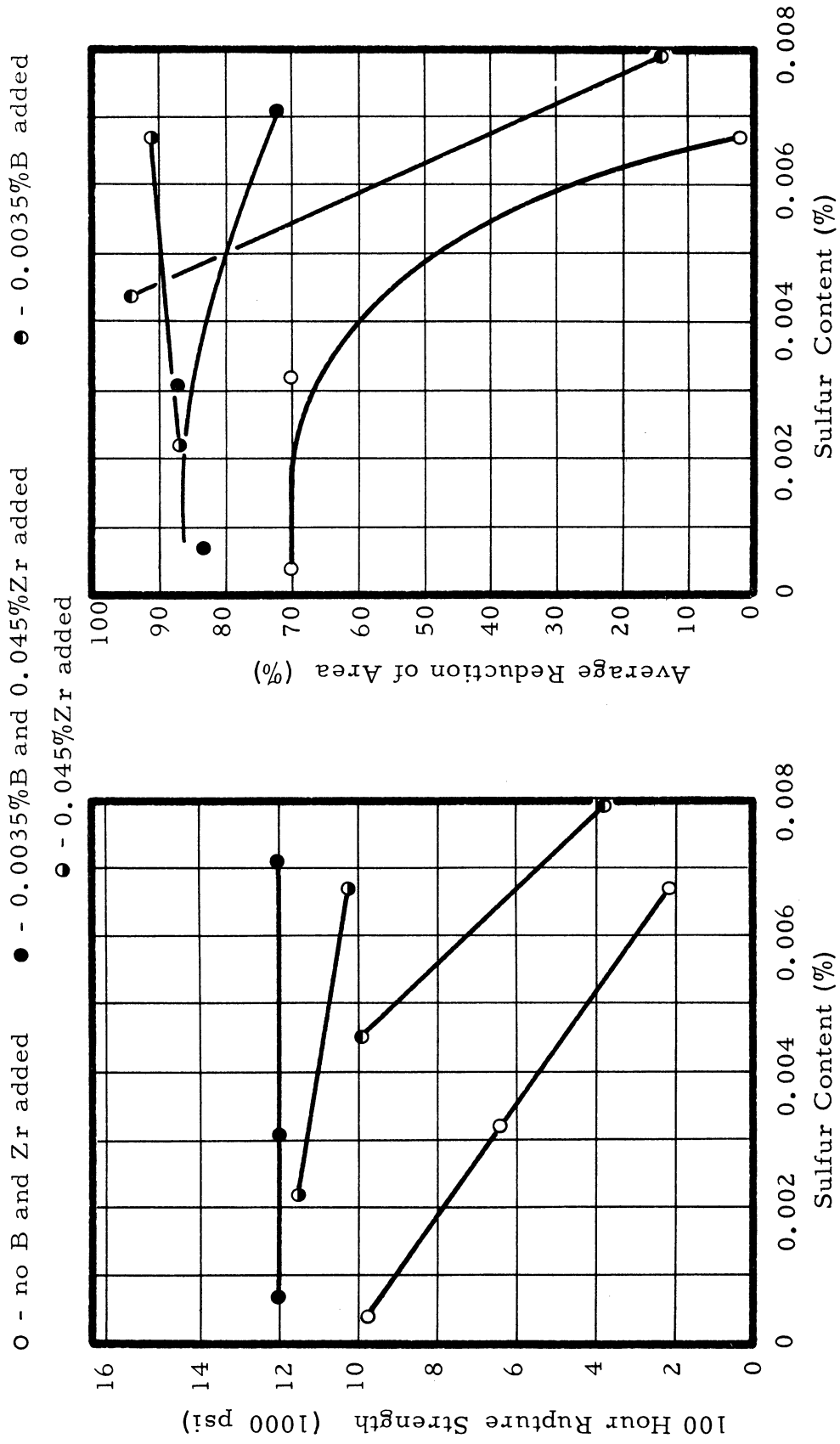
Figure 18. Influence of Sulfur on the Creep-Rupture Properties of Unalloyed Nickel at 1200°F
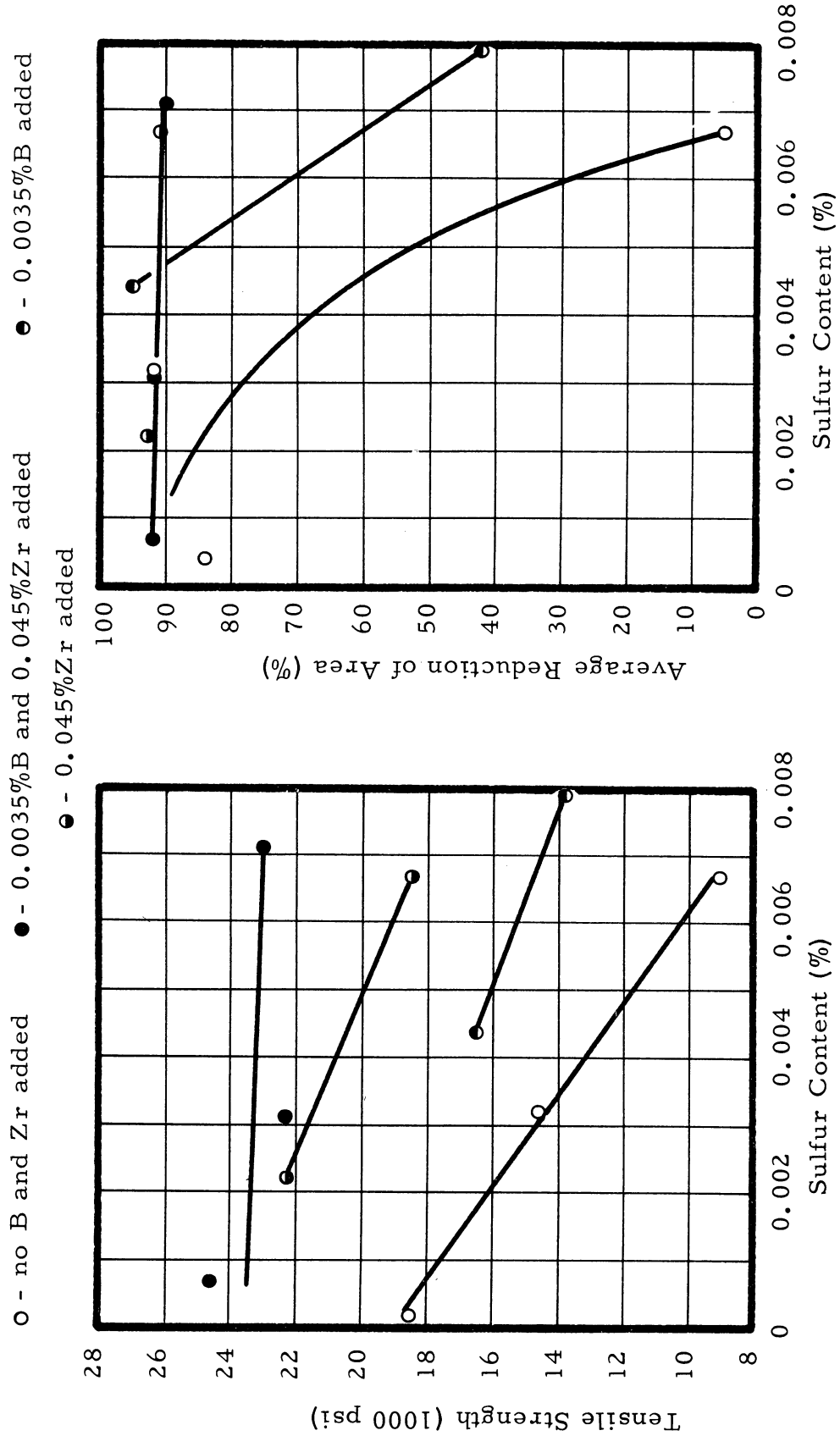
Figure 19. Influence of Sulfur Content on the Tensile Properties of Unalloyed Nickel at 1200°F

o - no B and Zr added

● - 0.0035%B added

● - 0.0035%B and 0.045%Zr added

⊙ - 0.045%Zr added

Average Reduction of Area (%)

Sulfur Content (%)

Tensile Strength (1000 psi)

Sulfur Content (%)
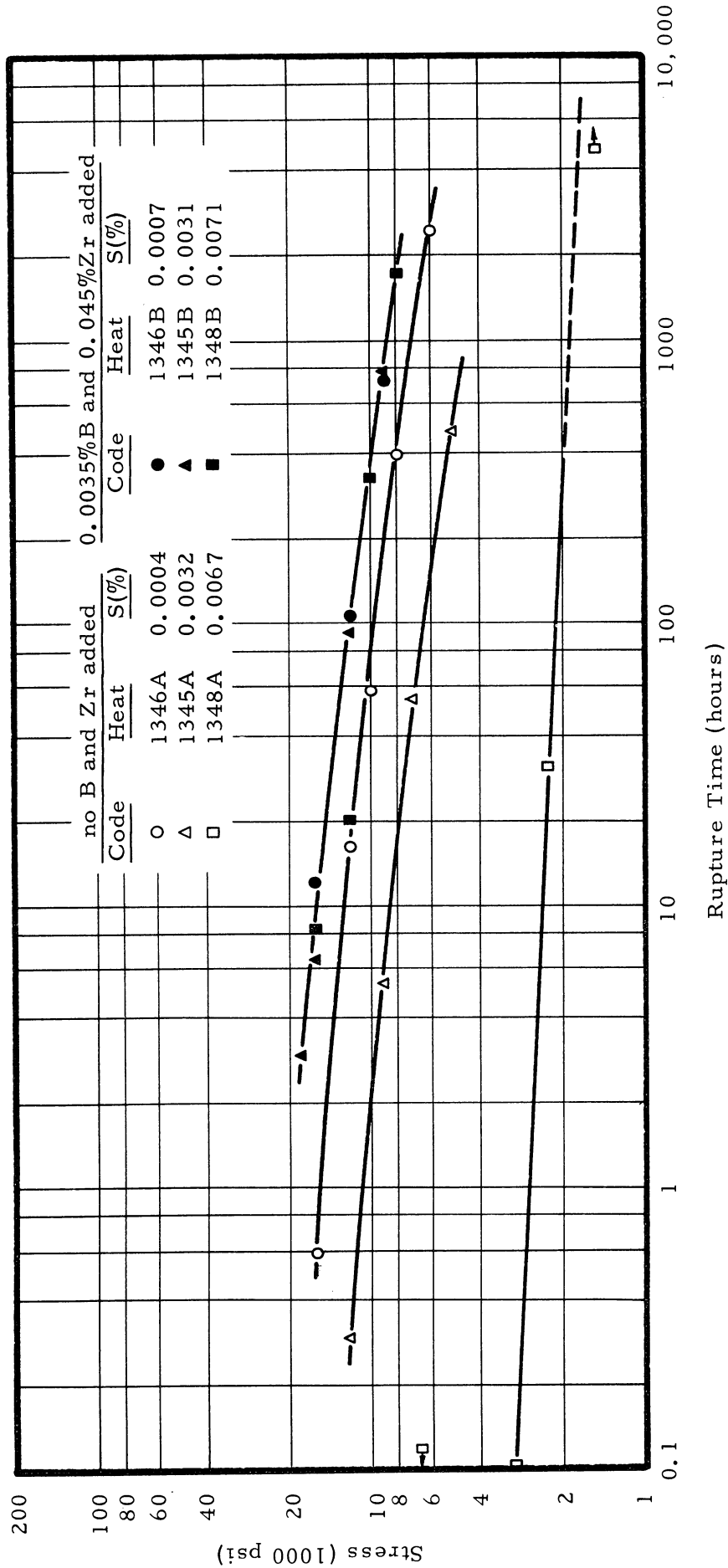
Figure 20. Comparative Stress-Rupture Time Curves at 1200.°F for Split Heats of Nickel with Three Levels of Sulfur
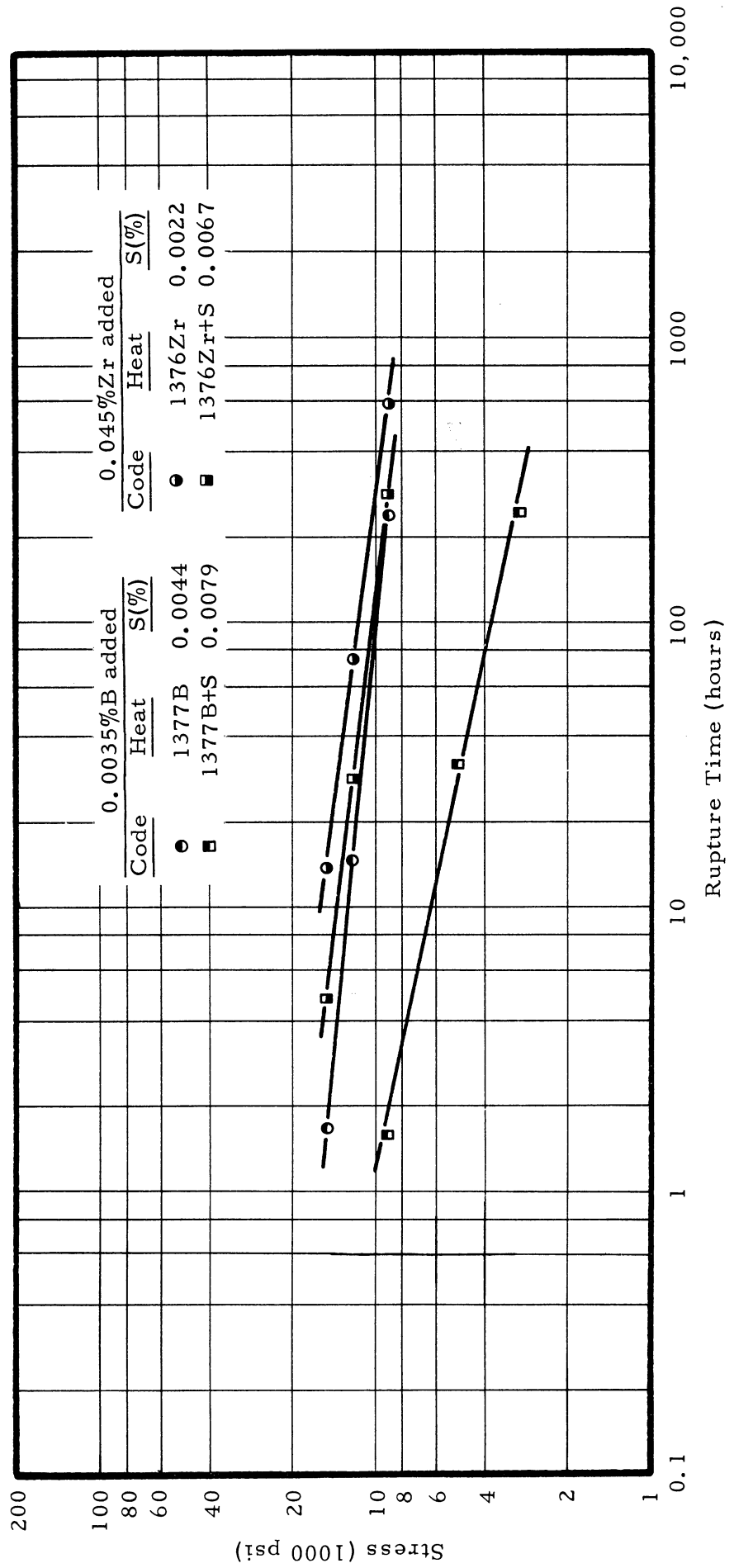
Figure 21. Comparative Stress-Rupture Time Curves at 1200° F for Heats of Nickel Containing Either Boron or Zirconium with Two Levels of Sulfur

no B and Zr added   0.0035%B and 0.045%Zr added

(a) Heat 1346A - 0.0004%S

(b) Heat 1346B - 0.0007%S

(c) Heat 1348A - 0.0067%S

(d) Heat 1348B - 0.0071%S
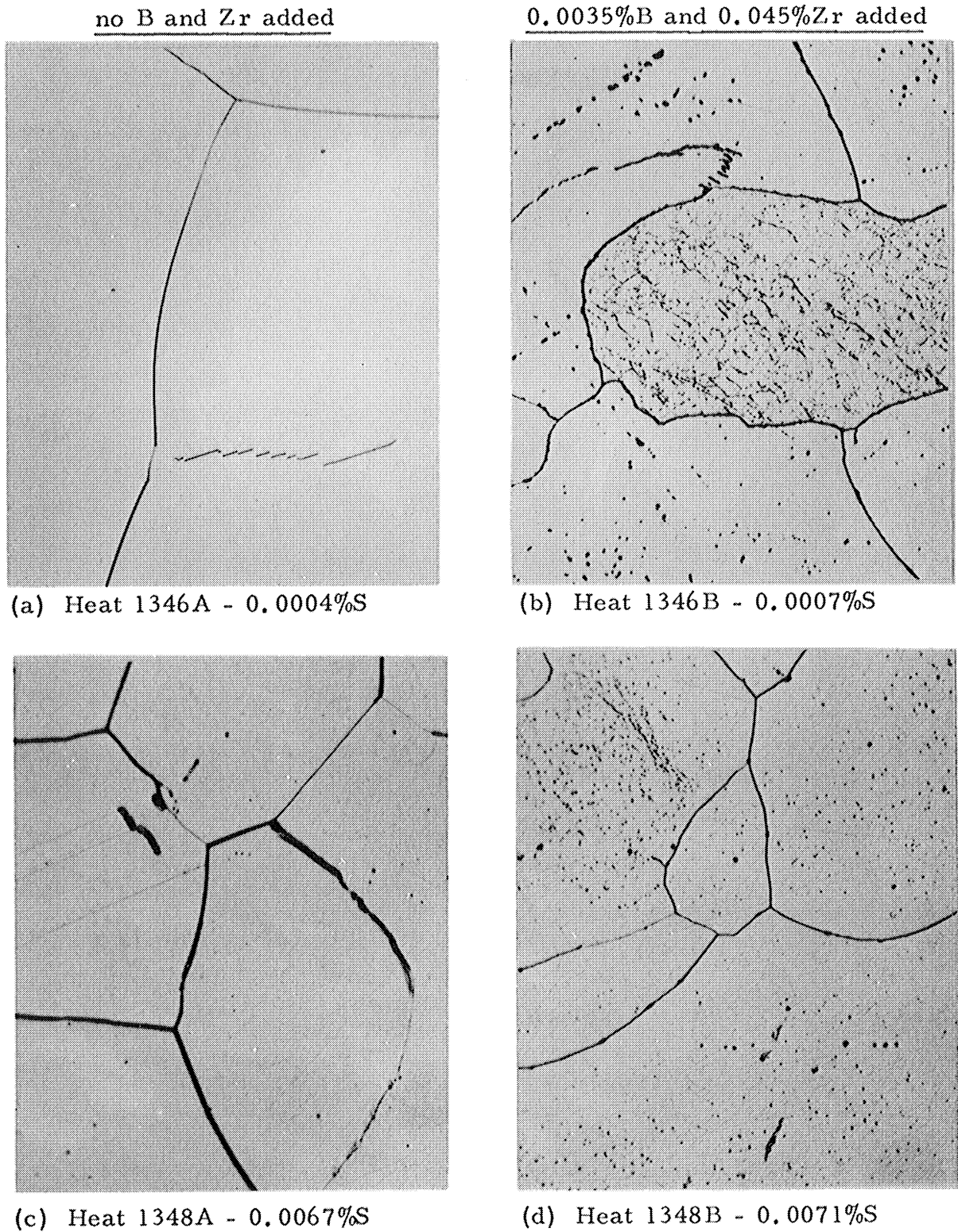
Figure 22. Influence of Sulfur and Boron and Zirconium on
the Microstructure of Nickel in the As-Heat
Treated Condition (1000X)
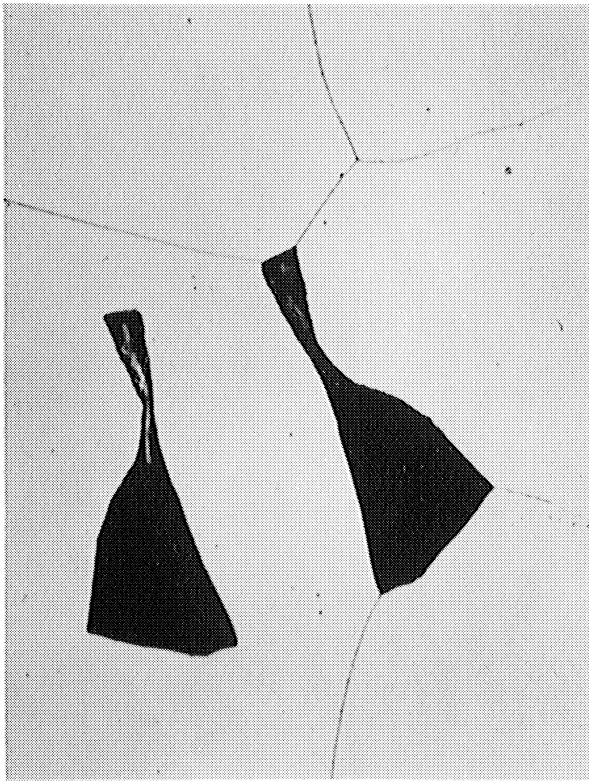
(a) stress - 3000 psi
rupt. time - 0.07 hrs.
RA - <1%

(b) stress - 2250 psi
rupt. time - 31.9 hrs.
RA - 3%

Figure 23.   High Sulfur Nickel without Boron and Zirconium
Added (Heat 1348A, 0.0067 percent Sulfur).
Microstructures After Creep-Rupture Testing
at 1200°F (1000X)
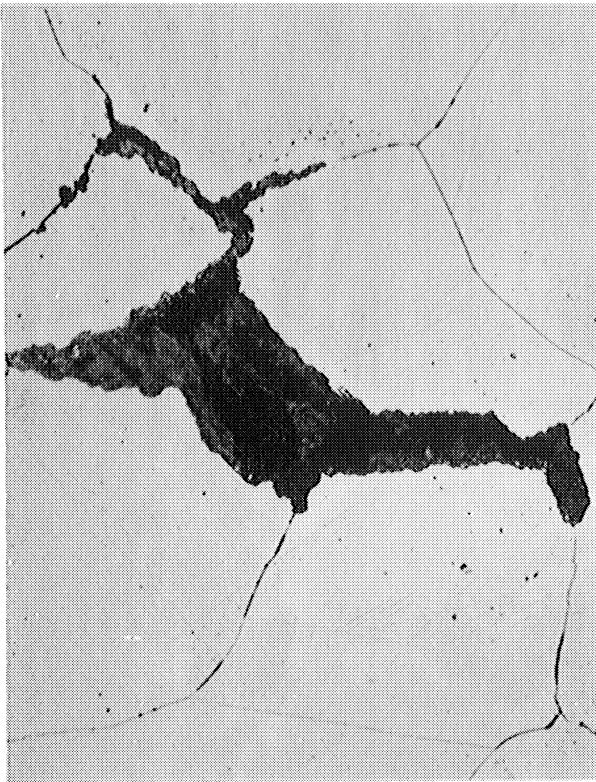
(c) stress - 1500 psi
     shut off after 4700 hrs.
     25% measured elongation

Figure 23 continued
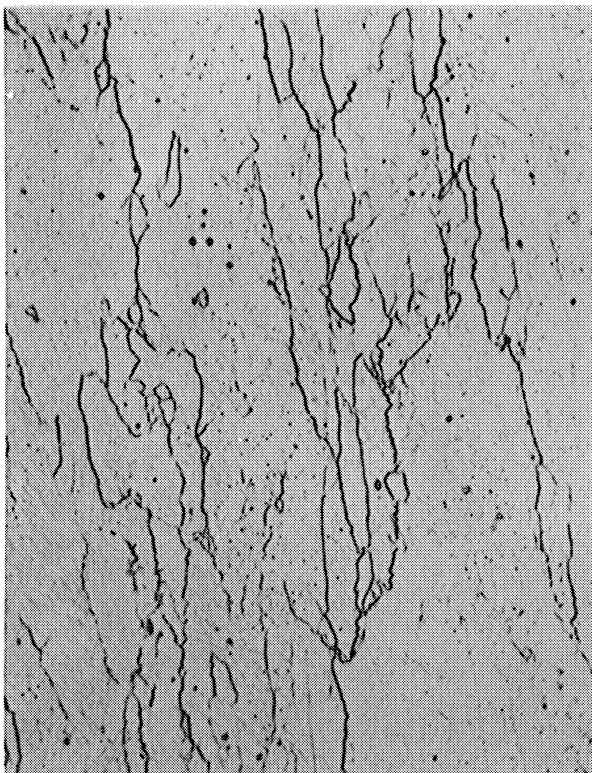
rupt. time - 1766.1 hrs.
RA - 64%

Figure 24. High Sulfur Nickel with 0.0035 percent Boron and
            0.045 percent Zirconium Added (Heat 1348B, 0.0071
            percent Sulfur). Microstructure After Creep-
            Rupture Testing at 1200°F and 8000 psi (1000X)
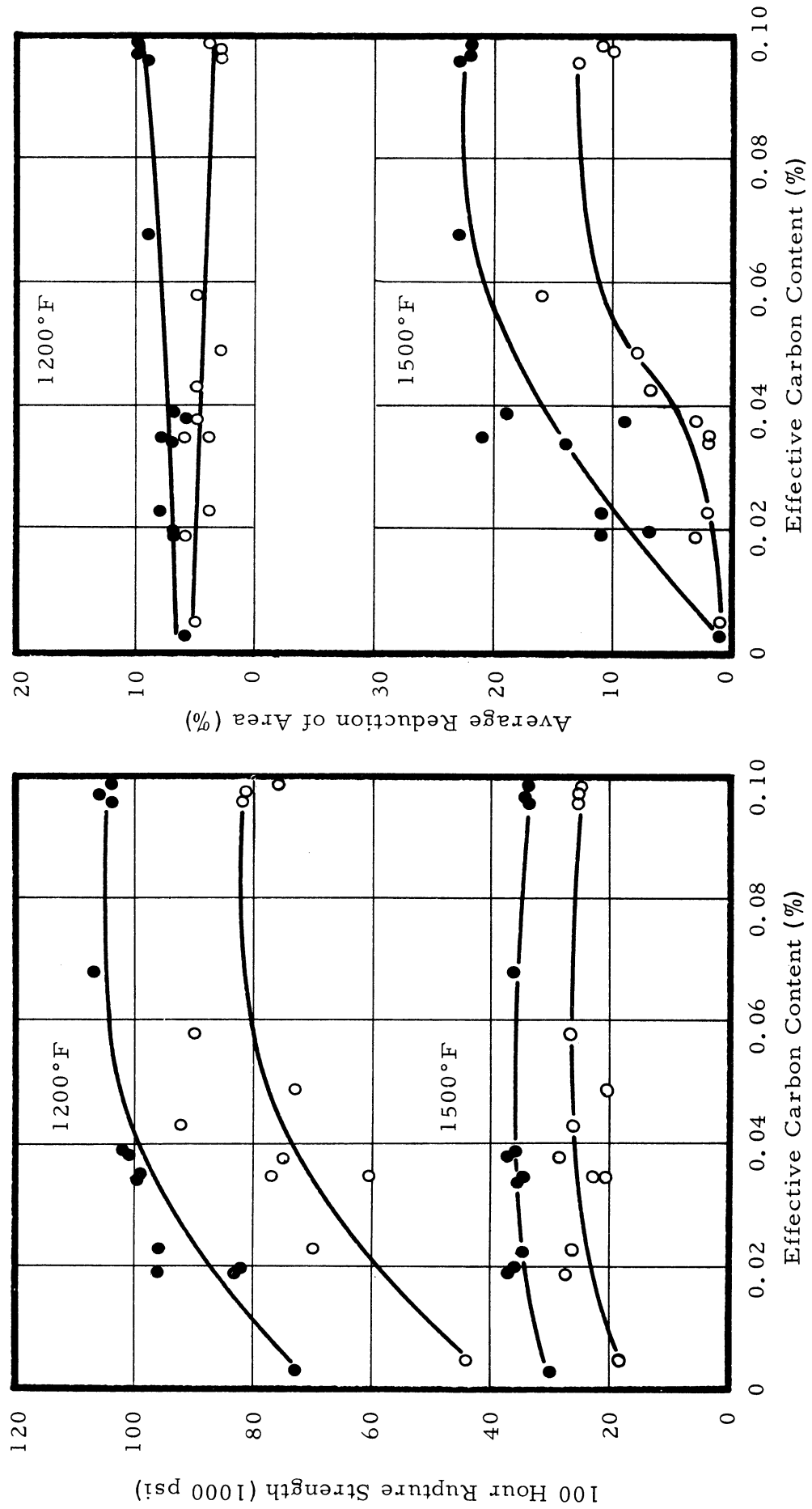
Figure 25. Relationships Between Creep-Rupture Properties and Effective Carbon Content for the 20Cr-1.2Al-3.8Ti alloy at 1200° and 1500°F
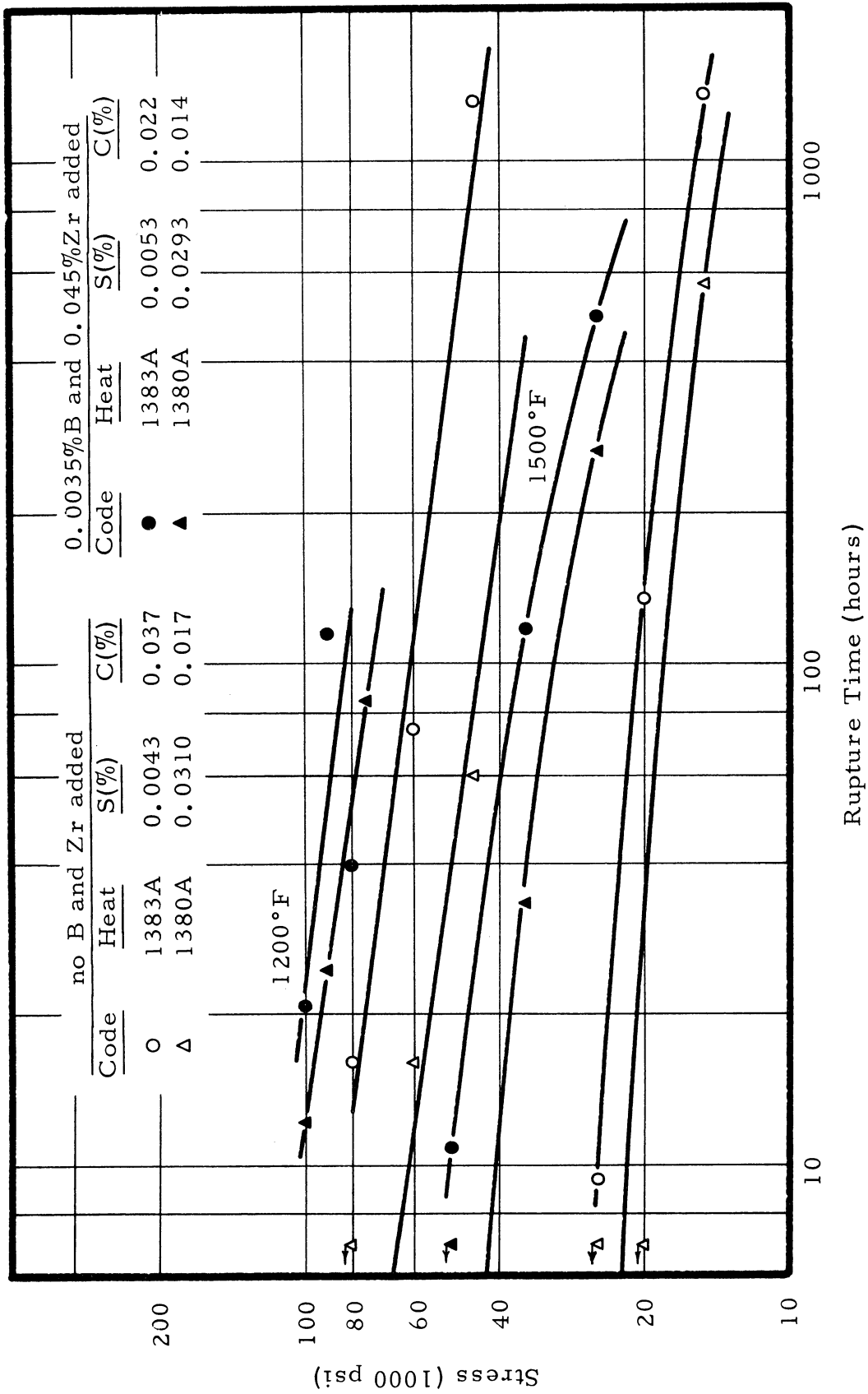
Figure 26. Stress-Rupture Time Curves for Intentionally Low Carbon Split Heats of the 20Cr-1.2Al-3.8Ti Alloy

no B and Zr added   0.0035%B and 0.045%Zr added
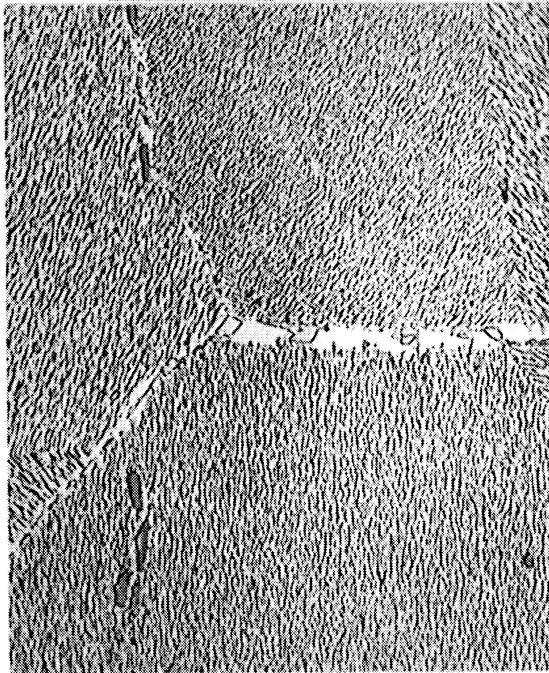
(a) Heat 1383A - 0.037%C
stress - 15,000 psi
rupt. time - 1368.8 hrs, RA - 2%
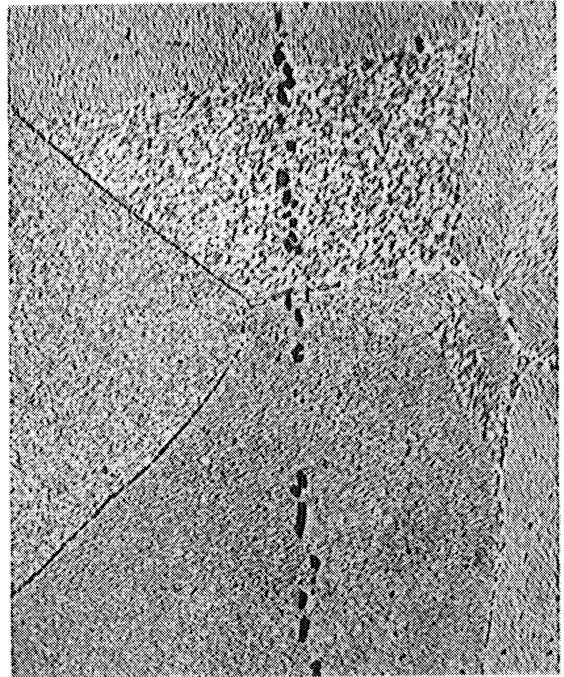
(b) Heat 1383B - 0.022%C
stress - 25,000 psi
rupt. time - 497.0 hrs, RA - 8%
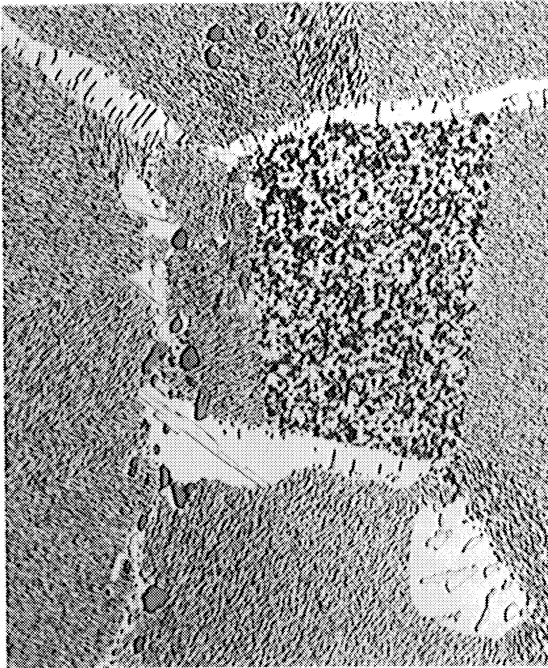
(c) Heat 1380A - 0.017%C
stress - 15,000 psi
rupt. time - 579.6 hrs, RA - 3%
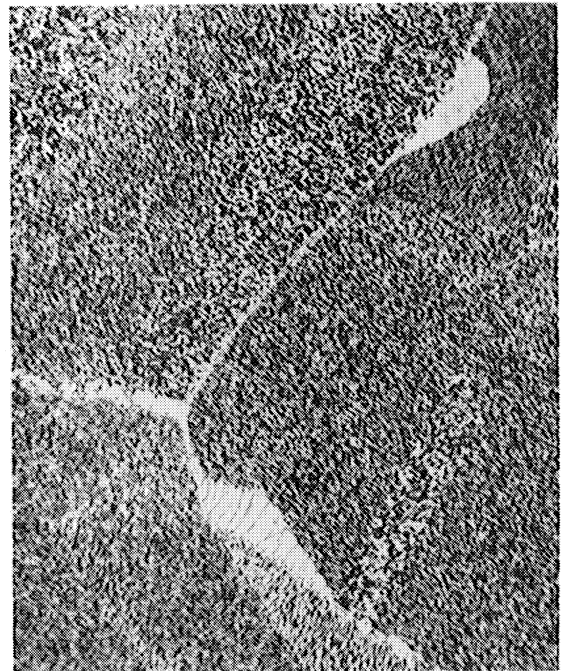
(d) Heat 1380B - 0.014%C
stress - 25,000 psi
rupt. time - 267.2 hrs, RA - 2%

Figure 27. Microstructures of Intentionally Low Carbon Split
Heats of the 20Cr-1.2Al-3.8Ti Alloy After Creep-
Rupture Testing at 1500°F (1000X)
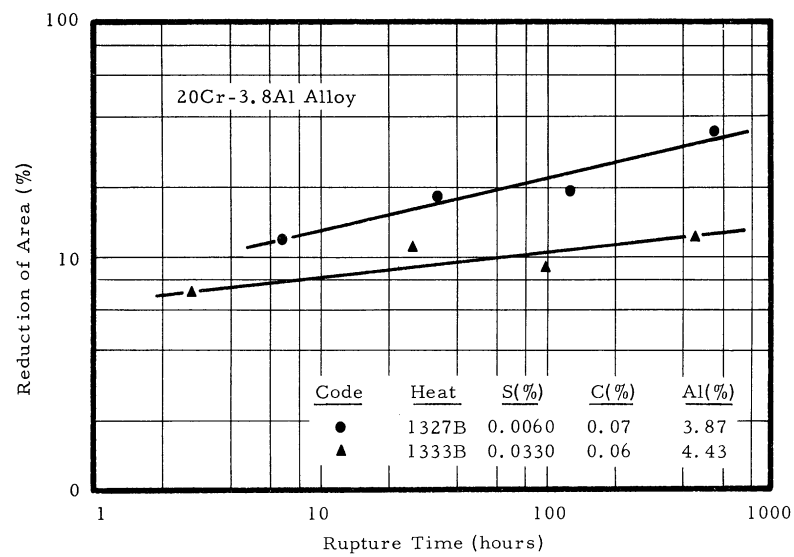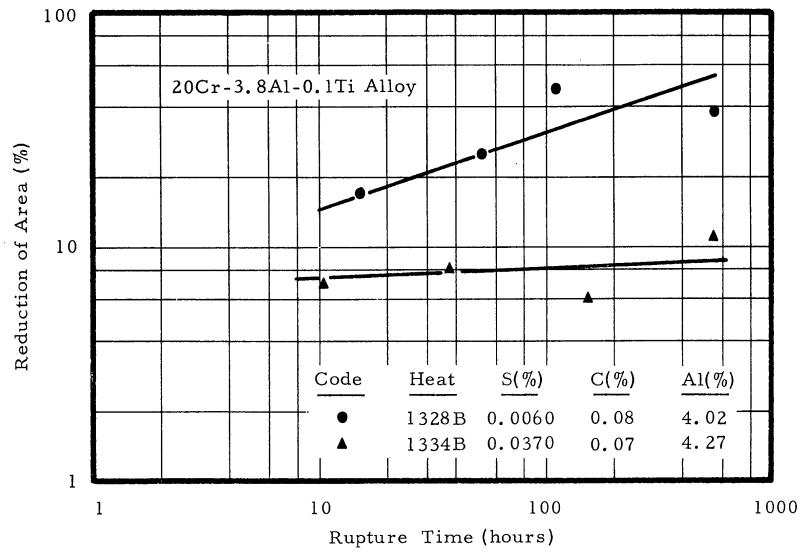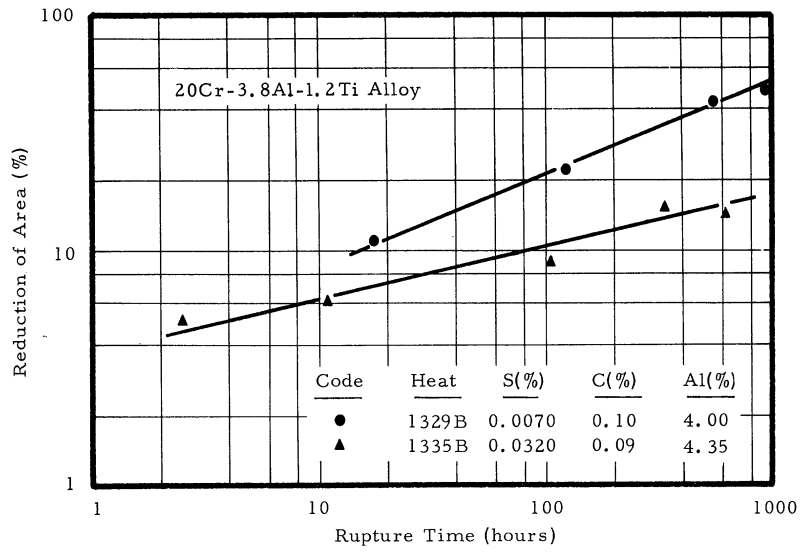
Figure 28. The Differences in Ductility at 1500°F Between High and Low
Sulfur Heats of the 20Cr-3.8Al-Varied Ti Alloys with 0.0035
percent Boron and 0.045 percent Zirconium Added
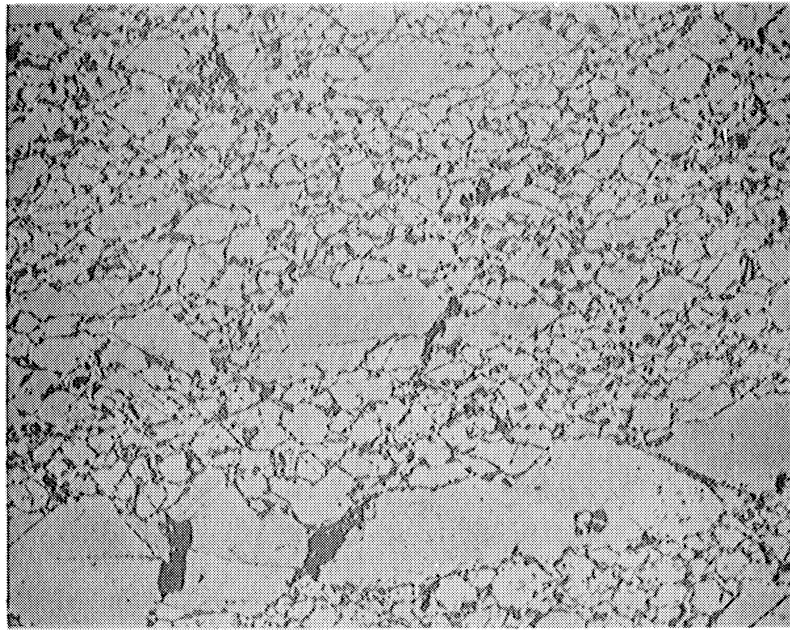
(a) Heat 1329B: rupt. time - 927.6 hrs, RA - 48%
(note carbide precipitation at boundaries and lack of cracks)
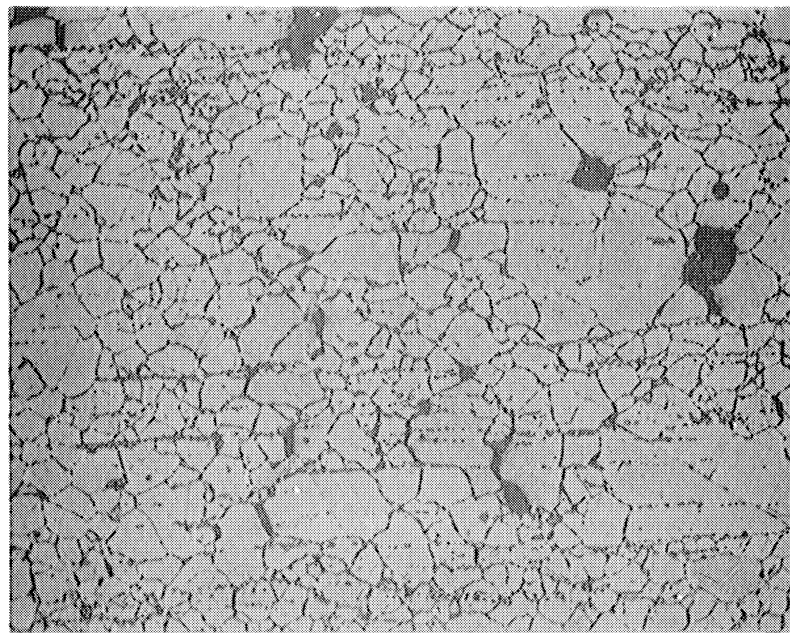
(b) Heat 1335B: rupt. time - 619.0 hrs, RA - 14%
(note lack of carbide precipitation and numerous cracks)

Figure 29. Difference Between Microstructures of Low and
High Ductility Creep-Rupture Specimens of the
20Cr-3.8Al-1.2Ti Alloy with 0.0035 percent
Boron and 0.045 percent Zirconium Added.
Tested at 1500°F and 15,000 psi (100X)

Code for Observations During Rolling

━━━━ no cracking or further cracking
▬ ▬ ▬ ▬ cracks start and become more severe

Ratings of Bar Quality After Rolling

4 - no cracks or defects
3 - slight defects
2 - definite corner cracks
1 - severe corner cracks
0 - almost catastrophic cracking

Heat	Sulfur Content (%)	Rolling Pass Number	Final Bar Quality
		20Cr-1.2Al-3.8Ti Alloy	
1289A	0.0024		4
1289B	0.0022		4
1313A	0.0017		4
1313B	0.0020		4
1247A	0.0035		4
1247B	0.0028		4
1290A	0.0059		4
1290B	0.0043		4
1314A	0.0049		4
1314B	0.0089		4
1291A	0.0145		4
1291B	0.0162		4
1315A	0.0092		3
1315B	0.0110		4
1316A	0.0310		3
1316B	0.0300		3
1317A	0.0540		3
1317B	0.0550		4
1349B	0.1510		2
		20Cr-1.2Al-3.8Ti Alloy Reneated After Every Three Passes	
1384B	0.0055		3
1379B	0.0400		3
1383A	0.0043		3
1383B	0.0053		3
1380A	0.0310		1
1380B	0.0293		1
		20Cr-3.8Al-1.2Ti Alloy	
1329A	0.0060		2
1329B	0.0070		2
1335A	0.0330		2
1335B	0.0320		2
		20Cr-3.8Al-0.1Ti Alloy	
1328A	0.0070		0
1328B	0.0060		1
1334A	0.0410		0
1334B	0.0370		0
		20Cr-3.8Al Alloy	
1327A	0.0080		0
1327B	0.0060		1
1333A	0.0320		0
1333B	0.0330		0
		80Ni-20Cr Alloy	
1331A	0.0080		4
1331B	0.0070		2
1332A	0.0310		1
1332B	0.0390		1

Figure 30. Visual Observations of Alloy Barstock During and After Rolling at 2150°F
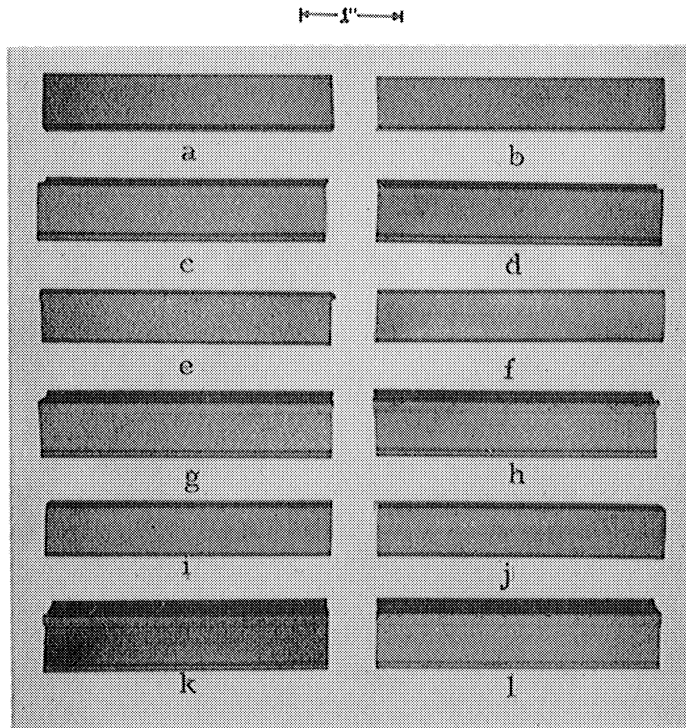
no B and Zr added			0.0035%B and 0.045%Zr added		
Code	Heat	S%	Code	Heat	S%
a	1289A	0.0024	b	1289B	0.0022
c	1313A	0.0017	d	1313B	0.0020
e	1290A	0.0059	f	1290B	0.0043
g	1314A	0.0049	h	1314B	0.0089
i	1291A	0.0145	j	1291B	0.0162
k	1315A	0.0092	l	1315B	0.0110

Figure 31. Quality of Low and Moderate Sulfur 20Cr-1.2Al-3.8Ti Alloy Barstock Hot Rolled at 2150°F

|⊢——1"——⊣|
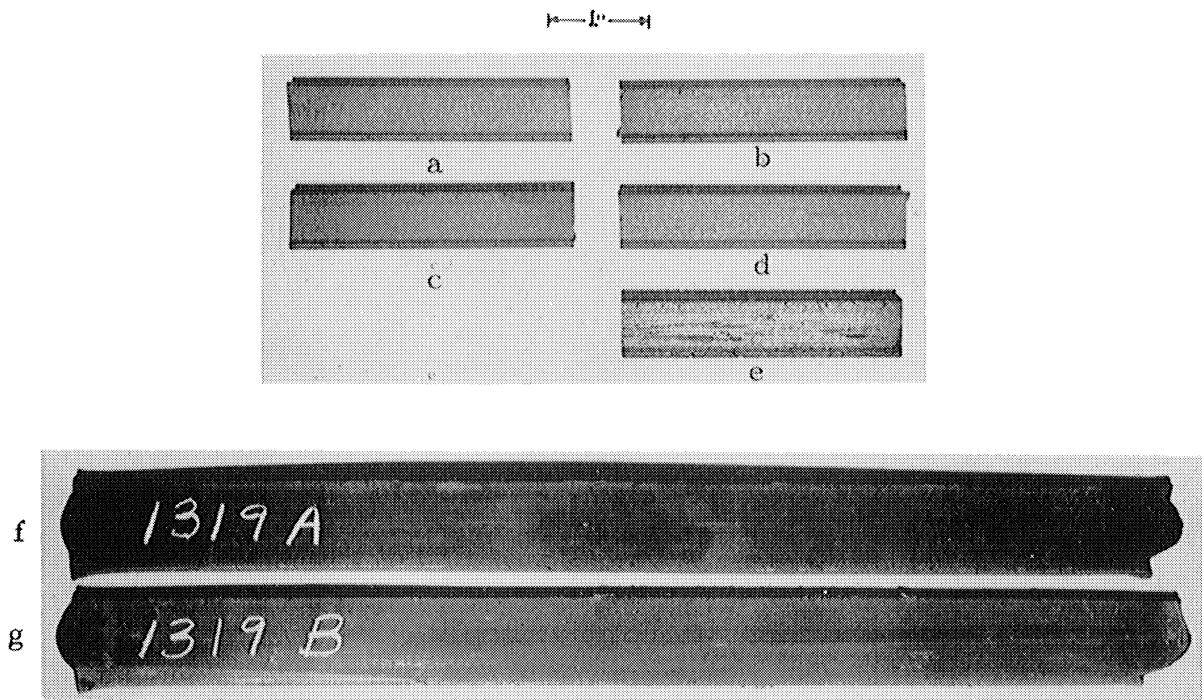
no B and Zr added			0.0035%B and 0.045%Zr added		
Code	Heat	S%	Code	Heat	S%
a	1316A	0.0310	b	1316B	0.0300
c	1317A	0.0540	d	1317B	0.0550
			e	1349B	0.1510
f	1319A	0.0700	g	1319B	0.0640

Figure 32. Quality of High Sulfur 20Cr-1.2Al-3.8Ti Alloy
Barstock and Plate Hot Rolled at 2150°F
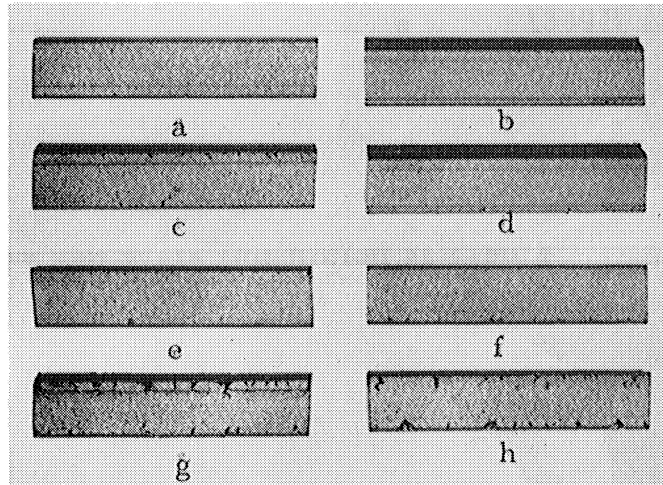
no B and Zr added				0.0035%B and 0.045%Zr added			
Code	Heat	S%	C%	Code	Heat	S%	C%
				a	1384B	0.0054	0.09
				b	1384B	0.0054	0.09
				c	1379B	0.0400	0.06
				d	1379B,	0.0400	0.06
e	1383A	0.0043	0.037	g	1383B	0.0053	0.022
f	1380A	0.0310	0.017	h	1380B	0.0293	0.014

Figure 33. Quality of 20Cr-1.2Al-3.8Ti Alloy Barstock Hot Rolled with Triple the Normal Severity at 2150°F (note cracking in high sulfur-low carbon Heat 1380)
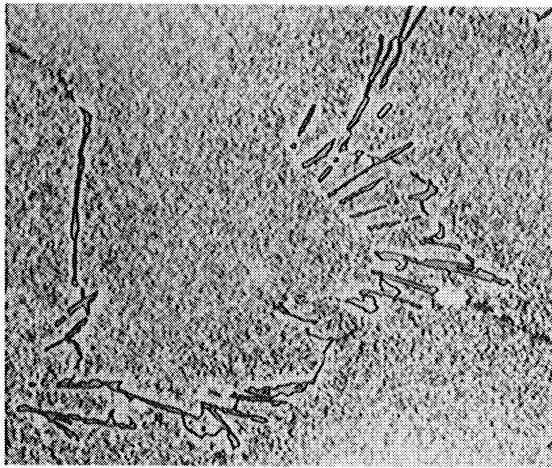
(a) Heat 1379B - 0.0400%S, 0.06%C   (b) Heat 1380A - 0.0310%S, 0.017%C

As-Cast
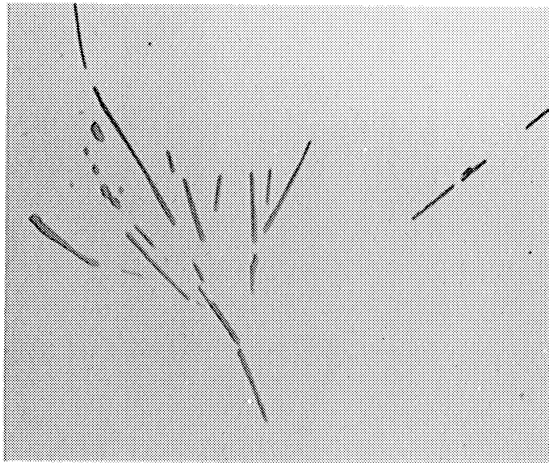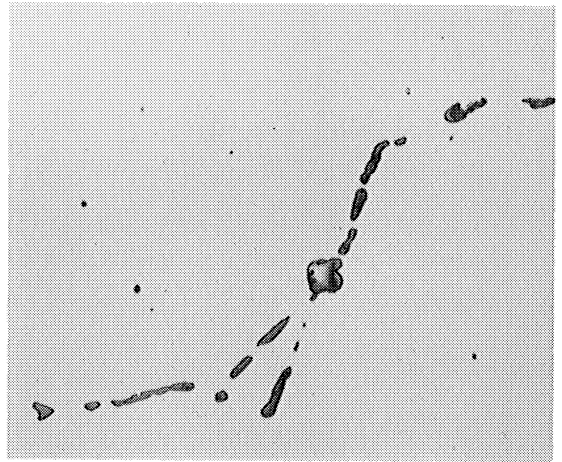
(c) Heat 1379B   (d) Heat 1380A

As-Cast plus 2 hours at 2150°F, W.Q.
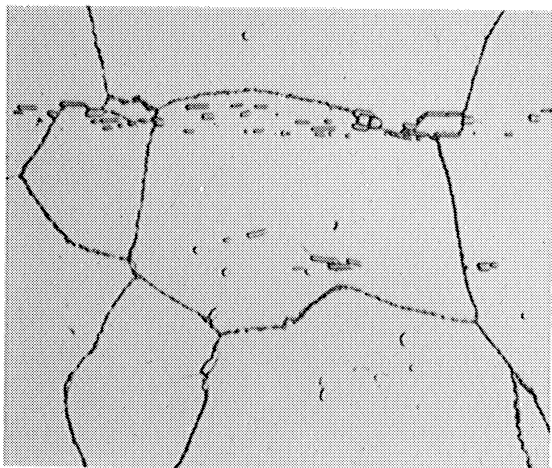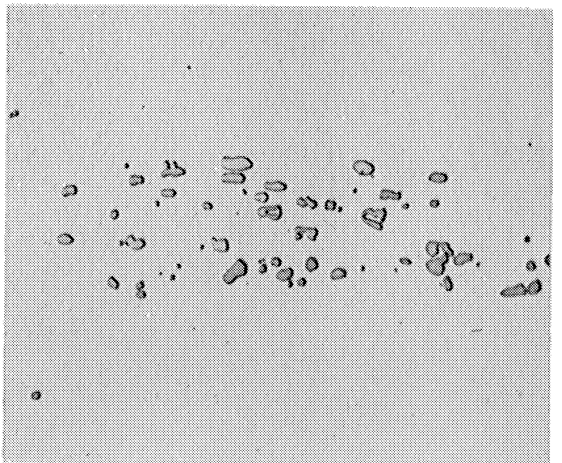
(e) Heat 1379B   (f) Heat 1380A

As-Rolled and Heat Treated

Figure 34. Influence of Processing on the Microstructures of
High Sulfur Heats of the 20Cr-1.2Al-3.8Ti Alloy
Having Normal and Very Low Carbon Contents (1000X)
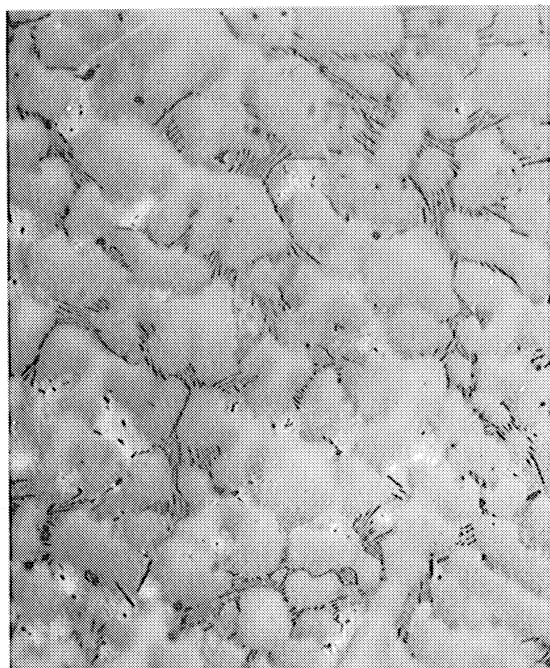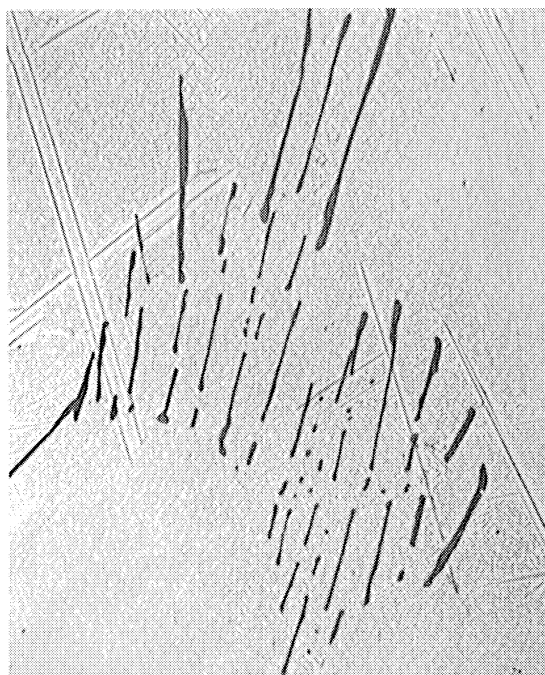
100X   1000X

As-Cast
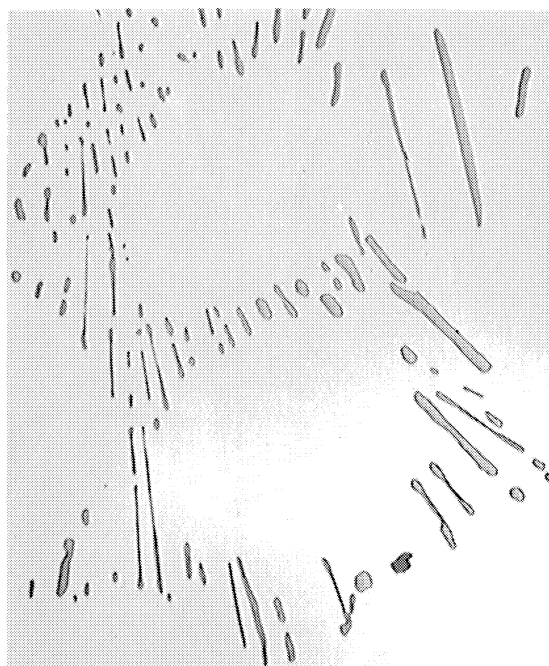
1000X   1000X
As-Cast plus 2 hours 2150°F, W. Q.   As-Rolled
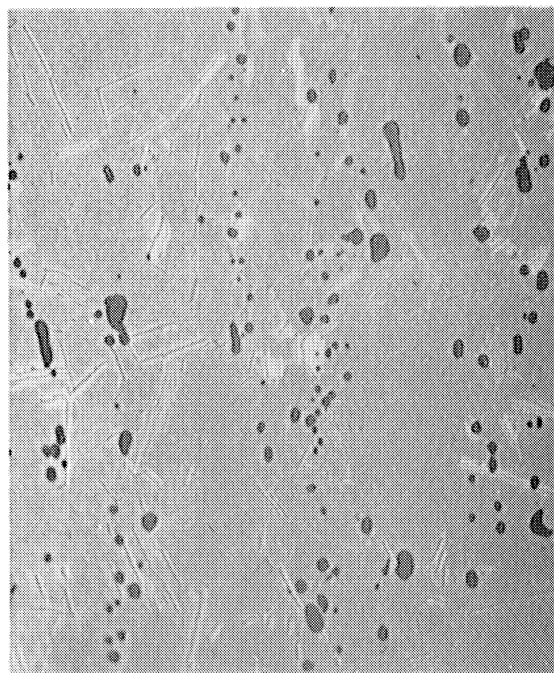
Figure 35. Influence of Processing on the Microstructure of
            a Very High Sulfur Heat of the 20Cr-1.2Al-3.8Ti
            Alloy. Heat 1349B with 0.1510 percent Sulfur
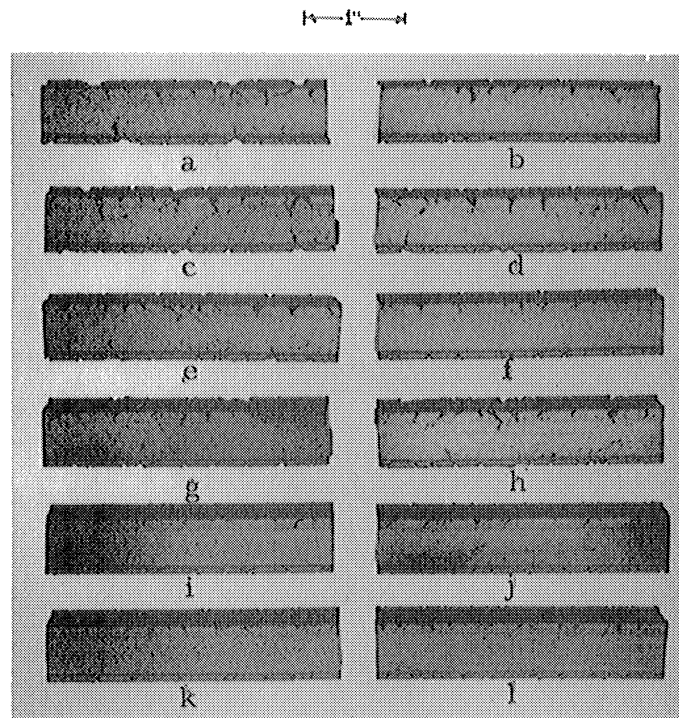
no B and Zr added			0.0035%B and 0.045%Zr added		
Code	Heat	S%	Code	Heat	S%
20Cr-3.8Al Alloy					
a	1327A	0.0080	b	1327B	0.0060
c	1333A	0.0320	d	1333B	0.0320
20Cr-3.8Al-0.1Ti Alloy					
e	1328A	0.0070	f	1328B	0.0060
g	1334A	0.0410	h	1334B	0.0370
20Cr-3.8Al-1.2Ti Alloy					
i	1329A	0.0060	j	1329B	0.0070
k	1335A	0.0330	l	1335B	0.0320

Figure 36. Quality of 20Cr-3.8Al-Varied Ti Alloy Barstock Hot Rolled at 2150°F
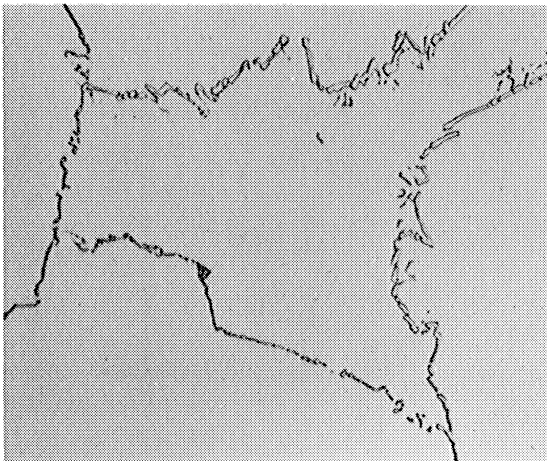
(a) Heat 1329A – 0.0060%S
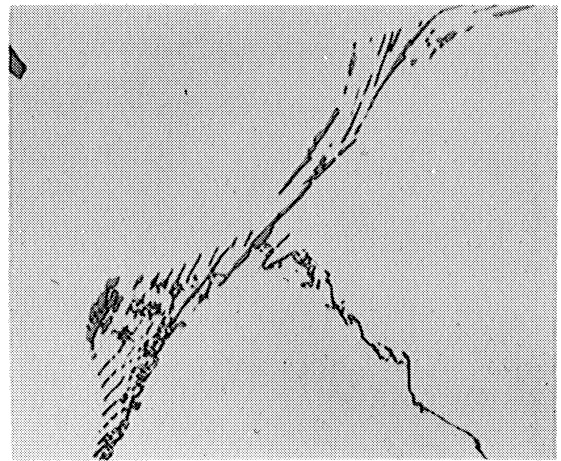
(b) Heat 1335A – 0.0330%S

As-Cast
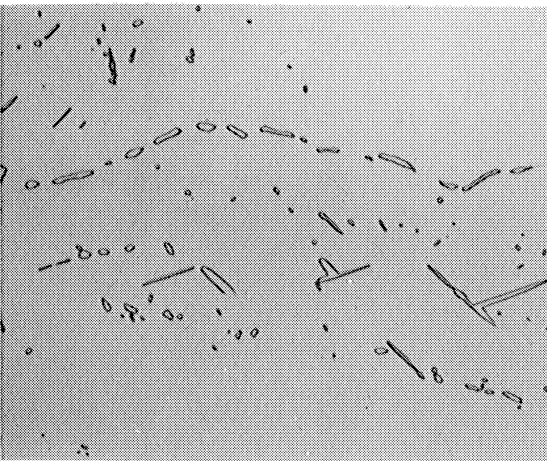
(c) Heat 1329A
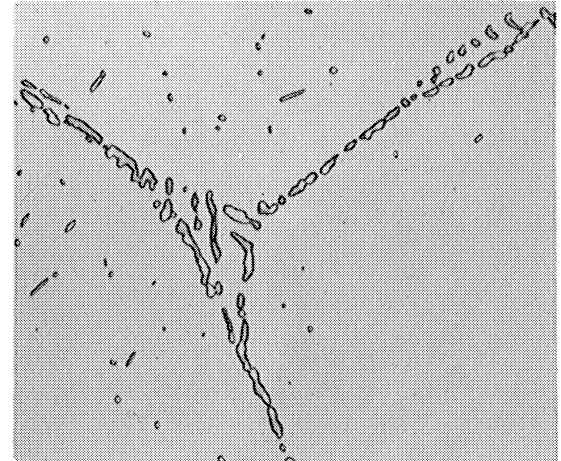
(d) Heat 1335A

As-Cast plus 2 hours at 2150°F, W.Q.
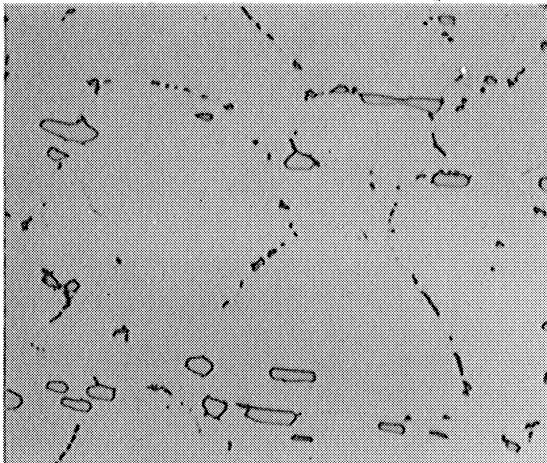
(e) Heat 1329A
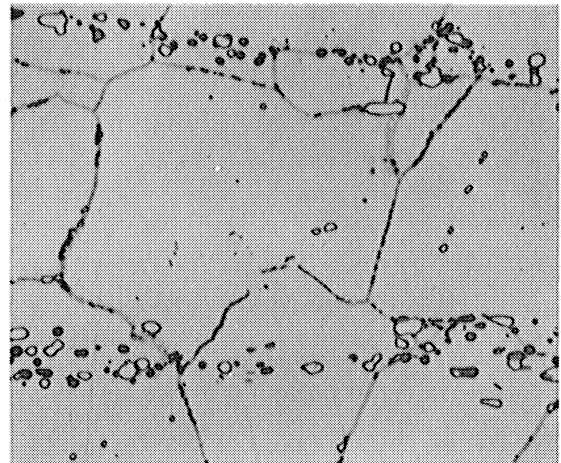
(f) Heat 1335A

As-Rolled and Heat Treated

Figure 37. Influence of Processing on the Microstructure of
Low and High Sulfur Heats of the 20Cr-3.8Al-1.2Ti
Alloy (1000X)
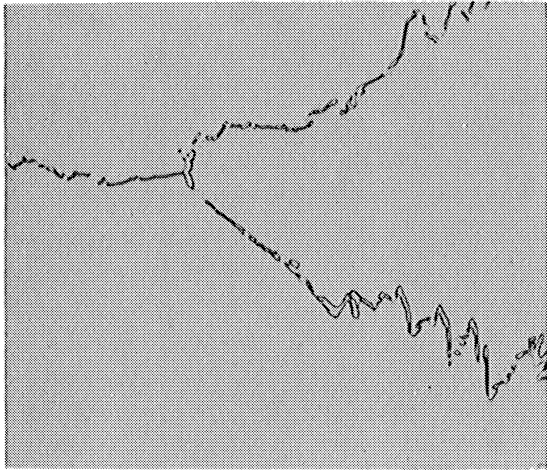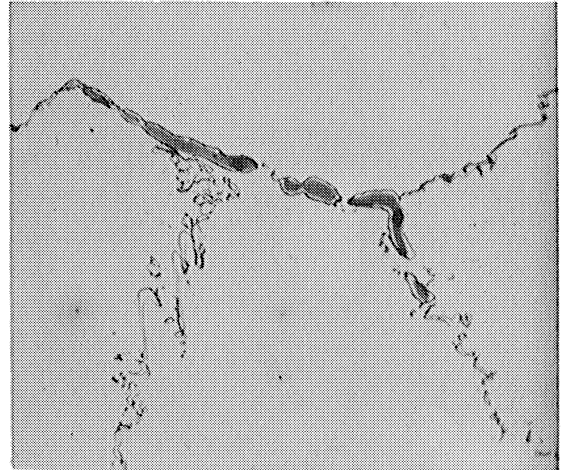
(a) Heat 1327A - 0.0080%S   (b) Heat 1333A - 0.0320%S

As-Cast
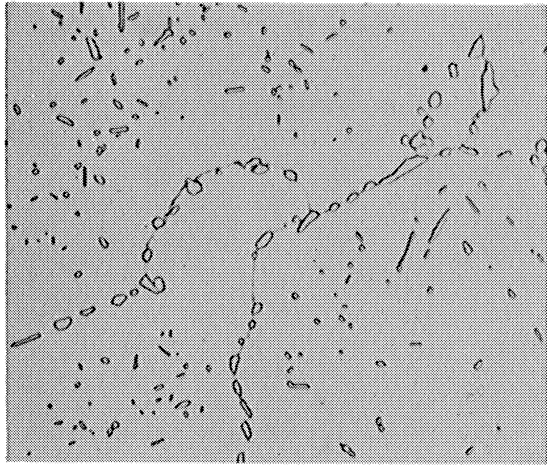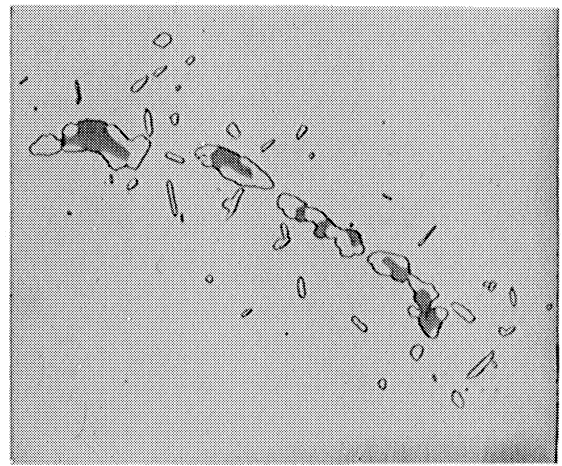
(c) Heat 1327A   (d) Heat 1333A

As-Cast plus 2 hours at 2150°F, W. Q.
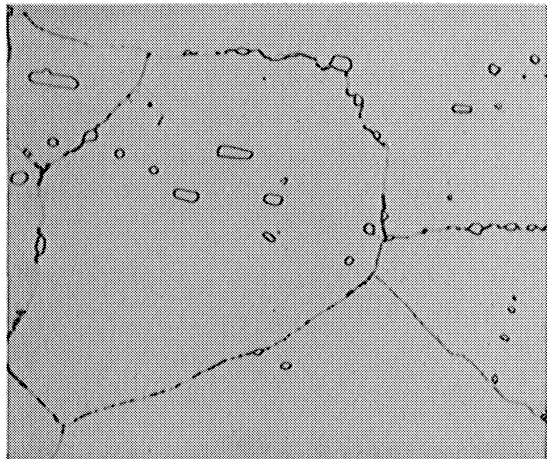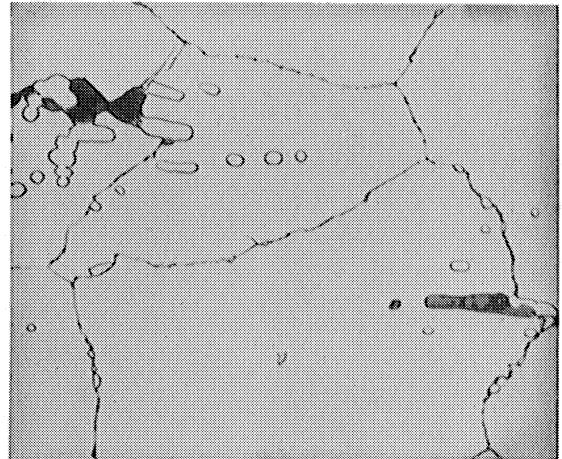
(e) Heat 1327A   (f) Heat 1333A

As-Rolled and Heat Treated

Figure 38. Influence of Processing on the Microstructure of
Low and High Sulfur Heats of the 20Cr-3.8Al Alloy
(1000X)
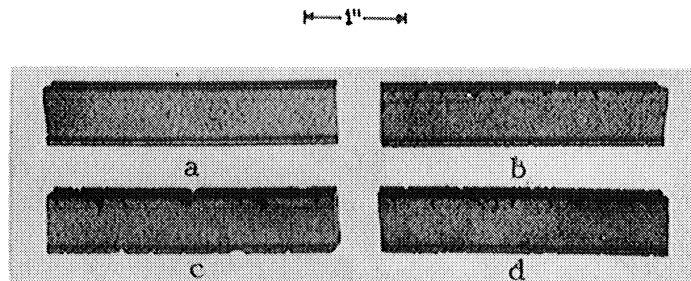
no B and Zr added			0.0035%B and0.045%Zr added		
Code	Heat	S%	Code	Heat	S%
a	1331A	0.0080	b	1331B	0.0070
c	1332A	0.0310	d	1332B	0.0390

Figure 39. Quality of 80Ni-20Cr Alloy Barstock Hot Rolled at 2150°F

no B and Zr added

(a) Heat 1331A - 0.0080%S

0.0035%B and 0.045%Zr added

(b) Heat 1331B - 0.0070%S
As-Cast

no B and Zr added

(c) Heat 1332A - 0.0310%S
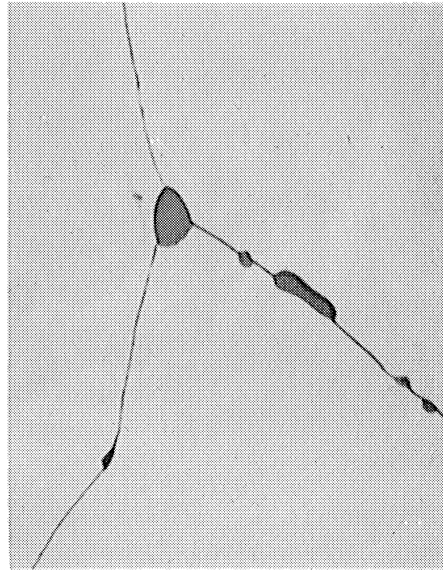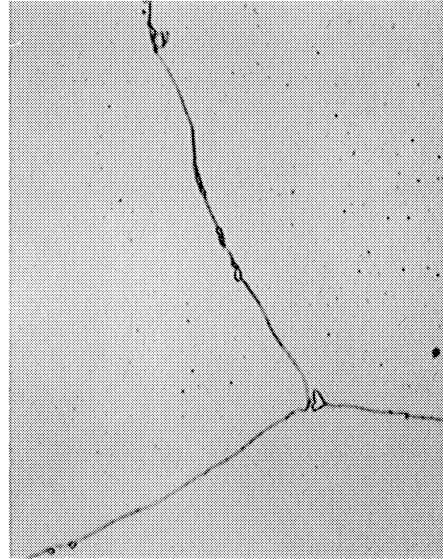
(d) Heat 1331A

(e) Heat 1331B
As-Cast plus 2 hours at 2150°F, W.Q.
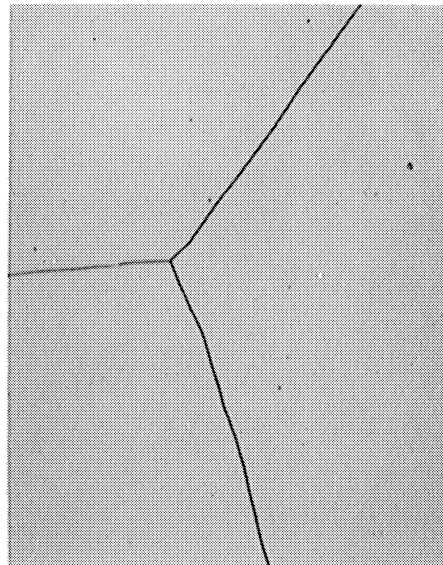
(f) Heat 1332A

Figure 40. Influence of the Pre-Rolling Solution Treatment, Boron and Zirconium, and Sulfur on the Microstructure of the 80Ni-20Cr Alloy (1000X)
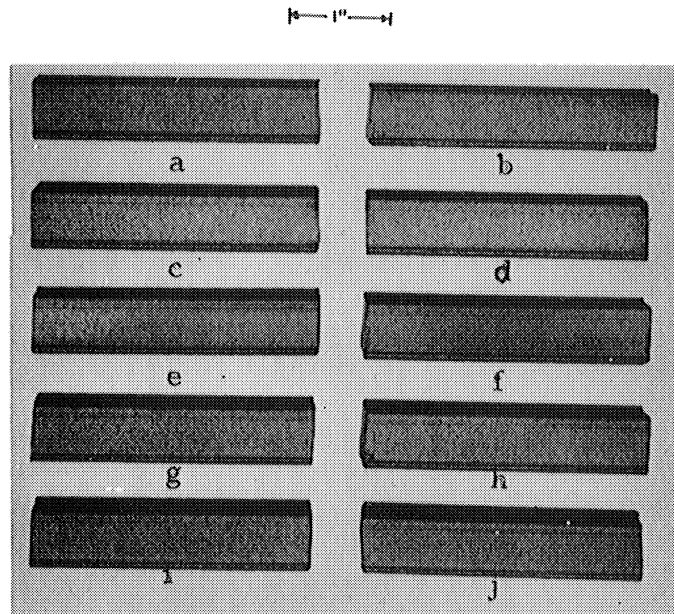
Code no	Heat B and Zr added	S%	Code	Heat 0.0035%B and 0.045%Zr added	S%
a	1346A	0.0004	b	1346B	0.0007
c	1345A	0.0032	d	1345B	0.0031
e	1348A	0.0067	f	1348B	0.0071
			0.045%Zr added		
g	1376Zr	0.0022	h	1376Zr+S	0.0067
			0.0035%B added		
i	1377B	0.0044	j	1377B+S	0.0079

Figure 41. Quality of Nickel Barstock Hot Rolled at 2000°F
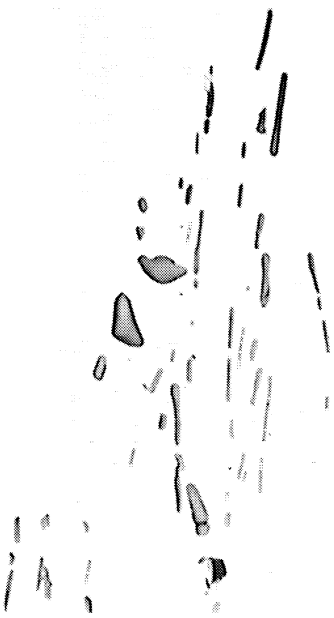
(a) Tau-$Ti_4C_2S_2$, bright field

(b) Tau-$Ti_4C_2S_2$, polarized

20Cr-1.2Al-3.8Ti Alloy (Heat 1319A, 0.0700%S)
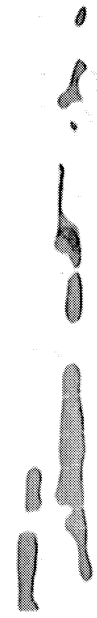
(c) Chromium sulfide, bright field

(d) Chromium sulfide, polarized

20Cr-3.8Al Alloy (Heat 1333A, 0.0320%S)

Figure 42. Optical Activity of Tau-$Ti_4C_2S_2$ and Chromium Sulfide When Examined Under Polarized Light (unetched, 1000X)
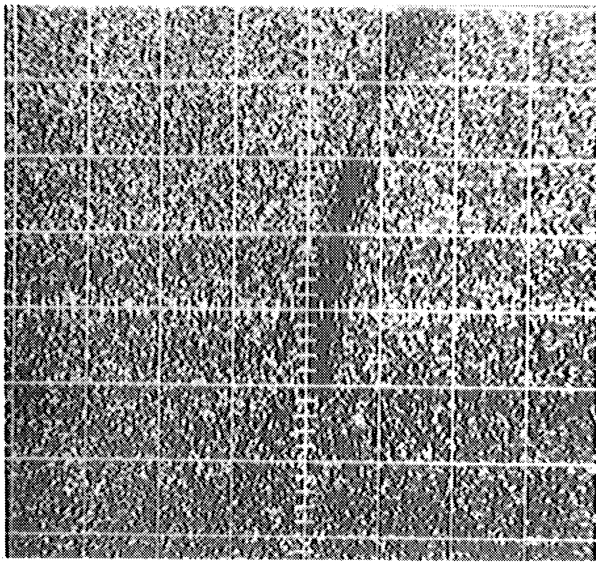
(a) Back scattered electron image

(intensity proportional to atomic number of elements in sample)
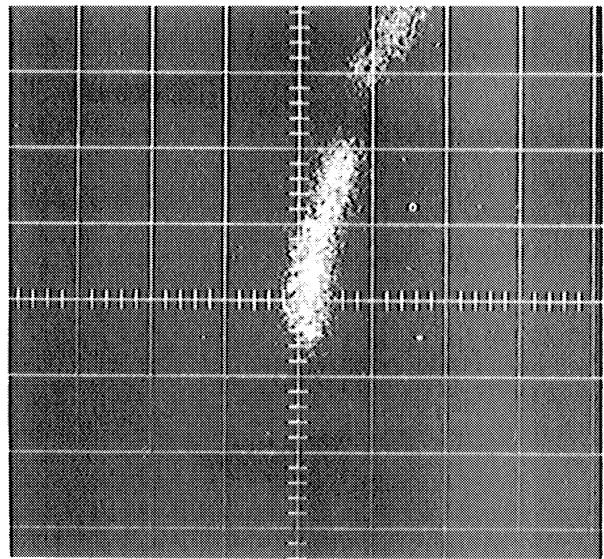
(b) Sulfur K_α intensity image

(intensity proportional to sulfur concentration)
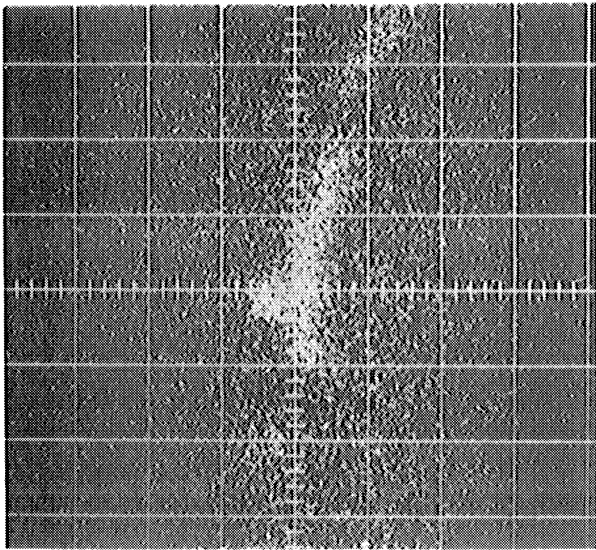
(c) Titanium K_α intensity image

(intensity proportional to titanium concentration)
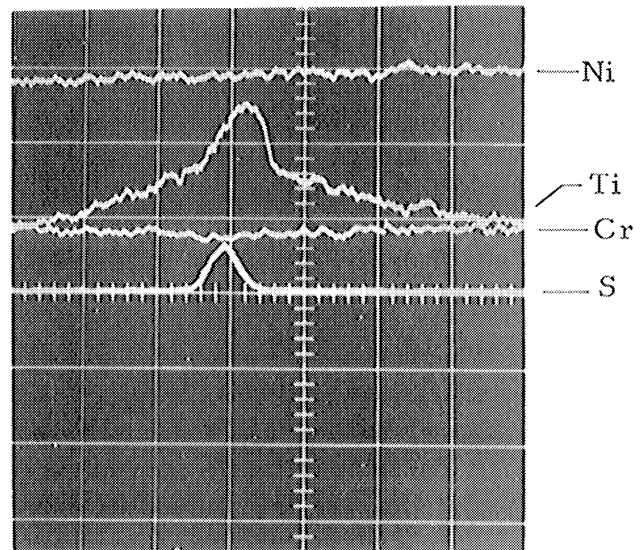
(d) Intensity profiles from linear beam scan

(intensities proportional to element concentration)

Figure 43. Electron Microprobe Analysis of a Lamellar Sulfide Particle in As-Cast Heat 1319A of the 20Cr-1.2Al-3.8Ti Alloy. Photographs of Oscilloscope Screen (1780X)
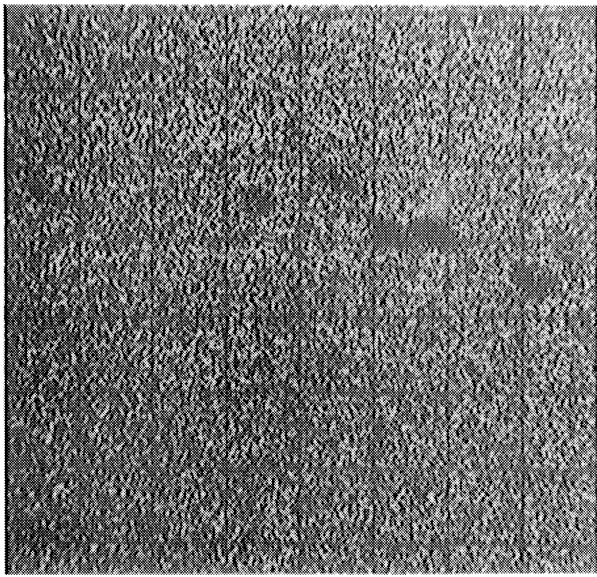
(a) Back scattered electron image

(intensity proportional to atomic
number of elements in sample)
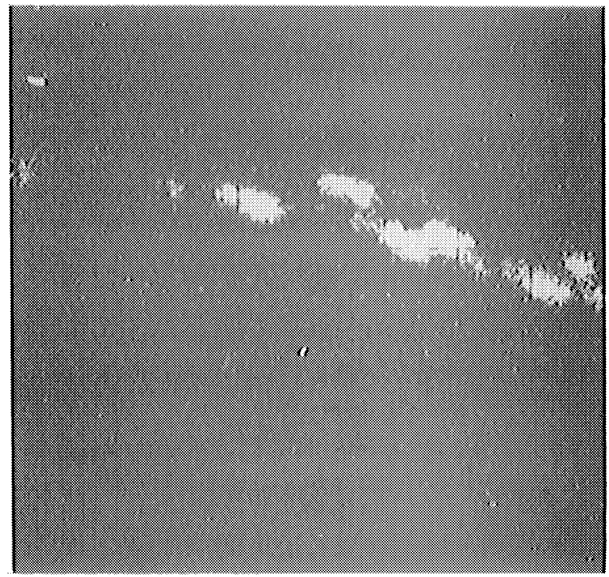
(b) Sulfur K_α intensity image

(intensity proportional to
sulfur concentration)
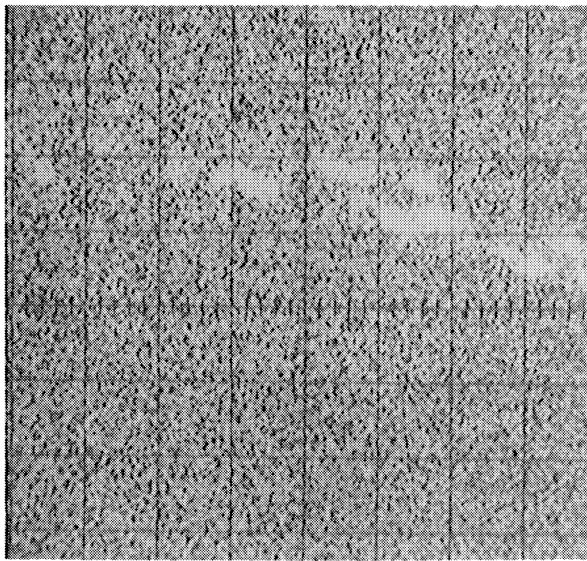
(c) Titanium K_α intensity image

(intensity proportional to
titanium concentration)
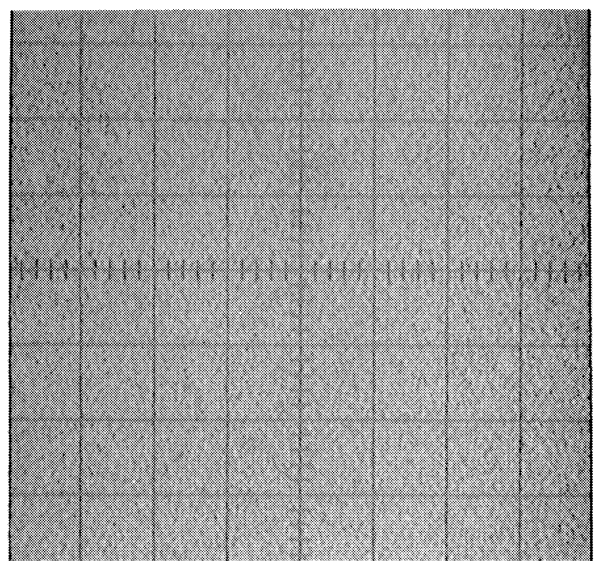
(d) Chromium K_α intensity image

(intensity proportional to
chromium concentration)

Figure 44. Electron Microprobe Analysis of Sulfide Particles in
As-Rolled Heat 1319A of the 20Cr-1.2Al-3.8Ti Alloy.
Photographs of Oscilloscope Screen (860X)
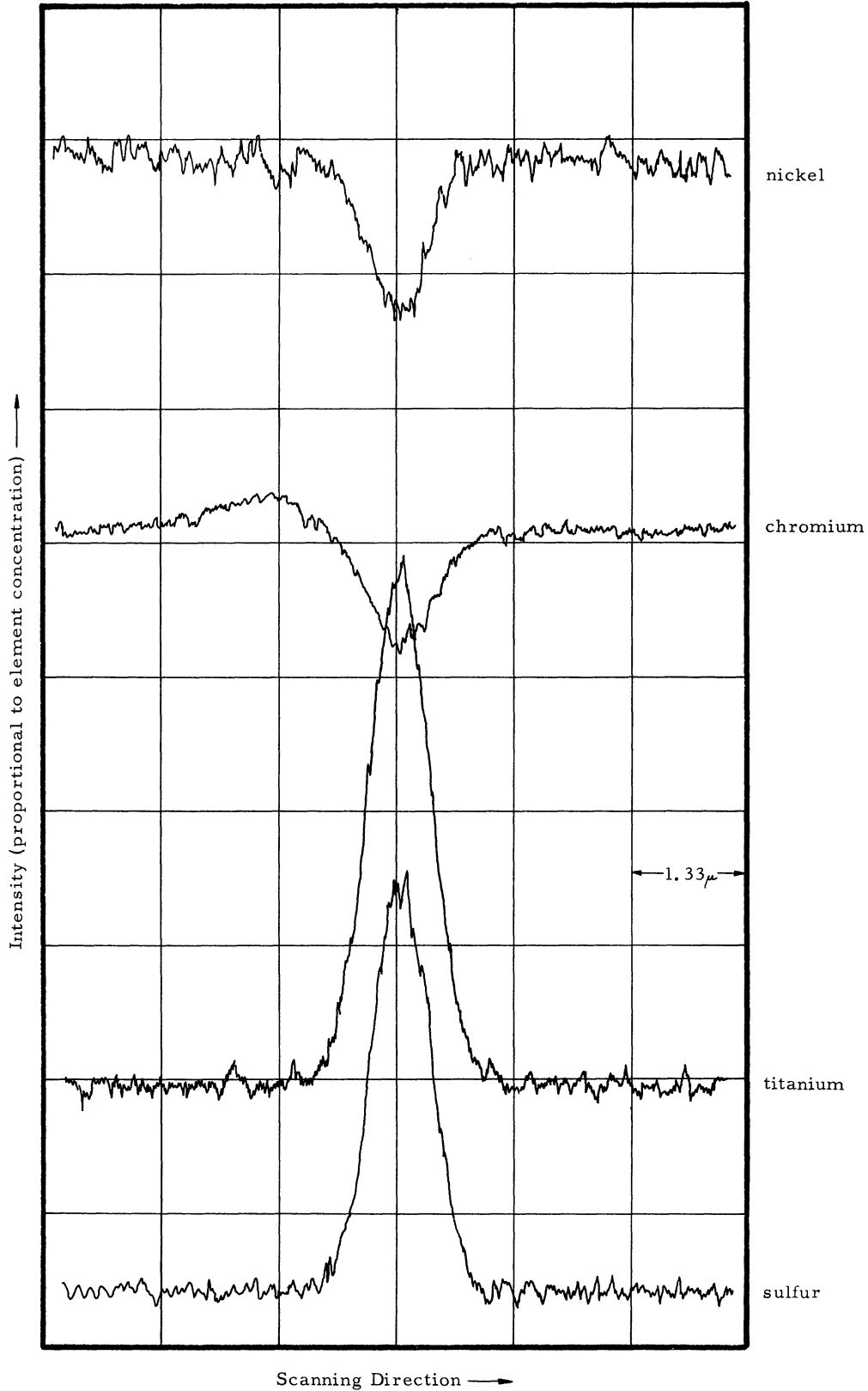
Figure 45. Electron Microprobe Analysis of Sulfide Particle in As-Rolled Heat 1319A of the 20Cr-1.2Al-3.8Ti Alloy. Composite Chart Record of Linear Beam Scan
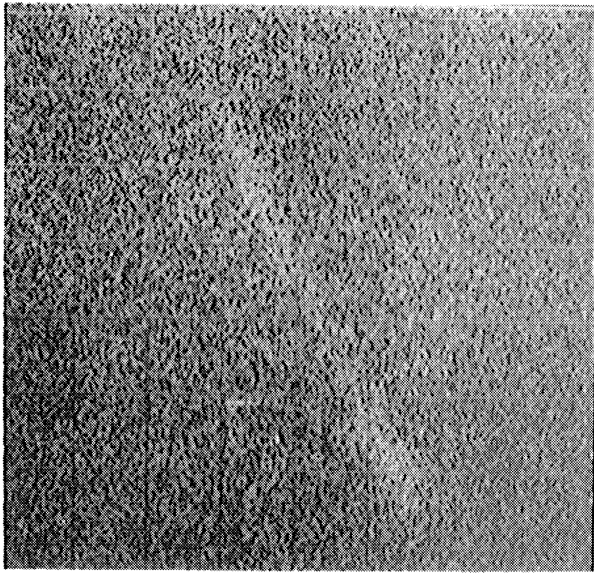
(a) Chromium K_α intensity image

    (intensity proportional to
    chromium concentration)
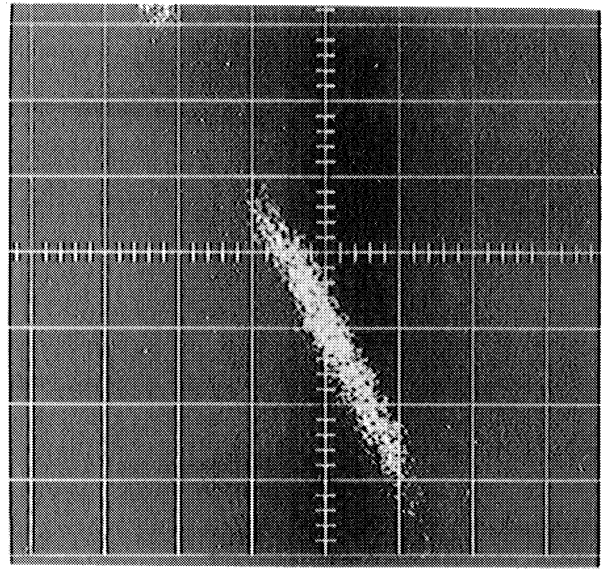
(b) Sulfur K_α intensity image

    (intensity proportional to
    sulfur concentration)
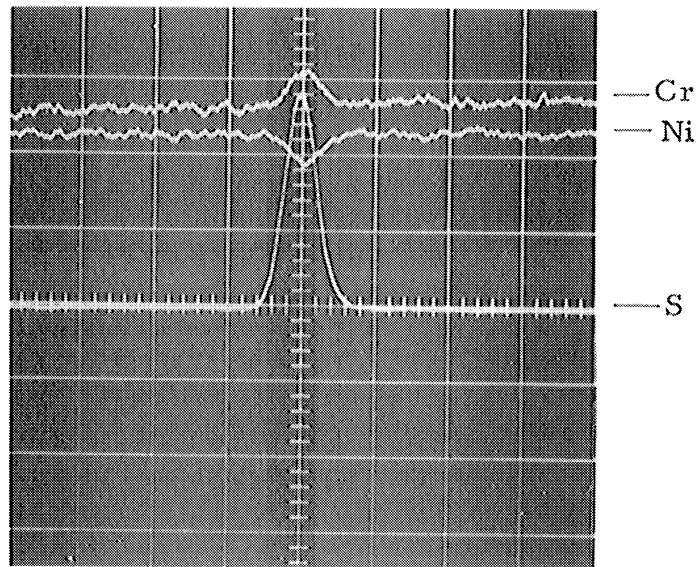
(c) Intensity profiles from linear
    beam scan

    (intensities proportional to
    element concentration)

Figure 46. Electron Microprobe Analysis of an Elongated Sulfide
Particle in As-Rolled Heat 1333A of the 20Cr-3.8Al
Alloy. Photographs of Oscilloscope Screen (1780X)

no B and Zr added   0.0035%B and 0.045%Zr added
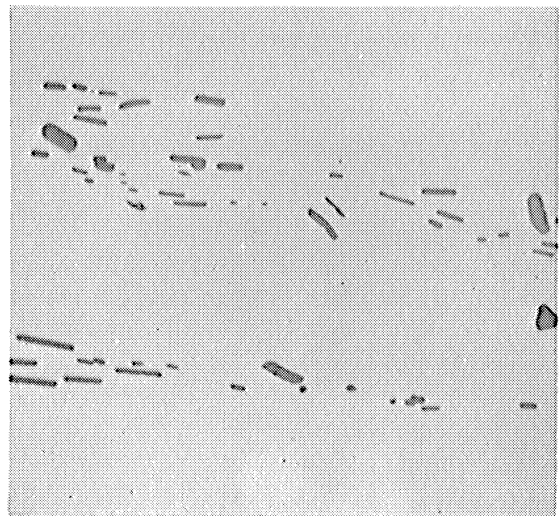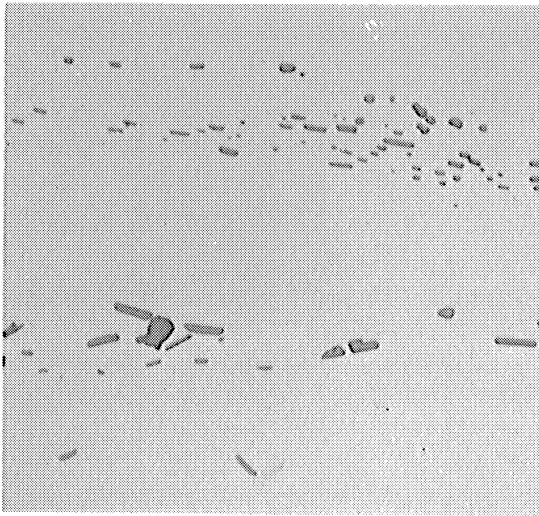
½ hour at 2300°F, W.Q.
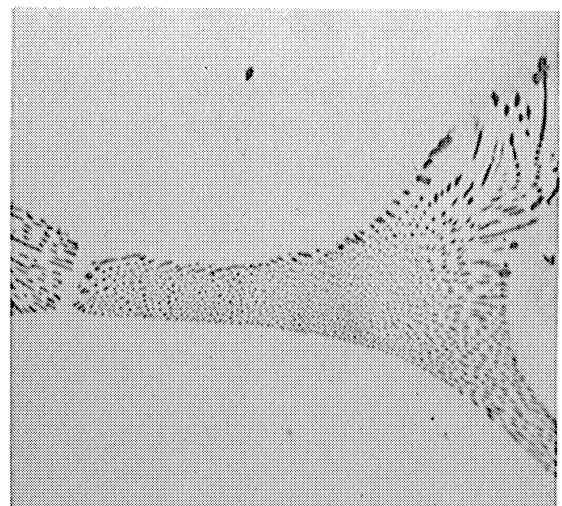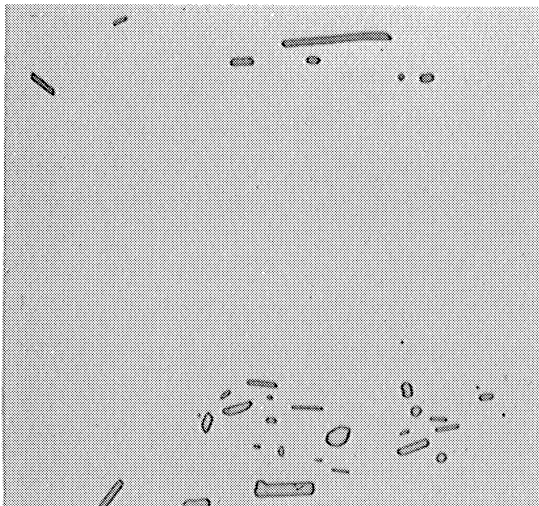
½ hour at 2400°F, W.Q.

½ hour at 2425°F, W.Q.

Figure 47. Influence of High Temperature Thermal Exposures
on Tau-$Ti_4C_2S_2$ in the 20Cr-1.2Al-3.8Ti Alloy with-
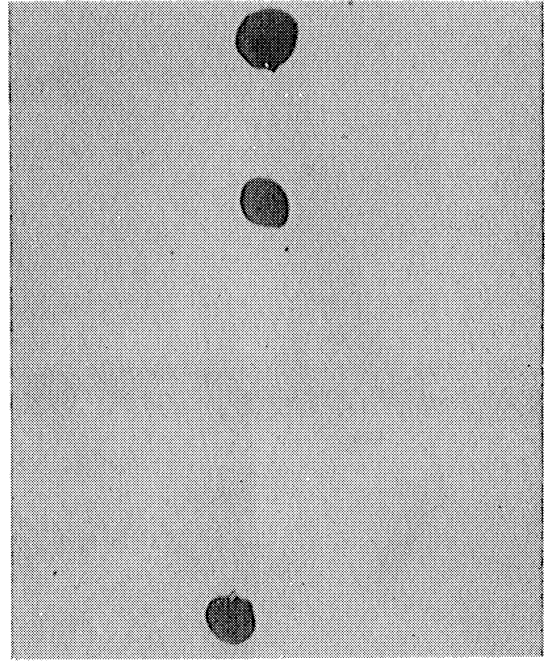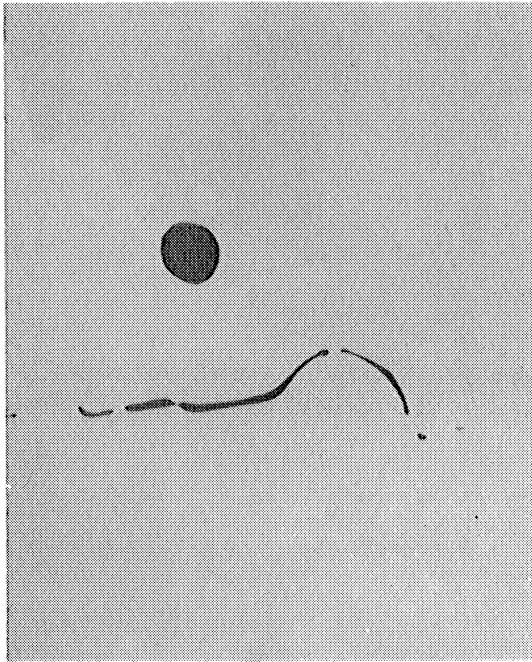out and with Boron and Zirconium Added (1000X)
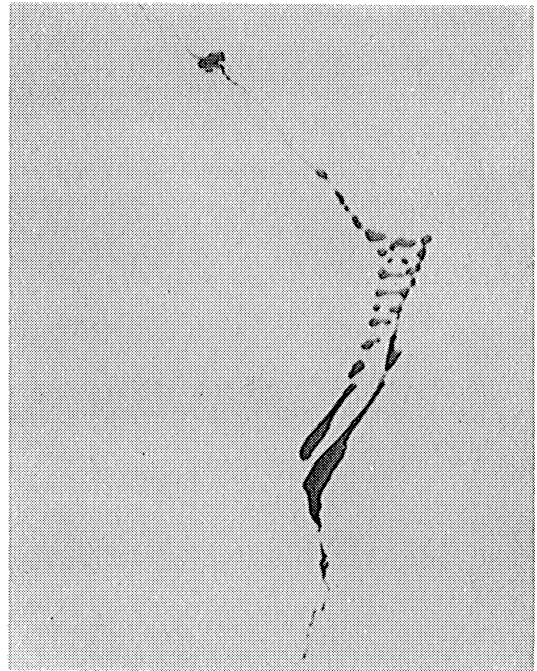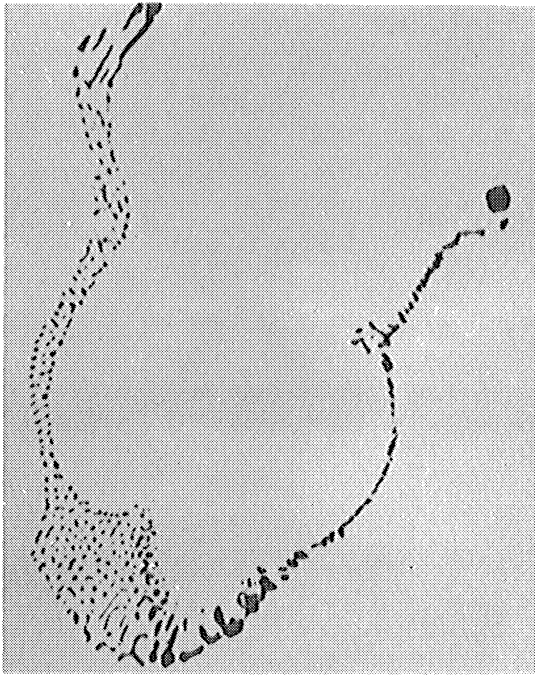
Tau-$Ti_4 C_2 S_2$ in Heat 1393
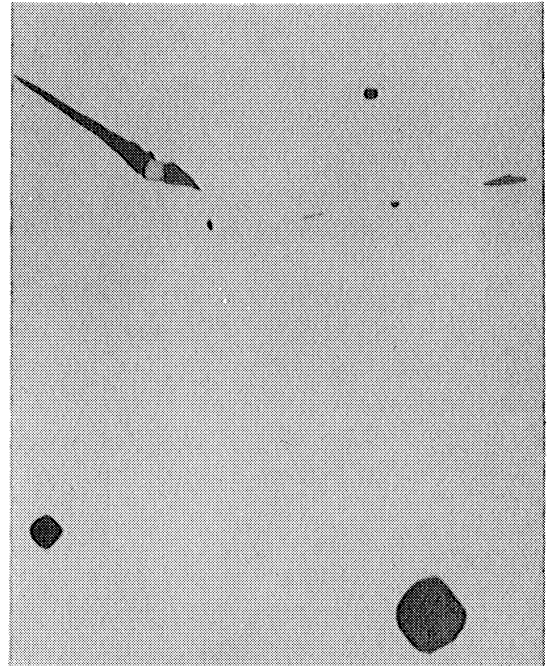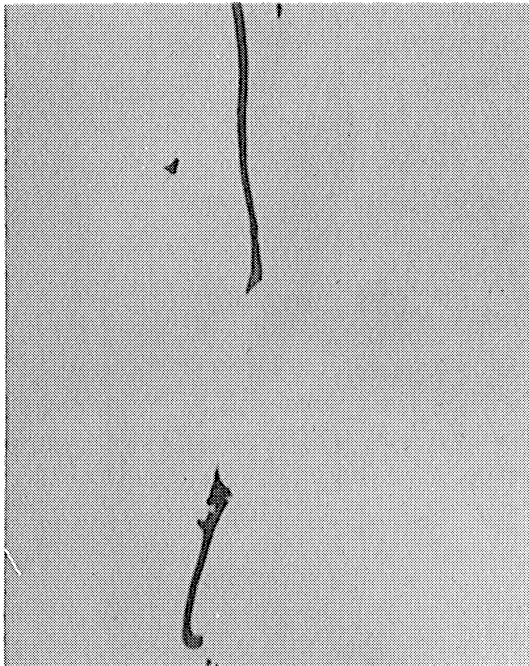(alloy nominally 20Cr-1.0Ti-0.1S-0.06C-bal. Ni)
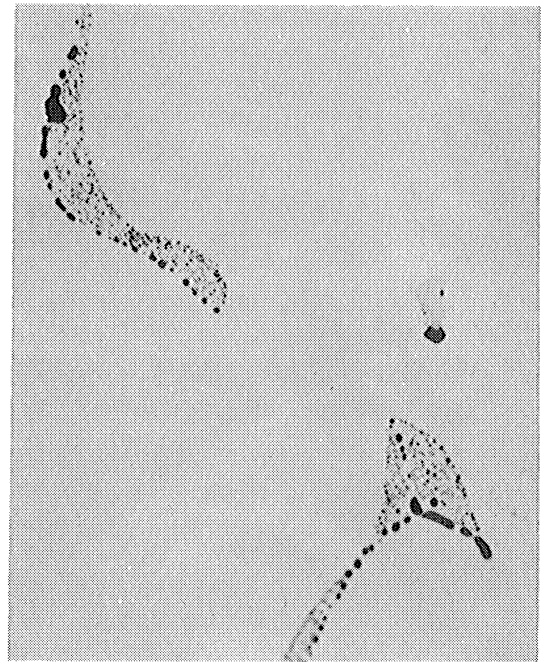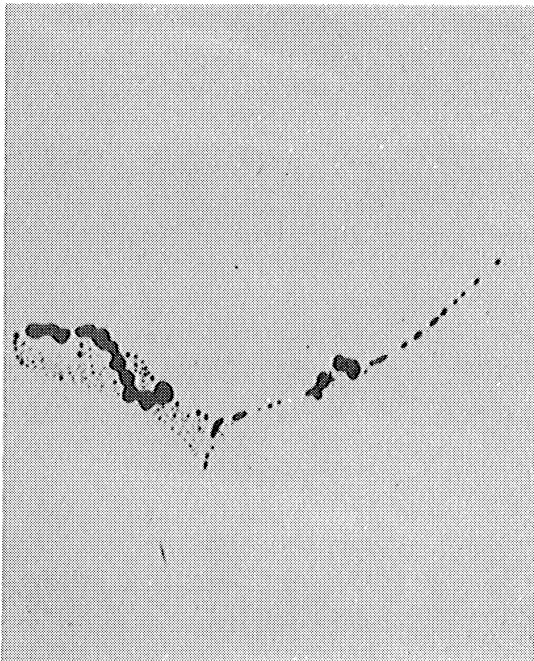
Unidentified Sulfide in Heat 1394
(alloy nominally 20Cr-1.0Ti-0.1S-<0.01C-bal. Ni)

Figure 48.   Influence of Composition on the Sulfides formed in
Ni-Cr-Ti-S-C Alloys (1000X)

Unidentified Sulfide in Heat 1395
(alloy nominally 1.0Ti-0.1S-0.06C-bal. Ni)

Unidentified Sulfide in Heat 1396
(alloy nominally 1.0Ti-0.1S-<0.01C-bal. Ni)

Figure 48. Continued